Efficient Interference Suppression and Resource Allocation in MIMO and DS-CDMA Wireless Networks

Patrick Clarke

P .D.

T U Y
D E

September 2011

Abstract

Direct-sequence code-division multiple-access (DS-CDMA) and multiple-input multiple-output (MIMO) wireless networks form the physical layer of the current generation of mobile networks and are anticipated to play a key role in the next generation of mobile networks. The improvements in capacity, data-rates and robustness that these networks provide come at the cost of increasingly complex interference suppression and resource allocation. Consequently, efficient approaches to these tasks are essential if the current rate of progression in mobile technology is to be sustained. In this thesis, linear minimum mean-square error (MMSE) techniques for interference suppression and resource allocation in DS-CDMA and cooperative MIMO networks are considered and a set of novel and efficient algorithms proposed

Firstly, set-membership (SM) reduced-rank techniques for interference suppression in DS-CDMA systems are investigated. The principals of SM filtering are applied to the adaptation of the projection matrix and reduced-rank filter in reduced-rank signal processing based on the method of joint iterative optimisation (JIO) of adaptive filters. The sparse updates and optimised step-sizes that form the basis of SM schemes are introduced to JIO in order to improve its convergence and complexity whilst maintaining its use of low-dimensionality filters. Analysis of the proposed schemes confirms their stability and establishes bounds on their performance. Through simulation in a DS-CDMA system, the proposed schemes are shown to outperform the existing JIO and reduced-rank schemes whilst achieving a significant reduction in computational complexity.

Secondly, resource allocation in multirelay cooperative MIMO systems is addressed. Jointly operating iterative discrete stochastic algorithms (DSA) are utilised to form a low-complexity transmit diversity selection (TDS) scheme optimised by a parallel relay selection (RS) procedure. The proposed scheme is shown to converge to the optimal exhaustive solution of the combinatorial TDS problem and enhance the performance of existing interference suppression methods. RS based on DSA is extended to continuous adaptive power allocation to form a joint discrete-continuous optimisation procedure that augments conventional iterative MMSE power allocation.

Lastly, an investigation into the use of bidirectional MMSE algorithms for interference suppression in DS-CDMA systems operating over severely fading channels is presented. The correlation present, even in fast fading environments, between 3 or more successive channel coefficients is exploited to enable improved reception and multiuser interference suppression (MUI) without tracking of the faded or unfaded symbols. A

set of adaptive mixing parameters is introduced to optimise the weighting of the correlation information from the considered channel coefficients in order to improve convergence and steady-state performance. An analysis of the proposed schemes is presented and the mechanisms behind their improved performance established. Accompanying signal-to-interference-plus-noise-ratio (SINR) analysis also provides analytical performance curves. The proposed schemes are compared to existing schemes and are shown to provide improved tracking and robustness, both in conventional and cooperative DS-CDMA networks.

Contents

List of Figures

List of Tables

Acknowledgements

I would like to express my sincere gratitude to my supervisor Dr. Rodrigo C. de Lamare for his support, advice, supervision and guidance throughout my research, without which much of this work would not have been possible.

I would also like to thank my girlfriend Laura for her unconditional support, Mungo for all the tea breaks and my family for their support and encouragement.

Finally, I would like to thank all members of the Communications Research Group for their support and advice.

Declaration

Elements of the research presented in this thesis have been published in academic journals and conference proceedings. A list of these publications can be found at the end of Chapter 1.

The work presented in this thesis is original to the best knowledge of the author. Where this is not the case, appropriate citations and acknowledgements have been given.

Chapter 1

Introduction

Contents

1.1 Overview

Recent advances in mobile communications have been made possible by the progression of the underlying wireless networks from analogue to direct-sequence code-division multiple-access (DS-CDMA) and, in the near future, to multiple-input multiple-output (MIMO) and cooperative systems. However, the improvements in data-rate, capacity and coverage are accompanied by multiuser interference (MUI), increased power consumption, intersymbol interference (ISI) and susceptibility to fading [1, 2]. Consequently, effective operation of these systems is reliant on the signal processing that performs interference suppression and resource allocation.

A vast array of research literature has been generated on interference suppression

and resource allocation algorithms, leading to well defined and documented optimal methods and solutions [2–8]. However, the computational complexity of obtaining the optimum solution generally prohibits their application to real-world systems. As a result, algorithms that efficiently obtain a near-optimal solution are of great interest. Training-based adaptive algorithms are a means to achieving this; however, a compromise between performance, complexity and convergence accompanies these algorithms.

In this thesis, a number of novel frameworks and accompanying adaptive algorithms are proposed that advance upon existing techniques in the field of interference suppression and resource allocation. Firstly, the set-membership (SM) [9–11] framework is applied to the promising area of reduced-rank signal processing based on joint iterative optimisation (JIO) of adaptive filters [12, 13]. Algorithms based on this framework are applied to a DS-CDMA system and improve upon the performance of existing reduced-rank schemes whilst achieving a significant reduction in complexity. Analysis is presented that confirms the convergence of the proposed algorithms and provides an improved steady-state error bound.

Secondly, interference suppression and resource allocation algorithms for cooperative MIMO systems are investigated. Low-complexity discrete stochastic algorithms (DSAs) [14] are utilised to a form joint transmit diversity and relay selection (RS) scheme for cooperative MIMO systems. Optimal 1-bit power allocation is obtained using low-complexity algorithms and discrete stochastic RS is shown to also bring improvements to continuous power allocation through zero constraints.

Lastly, the challenges of interference suppression for conventional and cooperative DS-CDMA systems in severely fading channels are addressed by the proposition of a set of bidirectional minimum mean-square error (MMSE) adaptive algorithms [15]. Correlation information from a plurality of time instants is utilised to avoid tracking of the channel or transmit symbols. Mixing parameters are also introduced to optimise the use of the correlation information. Analysis of the proposed algorithms provides analytical performance curves along with further insight into the operation of the proposed

schemes. The resulting algorithms improve upon the existing differential schemes in terms of convergence, steady-state performance, robustness to channel discontinuities and fading rate range.

1.2 Contributions

- The novel application of SM techniques to reduced-rank adaptive reception based on JIO of adaptive filters. Improved complexity, convergence and interference suppression performance are obtained by applying the principal of sparse, optimised updates to the joint iterative operation of the reduced-rank method. Algorithms based on mean square-error (MSE) and least-squares (LS) error criteria are derived and applied to the adaptation of the dimensionality reducing projection matrix and the reduced-rank filter. Error bounded sets containing valid filter estimates are formed at each time instant and optimised step-sizes are derived to ensure each adaptive structure lies within the relevant set. Variable errors bounds and rank selection are introduced to allow the proposed algorithms to adapt to non-stationary environments whilst also assisting in transferring the burden of bound and rank specification from the user to the algorithm. Stability and analytical convergence analysis are presented and used to provide an improved lower bound on the performance of the proposed scheme compared to the use of the error bound alone. Simulations in a DS-CDMA system with short spreading sequences over a wide range of scenarios confirm the improved performance of the proposed schemes and their effective interference suppression properties.

- Optimisation of RS and transmit diversity selection (TDS) in a two phase multi-relay cooperative MIMO system using joint discrete iterative algorithms. Sets of relay transmit antenna patterns are formed and then optimised, reduced, and searched by jointly operating DSAs at the destination node. Optimisation of the second phase is combined with selection of the data to forward from the relays in a

process where the burden of optimisation is concentrated at the receiver. Minimal 1-bit feedback is required for each relay antenna and both decode-and-forward (DF), and amplify-and-forward (AF) protocols are considered. The proposed schemes are then implemented with optimal and iterative, and linear and non-linear receivers and multiuser detection (MUD) methods. This results in a number of novel low-complexity implementations where discrete and iterative methods jointly operate and converge under a variety of optimisation criteria. Feedback analysis is given and the proposed schemes are shown to provide increased diversity and interference suppression, and achieve near optimal performance whilst entailing significantly reduced computational complexity.

- An improved relay power allocation scheme for cooperative multi-relay MIMO networks where a DSA is used to aid the continuous power allocation process. A DSA utilising forwarded error data iteratively selects sets of relay antennas and constrains their transmit power to zero in a manner not possible with continuous power allocation alone. This results in improved power allocation by introducing first phase performance information into the second phase power allocation process. Adaptive reception implementations are presented which involve a number of discrete and iterative algorithms that jointly operate and converge in parallel to form a low-cost joint receive and transmit parameter optimisation scheme.

- A linear reception framework for multi-relay MIMO networks that exceeds the performance of the Wiener filter. Fully iterative least mean-square (LMS) based MMSE receivers are used to exploit the non-Wiener behaviour of the LMS algorithm in the presence of interference. The non-Wiener behaviour is shown to extend beyond systems with narrow band interference and a low-complexity iterative reception scheme is formed. The results are validated using bit-error-rate (BER) and MSE simulation plots and the performance improvements are shown to be reliant upon the independence between the reception at the relay nodes.

- The formulation of a switching bidirectional MMSE-based adaptive reception and interference suppression scheme for severely fading channels. In rapidly time-varying fading channels the correlation between multiple adjacent fading coefficients, and therefore receive vectors, is exploited in order to provide improved detection and estimation without the need for channel tracking. A switching framework based upon an auxiliary metric is introduced to optimise performance when correlation properties are rapidly varying and channel discontinuities are present. The use of the correlation information corresponding to multiple received vectors is optimised and implemented adaptively. Signal-to-interference-plus-noise-ratio (SINR) analysis of the proposed algorithm is presented and analytical performance curves obtained. Conjugate gradient (CG) and stochastic gradient (SG) implementations are derived and applied to conventional and cooperative multiuser DS-CDMA systems.

1.3 Thesis Outline

The structure of the thesis is as follows:

- Chapter 2 presents a literature review of the trends in mobile communications and introduces the system models considered in the thesis. Alongside this, an introduction to the principles of estimation and detection theory, and a review of existing interference suppression and resource allocation techniques is given.

- Chapter 3 presents a novel low-complexity SM reduced-rank framework based on the JIO of adaptive filters. Efficient schemes based on adaptive algorithms are derived and their computational complexity given. Convergence and steady-state analysis is presented and the proposed algorithms are applied to the uplink of a multiuser DS-CDMA system.

- Chapter 4 presents a joint relay and TDS framework for resource allocation in

cooperative multi-relay MIMO networks. DSAs are utilised to obtain a low complexity transmit optimisation procedure that requires minimal 1-bit feedback and whose computational burden is centred at the receiver. Improved diversity and interference suppression are achieved by the proposed schemes and the ability of MMSE adaptive techniques in multi-relay MIMO networks to exceed the performance of the optimal Wiener filter is highlighted. Discrete stochastic RS is jointly applied to continuous power allocation and, through the enforcement of zeros constraints, improves relay power allocation.

- Chapter 5 presents a bidirectional MMSE interference suppression scheme for DS-CDMA systems operating over fast fading channels. Variable switching and mixing parameters are utilised to optimise the contribution towards the adaptation of the filter from each of the considered time instants. An SINR analytical framework is derived and applied to the proposed algorithms to obtain analytical performance curves. The proposed schemes exhibit improved performance and robustness over the existing schemes, and are also able to obtain an interference suppression filter suitable for compounded, highly dynamic relay channels.

- Chapter 6 presents conclusions and the possible future work based on the content of the thesis.

1.4 Notation

Throughout this thesis, bold lower case and upper case letters represent vectors and matrices, respectively, and scalar quantities are represented by standard weight letters. The expectation operator is denoted by $E(\cdot)$ and the trace and main diagonal of a matrix are denoted by trace$(\cdot)$ and diag$(\cdot)$, respectively. The notation $(\cdot)^*$, $(\cdot)^T$ and $(\cdot)^H$ denote the complex conjugate, standard transpose and Hermitian transpose, respectively. The Euclidean norm of a vector and the absolute value of a scalar are expressed as $\|\cdot\|$ and $|\cdot|$, respectively, and the cardinality of a set is given by $\#(\cdot)$. An identity matrix of

dimensionality $M \times M$ is denoted by $\mathbf{I}_M$ and a matrix with dimensions $M \times N$ populated with the scalar x is expressed as $\mathbf{X}_{M \times N}$. Reduced-rank vectors and matrices are given with the addition of a tilde ($\tilde{.}$) and estimated values are denoted by the addition of a hat ($\hat{.}$).

1.5 Publication List

Journal Papers

1. P. Clarke and R. C. de Lamare, "Joint Transmit Diversity Optimization and Relay Selection for Multi-relay Cooperative MIMO Systems Using Discrete Stochastic Algorithms ", *IEEE Communications Letters*, 2011 (accepted and awaiting publication).

2. P. Clarke and R. C. de Lamare, "Low-Complexity Reduced-Rank Linear Interference Suppression Based on Set-Membership Joint Iterative Optimization for DS-CDMA Systems ", *IEEE Transactions on Vehicular Technology*, 2011 (accepted and awaiting publication).

3. P. Clarke and R. C. de Lamare, "Transmit Diversity and Relay Selection Algorithms for Multi-relay Cooperative MIMO Systems ", *IEEE Transactions on Vehicular Technology*, 2011 (under review).

4. P. Clarke and R. C. de Lamare,"Bidirectional Algorithms for Interference Suppression in Fast Fading DS-CDMA Networks", *IEEE Transactions on Vehicular Technology*, 2011 (in preparation).

Conference Papers

1. P. Clarke and R. C. de Lamare, "Adaptive Set-Membership Reduced-Rank Interference Suppression for DS-UWB Systems", *IEEE International Symposium on Wireless Communications Systems*, September 2009.

2. P. Clarke and R. C. de Lamare, “Set-Membership Reduced-Rank Algorithms based on Joint Iterative Optimization of Adaptive Filters”, *43rd IEEE Asilomar Conference on Signals Systems and Computers*, November 2009.

3. R. Fa, R. C. de Lamare and P. Clarke, “Reduced-rank STAP for MIMO Radar Based on Joint Iterative Optimization of Knowledge-Aided Adaptive Filters ”, *43rd IEEE Asilomar Conference on Signals Systems and Computers*, November 2009.

4. P. Clarke and R. C. de Lamare, “Set-Membership Reduced-Rank BEACON Algorithm Based on Joint Iterative Optimization of Adaptive Filters”, *IEEE International Symposium on Circuits and Systems*, September 2009.

5. P. Clarke and R. C. de Lamare, “MMSE Transmit Diversity Selection for Multi-Relay Cooperative MIMO Systems Using Discrete Stochastic Gradient Algorithms”, *17th IEEE International Conference on Digital Signal Processing*, July 2011.

6. P. Clarke and R. C. de Lamare, “Joint MMSE Transmit Diversity Optimization and Relay Selection for Cooperative MIMO Systems Using Discrete Stochastic Algorithms”, *IEEE Online Conference on Green Communications*, September 2011.

7. P. Clarke and R. C. de Lamare, “Joint Iterative Power Allocation and Relay Selection for Cooperative MIMO Systems Using Discrete Stochastic Algorithms”, *IEEE International Symposium on Wireless Communications Systems*, November 2011.

8. P. Clarke and R. C. de Lamare,“Bidirectional MMSE Algorithms for Interference Suppression in DS-CDMA Systems Over Fast Fading Channels”, *IEEE International Conference on Acoustics, Speech, and Signal Processing*, March 2011 (submitted).

Book Chapters

1. R. C. de Lamare and P. Clarke, “Joint Resource Allocation and Interference Mitigation Techniques for Cooperative Wireless Networks”, *Using Cross-Layer Techniques for Communication Systems*, 2011.

Chapter 2

Literature Review

Contents

2.1 Introduction

This chapter presents an introduction to the progression of mobile network technology and the associated techniques and algorithms utilised for resource allocation and interference suppression. Firstly, a summary of the trends in mobile communications is given alongside an introduction to the associated system models, namely DS-CDMA, MIMO and cooperative systems. Following this, an overview and description of the detection and estimation techniques ubiquitous within wireless networks are presented. Finally, interference suppression and resource allocation are introduced along with the widely used optimal and adaptive methods.

2.2 Trends in Mobile Communications Systems

Since the advent of mass market mobile communications at the end of the 20th century, mobile communications have become an integral part of a modern ultra-connected lifestyle. This has led to a rapid increase in system capacity requirements but also to a shift in nature of the data transmitted, from low data-rate speech to bandwidth intensive multimedia content. Consequently, the underlying technology, standards and signal processing of the mobile network infrastructure have had to adapt to the changing requirements placed upon them.

The initial digital second generation networks based on time-division multiple-access (TDMA) and frequency division multiple access (FDMA) were primarily designed for the transmission of speech using a circuit switched network topology. These networks still account for the majority of world-wide mobile subscribers due to the mature status of the technology, ease of roaming and low cost handsets. However, even with the introduction of higher capacity packet switched methods, such as general packet radio service (GPRS) and enhanced data-rates for global system for mobile communications (GSM) evolution (EDGE) these networks were not able to provide the flexibility, data-rates and exponentially increasing capacity required as mobile internet use became increasing popular.

This brought about a shift to the spread spectrum DS-CDMA systems that are currently used in various standards around the world and in existing 3G networks in the UK [1]. Its flexibility, capacity and robustness suited DS-CDMA to mobile networks but has also made it a common choice of transmission method for the burgeoning area of wireless sensor networks (WSN). The benefits of DS-CDMA for mobile communications include robustness in multipath environments, flexible allocation of bandwidth, increased user capacity and reduced interference to co-spectrum users. However, these advantages come at the cost of the increased MUI and ISI, which are inherent to mul-

[1] In this work, the generations of mobile technology are referred to as they are commonly accepted in the UK; however, classification of this nature varies depending on the country and network operator.

tiple access spread spectrum systems where users transmit non-orthogonal signals over a shared channel. Consequently, the demands placed on the signal processing at the receiver and the transmitter have increased. Accordingly, to achieve the theoretical capacities on offer, advanced MUD, antennas techniques and power allocation are required.

The exponential increase in traffic over mobile networks is forecast to continue, therefore a new 4th generation of mobile wireless networks is required to supersede the current standards. Due to their increased diversity, multiplexing and spectral efficiency, MIMO and orthogonal frequency-division multiplexing (OFDM) techniques have been presented as a means to provide the extra capacity and robustness required. Although not yet commercially deployed in the UK [16], MIMO capability has been incorporated in to Third Generation Partnership Project (3GPP) Long term evolution (LTE) standards since release 8 [17]. Increased coverage whilst avoiding extensive and costly investment in new infrastructure is also essential if 4G generation standards are to be widely adopted and the deployment issues of the 3G roll-out avoided. Accordingly, relaying is anticipated to play a vital role in future network protocols due to its ability to increase coverage with low cost fixed or mobile relays, as opposed to conventional base stations. Consequently, relaying and cooperation between base stations and mobile users has been incorporated into 3GPP LTE advanced release 10 [17] and is anticipated to lead to fully cooperative MIMO networks. However, the increased performance brought about by MIMO systems and relaying is accompanied by a substantial increase in the complexity of the processing required at the transmitter, relays and receiver. Consequently, improved signal processing techniques are once again required to minimise the adverse impact that this additional processing has on the mobile user and the complexity of the user equipment.

2.2.1 Spread Spectrum Systems

The defining characteristic of spread spectrum systems is that their transmission bandwidth is significantly larger than the bandwidth of the data signal to be transmitted. As

a result, spread spectrum systems have a significantly broader but lower power spectral density (PSD) compared to equivalent power narrow band systems. This gives spread spectrum systems increased resistance to narrow band jamming, frequency selective fading and rudimentary eavesdropping but also allows it to present its signal as noise to co-system and co-spectrum users. These characteristics made spread spectrum systems ideally suited to military applications and it is this that accounted for their initial usage. More recently its DS-CDMA implementation has been adopted for commercial communications due to its multiuser properties and flexibility [2].

In DS spread spectrum systems, each transmitted data symbol is spread by modulating it with a higher frequency binary sequence made up of N bits or chips. The period of a chip, T_c, is significantly shorter than data symbol, T_s, where, for DS-CDMA with short spreading sequences $T_s/N = T_c$ and N is referred to as the processing or spreading gain. Through the selection of orthogonal or approximately orthogonal spreading codes, multiple access is possible over a shared channel. DS-CDMA in 3rd generation mobile networks operates on this principal and uses orthogonal codes when synchronicity between users signals can be ensured, and pseudo-random (PR) sequences when timing inaccuracies destroy the orthogonality between orthogonal codes. With the addition of chip pulse shaping to enable bandlimiting, the baseband continuous time receive signal in a K user system with a multipath channel can be expressed as

$$r(t) = \sum_{k=1}^{K} \sum_{l=1}^{L} \sum_{i=\infty}^{\infty} A_k b_k[i] h_{k,l} s_k[t - iT_s] + n[t] \tag{2.1}$$

where

$$s_k[t] = \sum_{n=1}^{N} c_k[n] p[t - iT_s - jT_c], \tag{2.2}$$

p is the chip pulse shaping waveform and c_k is the spreading sequence of the k^{th} user. For the k^{th} user, A_k and b_k are the transmit amplitude and symbol stream, respectively; $h_{k,l}$ is the gain of the l^{th} path of the k^{th} user's L path multipath channel and n is the additive white Gaussian noise (AWGN).

By assuming a synchronous system where the channel delay profile is an integer multiple of the chip period, the receive signal for the i^{th} symbol period at the receiver after chip pulse matched filtering can be expressed in the discrete time domain as

$$\mathbf{r}[i] = \sum_{k=1}^{K} A_k[i] b_k[i] \underbrace{\mathbf{H}_k[i]\mathbf{c}_k[i]}_{\mathbf{p}_s[i]} + \boldsymbol{\eta}[i] + \mathbf{n}[i] \tag{2.3}$$

where

$$\mathbf{H}_k[i] = \begin{pmatrix} h_{k,1}[i] & 0 & \dots & 0 \\ h_{k,2}[i] & h_{k,1}[i] & & \\ \vdots & h_{k,2}[i] & & \vdots \\ h_{k,L}[i] & \vdots & \ddots & \\ 0 & h_{k,L}[i] & & \\ & 0 & \ddots & 0 \\ \vdots & & & h_{k,1}[i] \\ & \vdots & \ddots & h_{k,2}[i] \\ & & & \vdots \\ 0 & 0 & \dots & h_{k,L}[i] \end{pmatrix}. \tag{2.4}$$

The ISI generated by the multipath channel is given by $\boldsymbol{\eta}[i]$, $\mathbf{p}_k[i]$ is the $M \times 1$ signature of the k^{th} user, $\mathbf{r}[i]$ is a $M \times 1$ column vector where $M = N + L - 1$ and $\mathbf{n}[i]$ is a vector of AWGN.

2.2.2 MIMO Systems

MIMO communications systems [1, 18–21] potentially offer significant advantages over single-input-single-output (SISO) systems in terms of diversity and multiplexing. The accompanying increases in capacity and robustness to narrowband fading have made them an attractive transmission scheme for high data-rate systems. In contrast to DS-CDMA, separation of channels is achieved through spatial separation of the transmit and receive antennas. However, due to the shared channel and correlation between co-

located antennas, orthogonality between data streams in a MIMO system is possible only with use of the space-time block coding (STBC) or code-division methods covered in Section 2.2.1. In spite of this, MIMO systems share an equivalence with DS-CDMA systems where the multi-antenna separation plays a similar role to the user separation allowed by the spreading sequences. Due to this, the receive signal in MIMO system can be expressed using (2.3) by substituting the signature sequence of the k^{th} user, $\mathbf{p}_k[i]$, for the spatial signature of the m^{th} transmit antenna, $\mathbf{h}_m[i]$. The result is an expression given by

$$\mathbf{r}[i] = \sum_{m=1}^{M} A_m[i] b_m[i] \mathbf{h}_m[i] + \mathbf{n}[i] \tag{2.5}$$

where

$$\mathbf{h}_m[i] = [h_{m,1}[i] \dots h_{m,n}[i]]^T \tag{2.6}$$

and $h_{m,n}$ denotes the complex path gain from the m^{th} transmit antenna to the n^{th} receive antenna. Although partially equivalent to DS-CDMA, MIMO systems are commonly expressed with the summation removed for ease of manipulation and calculation, resulting in

$$\mathbf{r}[i] = \mathbf{H}[i]\mathbf{A}[i]\mathbf{b}[i] + \mathbf{n}[i] \tag{2.7}$$

where

$$\mathbf{H}[i] = \begin{pmatrix} \mathbf{h}_1[i] & \dots & \mathbf{h}_m[i] \end{pmatrix} = \begin{pmatrix} h_{1,1}[i] & \dots & h_{m,1}[i] \\ \vdots & \ddots & \vdots \\ h_{1,n}[i] & \dots & h_{m,n}[i] \end{pmatrix}, \tag{2.8}$$

$\mathbf{A}[i] = \text{diag}[A_1[i] \dots A_M[i]]$ and $\mathbf{b}[i] = [b_1[i] \dots b_M[i]]^T$.

2.2.3 Cooperative Networks

The traditional point-to-point transmission techniques introduced thus far have a number of weaknesses associated with their power requirements, limited number of transmission paths and node cost [22–27]. Cooperative communications are concerned with

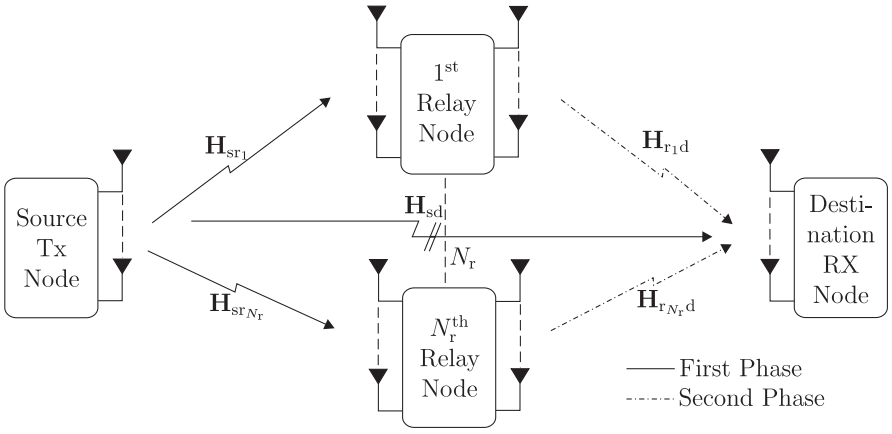

Figure 2.1: Cooperative MIMO system model

addressing these weaknesses and enabling the application of wireless networks to scenarios and environments previously not possible [28–31].

Initial studies on cooperative networks considered single relay implementations where the relay's primary use was to assist the communications of direct path in the presence of AWGN [22, 32]. However, more recently, complex systems with multiple fixed or mobile relays have been the focus of attention due to their flexibility, diversity, low-cost and distributed data sensing potential.

With regard to traditional mobile communications, cooperation is envisaged to form a part of future MIMO based mobile networks in order to provide low-cost coverage extension and capacity enhancement. However, with the advent of multi-relay multiantenna systems, allocation of the finite network resources of time and power has become vital if the optimum performance is to be obtained.

The relaying protocols of AF and DF prevail in cooperative communications due to their simplicity and intuitiveness. The optimum choice of the protocol has been shown to be dependent on respective performance of the first and second phases whereby DF is suited to scenarios where the first transmission is more reliable than the second phase and vice-versa for AF. The system model of a general cooperative two-hop MIMO network with a direct path and half duplex relays is given by Figure 2.1, where there are N_r relays and N_a forward and backwards antennas at each relay.

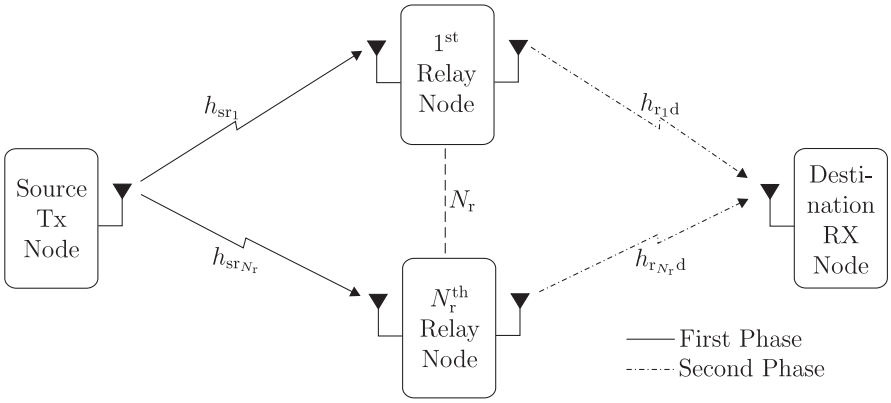

Figure 2.2: Cooperative DS-CDMA system model

Mathematically, the received signals of the first phase at the destination, first phase at the n^{th} relay and the second phase at the destination in a DF system are given by

$$\mathbf{r}_{sd}[i] = \mathbf{H}_{sd}[i]\mathbf{A}_s[i]\mathbf{b}[i] + \mathbf{n}_{sd}[i], \tag{2.9}$$

$$\mathbf{r}_{sr_n}[i] = \mathbf{H}_{sr_n}[i]\mathbf{A}_s[i]\mathbf{b}[i] + \mathbf{n}_{sr_n}[i] \tag{2.10}$$

and

$$\mathbf{r}_{rd}[i] = \sum_{n=1}^{N_r} \mathbf{H}_{r_nd}[i]\mathbf{A}_{r_n}[i]\hat{\mathbf{b}}_{r_n}[i] + \mathbf{n}_{rd}[i], \tag{2.11}$$

where $\hat{\mathbf{b}}_{r_n}$ is the decoded and estimated data at the n^{th} relay, and perfect synchronisation is assumed. For an AF system, $\hat{\mathbf{b}}_{r_n}$ is replaced with the received signal of the first phase, $\mathbf{r}_{sr_n}[i]$.

An alternative cooperative implementation is to use DS-CDMA based transmissions. This allows the benefits of DS-CDMA to be brought to cooperative networks. This has enabled the introduction of cooperative DS-CDMA to mobile networks but also the application of DS-CDMA to multi-hop WSN where low PSD and power consumption are key concerns [29,30,33]. The system model of a cooperative two-hop single antenna DS-CDMA network with single path channels, a negligible direct path and half duplex relays is given by Figure 2.2. The expression for the received signals at the relay and

destination nodes for a K user AF system are given by

$$\mathbf{r}_{\mathrm{sr}_n}[i] = \sum_{k=1}^{K} a_{\mathrm{s}_k}[i] b_k[i] h_{\mathrm{sr}_n}[i] \mathbf{c}_k[i] + \mathbf{n}_{\mathrm{r}_n}[i], \tag{2.12}$$

$$\mathbf{r}_{\mathrm{rd}}[i] = \sum_{n=1}^{N_{\mathrm{r}}} a_{\mathrm{r}_n}[i] h_{\mathrm{r}_n\mathrm{d}}[i] \mathbf{r}_{\mathrm{sr}_n}[i] + \mathbf{n}_{\mathrm{d}}[i] \tag{2.13}$$

and

$$\mathbf{r}_{\mathrm{rd}}[i] = \sum_{n=1}^{N_{\mathrm{r}}} \sum_{k=1}^{K} a_{\mathrm{s}_k}[i] a_{\mathrm{r}_n}[i] h_{\mathrm{sr}_n}[i] h_{\mathrm{r}_n\mathrm{d}}[i] \mathbf{c}_k[i] b_k[i] + \sum_{n=1}^{N_{\mathrm{r}}} a_{\mathrm{r}_n}[i] h_{\mathrm{r}_n\mathrm{d}}[i] \mathbf{n}_{\mathrm{r}_n}[i] + \mathbf{n}_{\mathrm{d}}[i]. \tag{2.14}$$

2.3 Parameter Estimation

Parameter estimation is a fundamental element of signal processing and is an essential tool in the implementation of communication systems. The estimation techniques covered in this thesis can be broadly classified into two families: classical and Bayesian [34–36]. These methods differ in their statistical assumption about input signals, the type of parameter to be estimated and the level of *a priori* knowledge. Accordingly, the resulting set of estimators from each approach have their own individual properties and preferred applications.

2.3.1 Bayesian Estimation

Bayesian methods [34, 35] address estimation problems where there is some level of prior knowledge on the quantity to be estimated and associated probabilistic assumptions can be made. The motivating factor of this methodology is to take advantage of the prior knowledge but also to provide an alternative method of estimation when a minimum variance unbiased estimator cannot be found [34].

In Bayesian estimation, the quantity to be estimated is assumed to be a random variable. This enables prior knowledge to be incorporated into an *a posterior* probability

density function (PDF) and an improved estimate obtained. To obtain such an estimator the definition of the Bayesian MSE is required

$$E[(\boldsymbol{\theta} - \hat{\boldsymbol{\theta}})] = \int \int (\boldsymbol{\theta} - \hat{\boldsymbol{\theta}})^2 p(\mathbf{x}, \boldsymbol{\theta}) d\mathbf{x} d\boldsymbol{\theta} \tag{2.15}$$

where the expectation is taken with respect to $p(\mathbf{x}, \boldsymbol{\theta})$ and $\boldsymbol{\theta}$ is a random variable [34]. To evaluate (2.15), $p(\mathbf{x}, \boldsymbol{\theta})$ is first obtained using Bayes theorem

$$p(\mathbf{x}, \boldsymbol{\theta}) = p(\boldsymbol{\theta}|\mathbf{x}) p(\mathbf{x}). \tag{2.16}$$

The minimiser of (2.15) can then found

$$\hat{\boldsymbol{\theta}} = E(\boldsymbol{\theta}|\mathbf{x}) \tag{2.17}$$

which is the MMSE solution and the mean of the posterior PDF of $\boldsymbol{\theta}$. A related estimator obtains the maximum value of posterior PDF of $\boldsymbol{\theta}$ and is accordingly termed the maximum a posterior (MAP) estimator.

However, in practice the MMSE estimator described above is not easily obtainable. Consequently, in most scenarios Bayesian estimators are limited to being linear and of the form

$$\hat{\boldsymbol{\theta}} = \mathbf{W}^H \mathbf{x} \tag{2.18}$$

where $\boldsymbol{\theta}$ and $\mathbf{x}$ are assumed to be zero mean and the estimation error, $\boldsymbol{\theta} - \hat{\boldsymbol{\theta}}$, is assumed orthogonal to the observation vector, $\mathbf{x}$. However, the linear MMSE filter will not be optimal unless the optimal filter is linear; for example, when the signal model is given by

$$\mathbf{x} = \mathbf{H}\boldsymbol{\theta} + \mathbf{n} \tag{2.19}$$

where $\mathbf{n}$ is AWGN.

The restriction to linear filters conveniently allows (2.15) to be expressed as

$$E||\boldsymbol{\theta} - \hat{\boldsymbol{\theta}}||^2 = E||\boldsymbol{\theta} - \mathbf{W}^H\mathbf{x}||^2. \tag{2.20}$$

To obtain the linear Bayesian MMSE estimator, (2.20) is minimised with respect to $\mathbf{W}^H$, yielding

$$\mathbf{W} = \mathbf{R}^{-1}\mathbf{P} \tag{2.21}$$

where $\mathbf{R} = E[\mathbf{r}\mathbf{r}^H]$, $\mathbf{P} = E[\mathbf{r}\boldsymbol{\theta}^H]$ and the resulting MMSE is $\sigma_{\boldsymbol{\theta}}^2\mathbf{I} - \mathbf{P}^H\mathbf{R}^{-1}\mathbf{P}$ where $\sigma_{\boldsymbol{\theta}}^2$ is the variance of the parameter vector. Thus to obtain the linear Bayesian MMSE estimator, or the Wiener filter as it is otherwise known, as in the problem defined by (2.20) and (2.19), the first two moments of the joint distribution $p(\mathbf{x}, \boldsymbol{\theta})$ are required.

2.3.2 Maximum Likelihood Estimation

Maximum likelihood (ML) estimation is a classical methodology which provides an asymptotically efficient and unbiased estimate via a straightforward but potentially computationally intensive procedure [2, 34, 35]. Fundamentally, ML estimation chooses the parameter(s) that maximises the probability of a chosen PDF distribution resulting in the observed data. However, with an incorrect choice of PDF an unreliable estimate may be obtained.

Mathematically, the maximum likelihood estimator (MLE) for a parameter is given by the value that maximise the likelihood function $p(\mathbf{x}; \boldsymbol{\theta})$. Analytically the parameter value that maximises the likelihood function can then be obtained by finding the stationary points of the probability distribution. For simplicity, in many practical estimators the log of the likelihood function is used, resulting in the following maximisation procedure

$$\boldsymbol{\theta} = \arg\max_{\boldsymbol{\theta}} \ln p(\mathbf{x}; \boldsymbol{\theta}). \tag{2.22}$$

Here it can be seen that the MLE is the limiting instance of the MAP estimator when no

prior knowledge is available. Consequently, it can be thought as a classical analogue to the MAP estimator.

Although simplistic in its approach, it is not always possible to obtain a closed form solution for the MLE and therefore numerical methods involving iterative maximisation and combinatorial searching are often required. This can lead to computationally intensive solutions especially when multiple parameters are to be estimated.

2.3.3 Least Squares Estimation

The LS estimator [34, 35, 37] is deterministic and, although it can converge to the minimum variance unbiased estimator under the correct conditions it cannot be considered optimal, unlike MMSE and ML based estimators. A significant benefit of the method of LS is that only a signal model is assumed and no statistical information or assumptions about the data or noise are necessary. This, along with its intuitiveness, has led to the LS estimator begin widely used. Focussing on linear estimation, the model assumed by the LS method for a unknown vector parameter is of the form

$$\mathbf{x} = \mathbf{H}\boldsymbol{\theta} + \mathbf{n} \tag{2.23}$$

where $\mathbf{n}$ is unknown additive noise. The LS estimator finds the parameter $\boldsymbol{\theta}$ that minimises the squared difference between the observed signal and the reconstructed signal. Mathematically the cost function is expressed as

$$J(\boldsymbol{\theta}) = ||\mathbf{x} - \mathbf{H}\hat{\boldsymbol{\theta}}||^2 \tag{2.24}$$

and when solved, yields

$$\boldsymbol{\theta} = (\mathbf{H}\mathbf{H}^H)^{-1}\mathbf{H}^H\mathbf{x} \tag{2.25}$$

as the LS solution. A solution has been found whilst making no statistical assumptions about the data, making it a highly useful if not optimal estimator. Furthermore, if the

errors represented by **n** are wide-sense stationary (WSS), independent, and normally distributed, the ML and LS estimators are equivalent [34]. Therefore the LS approach provides an alternative approach to establishing the MLE.

2.3.4 Reduced-Rank Techniques

In the traditional signal processing techniques covered up to this point, the adaptive estimation and filtering procedures operate directly on the raw observation signal. However, this leads to a dependency between the performance of a filtering process and the properties of the observed signal, such as eigenvalue spread, dimensionality, and noise and correlation characteristics. This can lead to problems including slow convergence, extended training, high computational complexity, susceptibility to interference, large memory requirements and isolation of the signals of interest. Reduced-rank techniques [12, 13, 38–43] can help alleviate these problems by mapping or projecting the observed signal onto a reduced-rank signal subspace, thus reducing the dimensionality of the signal and extracting features of interest. Ideally, the objective is to perform rank-reduction whilst preserving the signals of interest so that equivalent full-rank performance can be obtained by a subsequent reduced-rank filtering procedure. The advantages of this approach result from the use of reduced dimensionality filters but also the separation of the observation vector into signal and noise subspaces.

The rank-reduction process is performed using a projection matrix that maps the $M\times 1$ full-rank observation vector onto a $D\times 1$ reduced-rank signal subspace. The $M\times D$ projection matrix, $\mathbf{S}_D$, is designed in accordance with a chosen optimisation criterion where the exact nature of the sub-space onto which the full-rank signal is projected is determined by said criterion. This process is depicted in Figure 2.3 where $\tilde{\mathbf{r}}[i]$ is the $D \times 1$ reduced-rank signal vector and the input to reduced-dimensionality adaptive filter $\tilde{\mathbf{w}}[i]$. The main challenges in reduced-rank signal processing are the design of the projection matrix and selection of the rank of the subspace, D.

The earliest methods were inspired by principal components analysis in mathematics

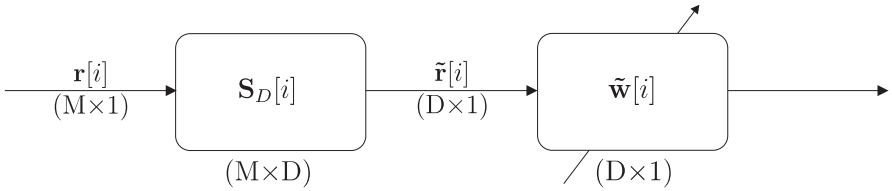

Figure 2.3: Reduced-rank projection matrix

and based upon eigendecomposition of the received signal's autocorrelation matrix [40, 41, 43]. By performing an eigendecomposition given by

$$\mathbf{R} = \mathbf{Q}\Lambda\mathbf{Q}^H = \sum_{i=1}^{M} \lambda_i \mathbf{q}_i \mathbf{q}_i^H, \tag{2.26}$$

where Λ is a diagonal matrix of eigenvalues and $\mathbf{Q} = [\mathbf{q}_1, \mathbf{q}_2, \ldots, \mathbf{q}_M]$ is a matrix formed from the corresponding eigenvectors, the D largest eigenvalues and their corresponding eigenvectors can be chosen and a reduced-rank approximation of the autocorrelation matrix formed [38, 44, 45]. Rearrangement of the eigenvalues of (2.26) into ascending order then allows the basic reduced-rank approximation of the autocorrelation matrix to be formed from the D largest eigenvalues and eigenvectors, yielding

$$\tilde{\mathbf{R}} = \sum_{i=M-D+1}^{M} \lambda_i \mathbf{q}_i \mathbf{q}_i^H. \tag{2.27}$$

However, correct selection of the rank D is required to ensure the majority of the signal of interest is projected on to the reduced-rank signal subspace and that the system is not under-modelled. This is a non-trivial task, especially when the optimum rank scales with system size. This in combination with the computational complexity of eigendecomposition and the fact the reduced-rank processing is not optimised according to a user specified criterion limits the applicability of the PC technique. A natural progression from this was the cross spectral technique. This improved technique selected D eigenvalues based on an auxiliary criterion but the problem of rank selection and eigendecomposition remained [43]. Consequently, subsequent research focussed on low-complexity reduced-rank methods which avoided eigendecomposition and whose

rank did not scale with system size. In 1998 the multi-stage Wiener filter (MSWF) was proposed by Goldstein, Reed and Scharf [42]. Based on a truncated form of a decomposition of the traditional Wiener filter, it had the desirable properties of avoiding eigendecomposition and the rank of its subspace not scaling with system size [41–43]. The MSWF forms the Krylov subspace through D recursions of a projection matrix construction algorithm and then projects the full-rank signal onto it. A form amenable to adaptive implementation is the 'Powers of R' approach which only requires the autocorrelation and cross-correlation matrices of the observation vector [42, 43]. Following this approach the projection matrix that mathematically maps the observation vector on the reduced-rank signal subspace is then formed by

$$\mathbf{S}_{D_k}[i] = \left[\bar{\mathbf{p}}[i],\ \bar{\mathbf{p}}_k[i]\mathbf{R}[i],\ \bar{\mathbf{p}}_k[i]\mathbf{R}^2[i],\ \bar{\mathbf{p}}_k[i]\mathbf{R}^3[i], \cdots, \bar{\mathbf{p}}_k[i]\mathbf{R}^{D-1}[i]\right] \tag{2.28}$$

where

$$\bar{\mathbf{p}}_k[i] = \frac{\mathbf{p}_k[i]}{\|\mathbf{p}_k[i]\|} \tag{2.29}$$

and $\mathbf{R}[i]$ and $\mathbf{p}[i]$ are the autocorrelation matrix and cross-correlation vector, respectively, at the i^{th} time instant. Although described as projection matrix here, it is often referred to as a linear transform or transformation matrix and expressed as $\mathbf{S}_{D_k}[i]\mathbf{S}_{D_k}^H[i]$ from a linear algebra perspective. However, in this work it shall be referred to as a projection matrix from this point onwards.

The MSWF and its equivalence with auxiliary vector filtering (AVF) marked a progression in reduced-rank signal processing but complexity remained an issue [46–48]. The most recent reduced-rank techniques focus upon fully adaptive implementations where the projection matrix is iteratively updated in conjunction with the adaptive structures in the reduced-rank signal subspace. Two methods emerged based on this approach: reduced-rank processing based on JIO of adaptive filters and joint interpolation, decimation and filtering (JIDF) [12, 13, 49, 50]. The advantages offered by these techniques stem from the exchange of information between the rank-reduction process

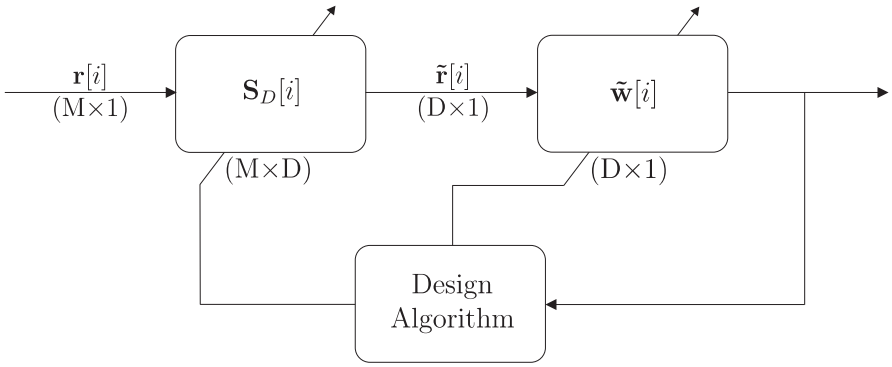

Figure 2.4: Reduced-rank JIO implementation

and the subsequent adaptive filtering but also their ability to be implemented with existing adaptive algorithms such as recursive least-squares (RLS) and LMS. An MMSE implementation of the scheme depicted in Figure 2.4 can be obtained by solving the following optimisation problem

$$[\mathbf{S}_{D_k,\text{opt}}, \tilde{\mathbf{w}}_{k,\text{opt}}[i]] = \underset{\mathbf{S}_{D_k},\tilde{\mathbf{w}}_\mathbf{k}}{\arg\min}\, E[|b_k[i] - \tilde{\mathbf{w}}_k^H[i]\mathbf{S}_{D_k}^H[i]\mathbf{r}[i]|^2]. \tag{2.30}$$

where $b_k[i]$ is the desired output.

2.4 Interference Suppression

Suppression of interference in wireless communications systems is essential if capacity is to be maximised and reliable transmission obtained. Approaches to interference suppression depend upon both the system and the nature of the interference. Consequently, a vast array of research literature has been generated on this topic and continues to be a focus of signal processing research efforts with books including Verdu [2] providing a unified treatment of the theory and established techniques. When considering the systems covered in this thesis, achieving robustness against multiuser, multistream and multipath interference are the most significant challenges.

In this section, the focus is on interference suppression in DS-CDMA systems. However, in a similar manner to the mathematical equivalence between DS-CDMA and

MIMO systems, the interference between antennas in a MIMO system can be likened to the MUI in DS-CDMA systems. Consequently, the methods given in this section are equally applicable to MIMO systems although their notation and naming in the literature may differ.

MUD addresses the need to suppress the multiuser interference created by co-system signals which share the same physical channel. Considering the output of the matched filter of user 1, the signal of interest and interference can be expressed as

$$\mathbf{r}[i] = A_1[i]b_1[i]\mathbf{H}_1[i]\mathbf{c}_1[i] + \underbrace{\sum_{k=2}^{K} A_k[i]b_k[i]\mathbf{H}_k[i]\mathbf{c}_k[i]}_{\text{MUI}} + \boldsymbol{\eta}[i] + \mathbf{n}[i]. \tag{2.31}$$

Improvements are sought by actively taking into account the interfering users' signals when performing detection and estimation. This is in contrast to single user detection which bases detection and estimation of a user's signal solely upon the characteristics of their desired signal [2, 51]. In DS-CDMA networks it can appear that MUD is a trivial or potentially unnecessary task due to orthogonal spreading codes. However, this requires synchronous operation and therefore places heavy demands on the users and timing within the system. Restricting DS-CDMA networks to orthogonal codes can also deprive them of a number of advantages, such as the ability to tradeoff capacity against performance in order to obtain a dynamic system that is able to adapt to the time-varying demands placed on it [2]. Additionally, even with asynchronous transmission it is possible to maintain quasi-orthogonality with correctly designed non-orthogonal signature sequences; therefore mitigating an element of the MUI. During the infancy of DS-CDMA communications, the single user matched filter that treated multiple-access-interference (MAI) as AWGN was thought to be the optimal reception technique. However, the study of MUD established that this is not the case if information on the interfering users is known. Single user detection was the dominant method when wireless communications were in their infancy prior to 1980s but the advent of advanced multiple-access schemes brought about the need for more sophisticated schemes

which did not simply treat multiple access interference as AWGN [2, 52].

2.4.1 Maximum Likelihood Detection

Optimum MUD is based upon ML detection and estimation of all MAI such that the likelihood or log-likelihood function is maximised. This results in a solution that obtains the symbols that are most likely to have resulted in the observed signal. This is also equivalent to the solution that results in minimum noise energy [2]. To obtain optimal MUD performance, the receiver requires knowledge of the system spreading sequences, user timing information, user receive amplitudes and noise power. When this information is known, the likelihood function is equivalent to the minimisation of the Euclidean distance, and is given by

$$\begin{aligned}\left[\hat{b}_1[i]\dots\hat{b}_K[i]\right] &= \underset{b_1[i]\dots b_K[i]}{\arg\max}\; p(\mathbf{r}[i]; b_1[i]\dots b_K[i]) \\ &= \underset{b_1[i]\dots b_K[i]}{\arg\min} \left\| \mathbf{r}[i] - \sum_{k=1}^{K} A_k[i] b_k[i] \mathbf{H}_k[i] \mathbf{c}_k[i] \right\|^2 .\end{aligned} \tag{2.32}$$

The solution to (2.32) can be found through analysis of all combinations of the user symbols $b_k[i]$. However, this is a prohibitively complex task for practical implementation due to the exponential relationship between the number of users and possible solutions. Specifically, there are $(O_M)^K$ possible solutions to (2.32) where O_M is the order of the modulation scheme. To alleviate this complexity, ML based schemes that operate over a reduced set of solution have been developed [53, 54]. These schemes attempt to place a constraint on the solution set in order to restrict searching to the candidates that are most likely to yield the ML solution. Sphere decoding is the most prominent member of this family of schemes and places a sphere with a predefined radius onto a lattice of potential solution so only candidates that fall within the sphere are considered for ML detection [53].

2.4.2 Linear Detection Techniques

Sub-optimal techniques such as sphere decoding go someway to reducing the computation burden of ML MUD but their complexity still substantially exceeds that of linear methods [53]. Furthermore, obtaining the required information on each user's signal is not always practical or possible. Consequently, investigation into linear detection methods that occupy the middle ground between optimality and complexity, and require only the decoding of the desired user have been a common focus of MUD research. As previously noted, linear correlating receivers are optimal for single user detection. However, their effectiveness declines when multiple users are present and they also fail to fully exploit data on interfering users. Accordingly, in the presence of MAI alternative linear methods are of more use.

MMSE Linear Detection

In contrast to the ML method given by (2.32), the MMSE MUD problem can be cast as a linear estimation problem where a finite impulse response (FIR) filter is used to minimise the MSE between the estimated data of the user of interest and the transmitted data, $E[b_k[i] - \hat{b}_k[i]]$. The relevant optimisation expression is given by

$$\mathbf{w}_{k,\text{opt}}[i] = \arg\min_{\mathbf{w}_k} E\left\|b_k[i] - \mathbf{w}_k^H[i]\mathbf{r}[i]\right\|^2. \tag{2.33}$$

By taking the gradient with respect to the complex vector $\mathbf{w}_k[i]$ and equating to zero, an expression for the optimum linear MMSE MUD filter can be formed

$$\mathbf{w}_{k,\text{opt}}[i] = \left(\sum_{n=1}^{K} \frac{A_n^2[i]}{A_k^2[i]}\mathbf{H}_k[i]\mathbf{c}_k[i]\mathbf{c}_k^H[i]\mathbf{H}_k^H[i] + \frac{\sigma^2}{A_k^2[i]}\mathbf{I}\right)^{-1} \mathbf{H}_k[i]\mathbf{c}_k[i]. \tag{2.34}$$

A linear estimate of the desired symbol can then be computed

$$z_k[i] = \mathbf{w}_{k,\text{opt}}^H[i]\mathbf{r}[i] \tag{2.35}$$

and processed by a detector given by

$$\hat{b}_k[i] = Q(z_k[i]), \tag{2.36}$$

where Q is a slicer dependent on the constellation scheme of the system.

Although the computational complexity advantages brought about by linear MMSE approaches are significant with respect to ML based schemes, a matrix inversion of cubic complexity is still required. Furthermore, the accurate determination of cross-correlations, channel coefficients, users' signal-to-noise-ratio (SNR) and spreading sequences may not always be possible in a time-varying environment.

Least Squares-Based Linear Detector

As with parameter estimation, an alternative deterministic approach based on the LS optimisation criterion can be used to derive an interference suppression filter. This removes the need for statistical assumptions about the input data but instead introduces a dependency on the number of data samples used in the calculation of the LS solution. Firstly, an estimation error based cost function is formed that utilises all data up to and including the i^{th} time instant and has an exponential forgetting factor, λ, to weight more recent samples more heavily.

$$J[i] = \sum_{i}^{l=1} \lambda^{i-l} \left\| b_k[l] - \mathbf{w}_k^H[l]\mathbf{r}[l] \right\|^2 = \|e_k[l]\|^2 . \tag{2.37}$$

Via the standard LS derivation [38], the resulting solution is given by

$$\mathbf{w}_k[i] = \mathbf{R}^{-1}[i]\mathbf{p}[i]. \tag{2.38}$$

where

$$\mathbf{R}[i] = \sum_{l=1}^{i} \lambda^{i-l}\mathbf{r}[l]\mathbf{r}^H[l] \tag{2.39}$$

and

$$\mathbf{p}[i] = \sum_{l=1}^{i} \lambda^{i-l} b_k^H[l]\mathbf{r}[l]. \tag{2.40}$$

Symbol estimation is then performed as for the linear MMSE detector given by (2.35)-(2.36).

2.4.3 Adaptive Linear Interference Suppression

To simplify the MMSE and LS interference suppression processes and remove the need for system knowledge, adaptive linear techniques can be used. These simply require an initial training sequence after which they switch to decision directed operation. However, if there are abrupt changes in the system channels or user power an additional training sequence may be required.

Least Mean-Square Algorithm

As with the optimal MMSE approach, the following optimisation function is utilised (2.33)

$$J[i] = E\left|b_k[i] - \mathbf{w}_k^H[i]\mathbf{r}[i]\right|^2 = E\left|e_k[i]\right|^2. \tag{2.41}$$

The LMS is then derived by placing (2.41) into a steepest descent framework as given by

$$\mathbf{w}_k[i+1] = \mathbf{w}_k[i] - \mu\nabla J[i]. \tag{2.42}$$

To avoid the use of a deterministic gradient an instantaneous gradient estimate is taken with respect to the linear filter

$$\underset{\mathbf{w}_k^H[i]}{\nabla} J[i] = -\mathbf{r}[i]\underbrace{\left(b_k[i] - \mathbf{w}_k^H[i]\mathbf{r}[i]\right)^H}_{e_k[i]}. \tag{2.43}$$

This gradient estimate can then be placed into (2.42) to form a SG algorithm

$$\mathbf{w}_k[i+1] = \mathbf{w}_k[i] - \mu\mathbf{r}[i]e_k^*[i]. \tag{2.44}$$

The LMS algorithm presented above was first proposed in 1960 [55,56]. Since its invention, its behavioural and convergence properties have been thoroughly investigated and established. This coupled with its low complexity has led to the LMS being adopted in a wide-variety of estimation and signal processing applications. Although widely used, the low complexity of the LMS is accompanied by a slow rate of convergence compared to other adaptive filtering algorithms due to its stochastic nature and discarding of past data [34, 38]. Consequently, other methods achieve faster convergence at the expense of increased complexity.

Recursive Least Squares Algorithm

The RLS utilises the entire data record from the point in time the algorithm commenced and therefore achieves a rate of convergence that is typically an order of magnitude faster than the LMS. However, this is at the cost of increased complexity and memory requirements [34, 38]. To perform the algorithms's derivation a solution to the weighted LS cost function (2.37) is first obtained from the recursive forms of (2.39) and (2.40) given by

$$\mathbf{R}[i] = \lambda \mathbf{R}[i-1] + \lambda^{i-l}\mathbf{r}[l]\mathbf{r}^{H}[l] \tag{2.45}$$

and

$$\mathbf{p}[i] = \lambda \mathbf{p}[i-1] + \lambda^{i-l}b_k^*[l]\mathbf{r}[l][l]. \tag{2.46}$$

Although in a recursive form, the solution given by (2.38), (2.45) and (2.46) involves a computationally intensive matrix inversion. To address this the RLS algorithm utilises the matrix inversion lemma, or Woodbury identity as it is also commonly known, to avoid the matrix inversion. The identity is given by

$$(\mathbf{A}+\mathbf{BDC})^{-1} = \mathbf{A}^{-1} - \mathbf{A}^{-1}\mathbf{B}(\mathbf{C}^{-1}+\mathbf{DA}^{-1}\mathbf{B})\mathbf{DA}^{-1}. \tag{2.47}$$

By equating (2.45) to the matrix inversion lemma and performing some algebraic ma-

nipulation, the recursive equations for the RLS algorithm can be reached. The full RLS algorithm is given by (2.48) to (2.51), where λ is an exponential forgetting factor close to unity used to decrease the weighting of past data.

$$\mathbf{k}[i] = \frac{\lambda^{-1}\mathbf{P}[i-1]\mathbf{r}[i]}{1+\lambda^{-1}\mathbf{r}^H[i]\mathbf{P}[i-1]\mathbf{r}[i]} \tag{2.48}$$

$$e_k[i] = b_k[i] - \mathbf{w}_k^H[i-1]\mathbf{r}[i] \tag{2.49}$$

$$\mathbf{w}_k[i] = \mathbf{w}[i-1] + \mathbf{k}[i]e_k^H[i] \tag{2.50}$$

$$\mathbf{P}[i] = \lambda^{-1}\mathbf{P}[i-1] - \lambda^{-1}\mathbf{k}[i]\mathbf{r}^H[i]\mathbf{P}[i-1] \tag{2.51}$$

Conjugate Gradient Algorithm

The motivation behind the formation of the CG method was to improve upon the convergence speed of the steepest descent method whilst avoiding the complex matrix inversion required for the conventional LS solution [57]. Although designed for quadratic problems of the form

$$\frac{1}{2}\mathbf{w}^H\mathbf{R}\mathbf{w} - \mathbf{p}^H\mathbf{w}, \tag{2.52}$$

the unique minimiser is also the solution to the more common problem formation

$$\mathbf{R}\mathbf{w} = \mathbf{p} \tag{2.53}$$

and can also be extended to non-quadratic problems.

The CG method is based upon the principal of R-orthogonality or conjugacy between a set of vectors, $\mathbf{d}_{1\ldots l}$, where they are defined as R-orthogonal, and therefore linearly independent, if $\mathbf{d}_l^H\mathbf{R}\mathbf{d}_j = 0$ for all $l \neq j$ [57]. These linearly independent vectors can then be used to expand the solution such that it can be obtained by the evaluation of a number of low complexity products.

The implementation of the conjugate gradient method in an iterative fashion leads

to the conjugate gradient algorithm. At each time instant a finite number of iterations, J, are performed and a succession of direction vectors, d_j, which are orthogonal to d_{j-1}, are generated from a combination of past direction vectors and optimisation function gradient [58]. Consequently, no matrix inversion is required and the method rapidly proceeds to the solution. Firstly in the derivation, the gradient and direction vectors for the k^{th} user require initialisation

$$\mathbf{g}_{k,0}[i] = \nabla_{\mathbf{w}_k[i]} J_k[i] = \mathbf{R}[i]\mathbf{w}_{k,0}[i] - \mathbf{p}_k[i], \mathbf{d}_{k,0}[i] = -\mathbf{g}_{k,0}[i] \tag{2.54}$$

The algorithm commences at each iteration with a steepest descent style filter update

$$\mathbf{w}_{k,j+1}[i] = \mathbf{w}_{k,j}[i] + \alpha_{k,j}[i]\mathbf{d}_{k,j}[i] \tag{2.55}$$

where

$$\alpha_{k,j}[i] = \frac{\mathbf{g}^H_{k,j}[i]\mathbf{d}_{k,j}[i]}{\mathbf{d}^H_{k,j}[i]\mathbf{R}[i]\mathbf{d}_{k,j}[i]}. \tag{2.56}$$

and is found by the minimisation of $J(\mathbf{w}_{k,j}[i])$ with respect to $\alpha_{k,j}[i]$. The direction vector is then updated for the next iteration

$$\mathbf{d}^H_{k,j+1}[i] = -\mathbf{g}^H_{k,j+1}[i] + \beta_{k,j}[i]\mathbf{d}^H_{k,j}[i] \tag{2.57}$$

where

$$\beta_{k,j}[i] = \frac{\mathbf{g}^H_{k,j+1}[i]\mathbf{R}[i]\mathbf{d}^H_{k,j}[i]}{\mathbf{d}^H_{k,j}[i]\mathbf{R}[i]\mathbf{d}_{k,j}[i]}. \tag{2.58}$$

The number of iterations, J, can either be predetermined or the algorithm terminated when a desired error residual level is achieved.

2.4.4 Non-Linear Detection Techniques

Non-linear suboptimal MUD offers significant performance advantages over linear methods whilst maintaining a complexity significantly below that of optimal techniques [2].

Subtractive interference cancellation is a popular decision driven subset that operate on the principal of MAI estimation and subtraction. Such methods are often implemented in multiple stages where each stage removes a proportion of the interference created by one of the interfering users [51]. However, their effective operation is reliant on reliable knowledge or each user's receive power, spreading code and channel. Consequently, their use is often limited to base stations where power constraints and spreading sequence estimation are of less of a concern. Although subtractive interference suppression is non-linear, its constituent estimation procedures can be linear and methods such as the decorrelating, MMSE or LS are commonly used. In the following examples, MMSE based estimation is utilised to illustrate the operation of the subtractive schemes.

Successive Interference Cancellation

Successive interference cancellation (SIC) is the most popular of the subtractive methods and is suited to scenarios where a large power differential exists between users' signals. It operates in a serial fashion where at each successive stage a user's transmitted data is estimated and their receive signal recreated. This signal is then subtracted from the total receive signal in an effort to remove their MAI contribution and increase the SINR ratio of subsequently decoded users [59, 60]. The modified receive signal for the n^{th} stage of SIC is given by

$$\mathbf{r}_n[i] = r[i] - \sum_{k=1}^{n-1} A_k[i]\hat{b}_k[i]\mathbf{H}_k[i]\mathbf{c}_k[i] \tag{2.59}$$

where $\hat{b}_k[i]$ is the estimated user data given by

$$\hat{b}_n[i] = \text{sgn}[\mathbf{w}_n^H[i]\mathbf{r}_n[i]], \tag{2.60}$$

$\mathbf{w}_n[i] = \mathbf{R}_n^{-1}[i]\mathbf{p}_n[i]$, $\mathbf{R}_n[i] = E[r_n[i]r_n[i]]$ and $\mathbf{p}_n[i] = E[r_n[i]b_n^*[i]]$ when linear MMSE estimation and binary phase shift keying (BPSK) modulation is used. The performance of SIC can be improved by optimising the order of decoding in terms of received signal

strength. Decoding and subtracting the user's signal with the highest power will achieve the largest reduction in MAI and schemes that do this are termed ordered SICs.

Parallel Interference Cancellation

Parallel interference cancellation is a concurrent form of subtractive interference suppression which is suited to scenarios where users have approximately equal receive power [2, 60]. PIC attempts to subtract all MAI for each user by detecting and estimating each user's signal in parallel. Conventional detection for all users is performed on the received signal to provide the estimates necessary for the reconstruction of the MAI. A second stage of conventional estimation then takes place on the MAI compensated received signal for each user and a set of improved estimates obtained. PIC can also be extended to multiple stages where the improved set of estimates from the previous stage is used to recreate the MAI for each user. In turn a further improved set of symbol estimates is achieved. The interference suppression operation for the k^{th} user at the n^{th} stage can expressed as

$$\mathbf{r}_n[i] = \mathbf{r}[i] - \sum_{k=1,k\neq n}^{K} A_k[i]\hat{b}_{k,n}[i]\mathbf{H}_k[i]\mathbf{c}_k[i]. \tag{2.61}$$

Subtractive interference suppression can alleviate MAI and reduce the limits it places on capacity and performance of DS-CDMA systems. However, effective operation is heavily reliant on accurate estimation of the interfering users' signals and their transmit symbols. If an incorrect symbol estimate is utilised in the cancellation procedure this has the effect of quadrupling the interfering power of that user. Consequently, reliable estimation of the interfering symbols is essential if improved performance compared to convention detection is to be obtained [51, 61].

2.5 Resource Allocation

Allocation of the finite resources in communications networks is a vital task if capacity, robustness and efficiency are to be maximised. The advances in wireless networks and the system complexity that accompanies this has led to an increase in the need for cross-layer optimisation and accurate allocation of transmit power, spectrum, transmit time and rate, and antennas, among others [62]. The selection of the optimisation criteria is of central importance and is heavily dependent on the system application and the nature of the transmitted data. Common criteria include capacity, quality of service, MUI and power consumption. The method of implementation is also a key consideration when performing resource allocation and is linked to the topology and operation of the considered system. Closed-loop and open-loop individual, distributed and centralised techniques and constraints are the most prevalent with the characteristics of each formed from a trade-off between performance, complexity and communications requirements. A requirement for the implementation of centralised open-loop schemes is a feedback channel. The higher the capacity of the feedback channel the better performance obtained due to reduced quantisation distortion and higher update rates. However, the addition of a feedback channel causes a reduction in system capacity.

In DS-CDMA one of the most critical roles of resource allocation is power control to ensure the near-far problem is avoided [2]. DS-CDMA systems are particulary susceptible due to the shared physical channel and the simultaneous transmission over it. Specifically, it occurs when the difference in receive power between two users in a single cell is so great that decoding of the weaker signal is not possible. Although such a problem can be overcome once sampling has taken place using subtractive interference cancellation, this relies upon the physical limits of the analogue-to-digital converter (ADC) to ensure the weaker signal is effectively sampled. Consequently, power allocation in DS-CDMA is vital; a fact that is reflected in the frequency and resolution of DS-CDMA power update schemes compared to GSM whose TDMA/FDMA access schemes lessen the effect of the near-far problem. An example power allocation optimisation problem

for a DS-CDMA system with a centralised power constraint is given by

$$\begin{aligned}[A_1[i]\cdots A_K[i]] &= \underset{A_1[i]\cdots A_K[i]}{\arg\min}\ E\left[|b_k[i]-\mathbf{w}_k^H[i]\mathbf{r}[i]|\right] \\ \text{subject to} &\sum_{k=1}^{K}|A_k|^2 = p\end{aligned} \tag{2.62}$$

where $\mathbf{r}[i]$ is given by (2.3), p is a system transmit power constraint and $\mathbf{w}_k[i]$ is an interference suppression filter for the k^{th} user [63]. This yields the MMSE solution for the k^{th} user

$$A_k[i] = R_{A_k}^{-1}[i]p_{A_k}[i] \tag{2.63}$$

where $R_k[i] = E\left[\mathbf{c}_k^H[i]\mathbf{H}_k[i]b_k^*[i]\mathbf{w}_k[i]\mathbf{w}_k^H[i]b_k[i]\mathbf{H}_k[i]\mathbf{c}_k[i]\right]$ and $p_k[i] = E\left[\mathbf{c}_k^H[i]\mathbf{H}_k[i]b_k^*[i]\mathbf{w}_k[i]b_k[i]\right]$. Extending resource allocation to cooperative networks is essential if their full potential is to be realised. However, the additional challenges of providing feedback over multihop cooperative networks complicates the task. The issue is further complicated by the need to achieve a balance between relay battery life, spatial diversity, spatial multiplexing, and feedback requirements. Established methods such as the water filling algorithm can require global channel knowledge and a high number of feedback bits, both of which require significant system resources to implement. Consequently, distributed and minimal feedback schemes are a significant focus of research.

Chapter 3

Set-Membership Reduced-Rank Joint Iterative Algorithms for DS-CDMA Systems

Contents

3.1 Introduction

Reduced-rank signal processing has been promoted in the last decade as a viable and attractive solution to a range of applications where the number of elements in adaptive fil-

ters have become prohibitively high [13,39,41,42,44,45,47,49,50,64–71]. Due to their performance in the presence of MUI, narrow band interference and fading channels, a resurgence of interest has also occurred in spread-spectrum systems such as DS-CDMA and ultra-wide-band (UWB). A key feature of these systems is their use of extended spreading codes which act to suppress multiuser and intercell inference. However, due to the problem of chip synchronisation in the uplink of DS-CDMA systems, the use of orthogonal codes to suppress MUI is restricted to the downlink. Consequently, in the uplink pseudo-random (PR) codes are utilised to randomise each user's signal to co-system and co-spectrum users, however this leads to increased multiuser interference compared to the downlink. Therefore interference suppression techniques are required. Linear and non-linear approaches including direct equalisation, SIC and decision feedback have been proposed as interference suppression and reception techniques for DS-CDMA systems with short spreading sequences [61, 72, 73]. However, the significant dimensionality of the structures necessary for both linear and non-linear reception and interference suppression of these spread signals result in a trade-off between complexity, convergence, training sequence length and tracking performance [38], whether implemented optimally or iteratively. These factors also impact upon the power consumption and robustness of a system, both of which are critical in mobile systems and wireless sensor networks.

Reduced-rank signal processing offers an alternative to conventional interference suppression techniques and has the ability to combat a number of the aforementioned drawbacks. By introducing a layer of preliminary signal processing that reduces the dimensionality of the input signal, smaller receive and interference suppression filters can be used. However, this extra layer of processing comes at a cost of increased complexity and consequently there is a quest for low-complexity reduced-rank methods. In communications theory, reduced-rank techniques originated from eigendecomposition of the received signal's autocorrelation matrix. Following decomposition, the largest eigenvalues and corresponding eigenvectors are then selected to form the reduced-rank signal

subspace and the dimensionality/rank reducing projection matrix which transforms the full-rank signal [13]. The PC and cross-spectral metric are two early techniques based on singular value decomposition (SVD) of an estimate of the autocorrelation matrix. These schemes operate via optimisation functions based on the optimum reduced-rank representation and a secondary error criterion [40,43], respectively. However, the inherent complexity of SVD fuelled the search for alternative reduced-rank methods. This led to the emergence of two approaches: the MSWF [41–43] and the AVF [46,47]. Both of these techniques possess the desirable characteristic of the subspace rank or number of auxiliary vectors not scaling with full-rank system dimensionality. However, complexity remained a major issue. The most recent method, reduced-rank signal processing based on JIO of adaptive filters, combats the issue of complexity by interpreting the projection or transformation matrix as a bank of adaptive filters. These filters are then jointly adapted with the reduced-rank filter in order to arrive at an effective projection matrix and interference suppression filter [12]. The majority of existing reduced-rank algorithms for communications perform the dimensionality-reduction process and interference suppression as independent tasks and use a conventional algorithm such as the LMS only to perform the adaptation of the reduced-rank interference suppression filter. In contrast, JIO uses conventional algorithms to adapt both structures and introduces an exchange of information between the two processes; a combination which results in performance benefits. However, this method has a complexity that still exceeds that of the full-rank LMS by up to an order of magnitude[1]. Consequently, the formulation of a technique to reduce this complexity is of great interest and central to this chapter.

SM techniques are a low-complexity approach to established adaptive filtering and have been applied to linear receivers in DS-CDMA and channel estimation with promising results [10, 11, 74]. Consequently, the combination of these and reduced-rank techniques for DS-CDMA interference suppression form an attractive proposition which has the potential to achieve the gains of reduced-rank signal processing without the associ-

[1] Depending upon the rank of the scheme

ated complexity.

The basis of SM filtering lies in set theory and the generation of a set of solutions to a bounded optimisation problem as opposed to a single solution [10]. First proposed for systems where a bound could be placed on the noise variance, it was later reformulated for a bounded error specification which allowed it to be applied to channel equalisation and interference suppression [10]. Two predominant error bounded SM implementations exist; the normalised LMS (NLMS) and RLS algorithms. The latter of which is in fact rooted in optimal bounding ellipsoids (OBE) techniques but conveniently lends itself to a LS interpretation [9]. Performance and complexity improvements over conventional adaptive methods result from SM filtering because an 'optimised' step-size is utilised and an element of the redundancy in the adaptation process eliminated. This redundancy removal stems from the definition of a bounded set of valid estimates as opposed to a point estimate at each time instant such that it is possible that a previous solution to the optimisation problem lies within the current set of solutions. Thus removing the need to update the solution (filter coefficients) whilst not sacrificing performance. Further improvements in performance and complexity can be obtained by implementing a variable error bound which adapts the solution sets to suit the environment and assists in preventing over and under bounding [74, 75] of the solution set. However, compared to the complexity savings brought about by the removal of redundancy, the improvements in convergence brought about by SM techniques are less significant and the overriding limiting factor remains the length of the filter. This shortfall of SM techniques can be addressed by introducing reduced-rank methods to alter the dimensionality of the signals under consideration. Consequently, investigation into a combination of SM and reduced-rank schemes has the potential to bear significant advances in low-complexity reduced-rank interference suppression.

This chapter proposes the integration of SM filtering with the JIO reduced-rank method for linear MUI suppression in DS-CDMA systems. A framework for the integration is set out and the unique properties of JIO which allow SM techniques to be ele-

gantly applied to reduced-rank methods, where previously not possible, are highlighted. The generation of sets of solutions from which the reduced-rank subspace and filter are chosen allow the selective updating capabilities and step-size optimisation of SM schemes to be applied to the adaptation of these structures. This gives the JIO reduced-rank procedure an added element of adaptivity which enables it to operate more reliably but also improves its convergence and steady state performance. The overall result is a sparsely updating implementation of the JIO whose complexity and performance can be controlled by manipulating the SM error bound and hence the bounded set of solutions. This makes the schemes especially suited to mobile communications and WSN where battery life is a major consideration and demands on the system are dynamic [76]. The derivation and implementation of two SM reduced-rank algorithms based on the SM-NLMS and Bounding Ellipsoid Adaptive Constrained Least Squares (BEACON) algorithms are presented. Analysis which unifies and extends that currently available is then given for their stability, convergence properties and steady-state error performance. In addition to this, a novel automatic SM rank-selection algorithm is presented along with a variable error bound implementation where the error bound is determined adaptively in order to arrive at an optimised bound, prevent over and under-bounding, and address the problem of bound selection when limited system knowledge is available. The performance of the proposed algorithms is evaluated and compared against existing methods for interference suppression in the uplink of a DS-CDMA system [2, 76].

This chapter is organised as follows: Section 3.2 introduces the system model and the linear reception of DS-CDMA signals, and Section 3.3 gives the integration of SM filtering with JIO of adaptive filters and the formulation of a JIO-SM framework. Section 3.4 derives and presents two algorithms based on the MMSE and LS error criteria. This is followed by an analysis of their complexity, automatic rank-selection and adaptive error bound variants of the proposed algorithms. Section 3.5 presents the stability and MSE analysis of the proposed algorithms along with limitations of the analysis resulting from the complex interdependent relationship between the adaptive structures

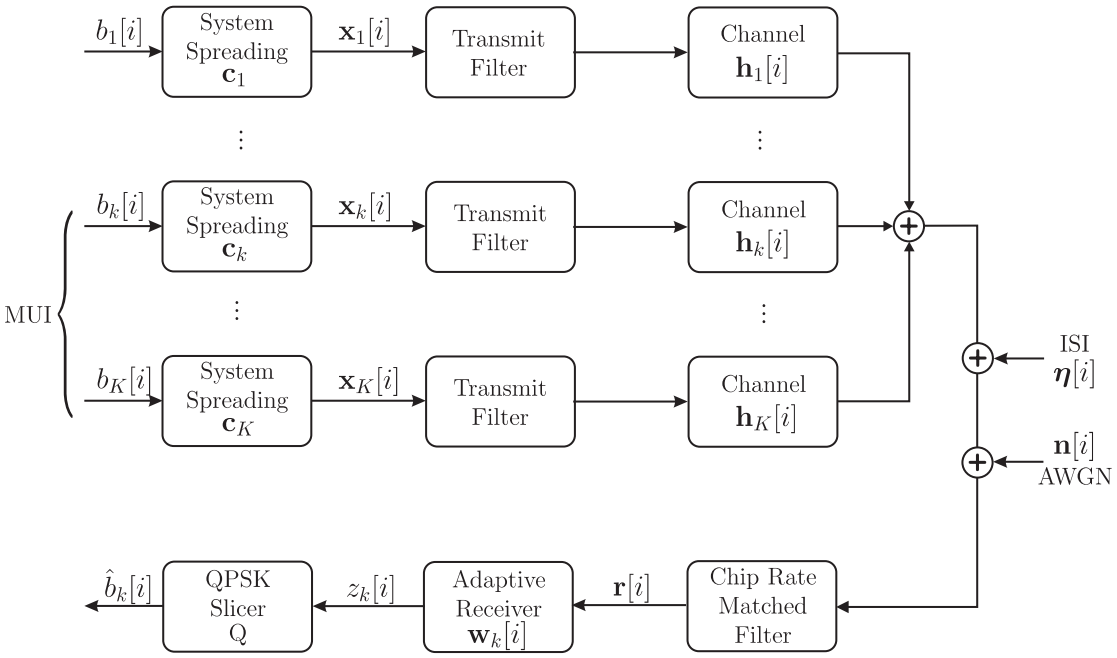

Figure 3.1: DS-CDMA uplink system model.

of the schemes. This is followed in Section 3.6 by the application and simulation of the proposed and existing algorithms to the DS-CDMA system and evaluation of their performance. Finally, Section 3.7 gives the conclusions.

3.2 DS-CDMA System Model and Linear Receivers

In this chapter, a discrete time model of the uplink of a symbol synchronous UMTS DS-CDMA system with short spreading sequences, K users and N chips per symbol is considered. This system is illustrated in Figure 3.1 [77]. The system has a chip rate of 3.84Mchips/s, an assumed bandwidth of 5MHz and uses quadrature phase shift keying modulation (QPSK). The multipath channel of each user is modelled in accordance with the UMTS Vehicular A channel model [78] and each path delay is assumed to be a multiple of the chip rate. For every user in the uplink an independent L path time-varying channel is generated. Each user's channel realisation is assumed to be constant over each symbol period and to have a maximum delay spread of $T_{D_{max}} = (L-1)T_c$

where $T_c = \frac{1}{3.84\times10^6}s$ is the chip duration. The channel for user k is given by

$$\begin{aligned}\mathbf{h}_k[i] &= [h_{k,1}[i]\ h_{k,2}[i]\ \cdots\ h_{k,L}[i]] \\ &= [\alpha_{k,1}[i]p_{k,1}\ \alpha_{k,2}[i]p_{k,2}\ \cdots\ \alpha_{k,L}[i]p_{k,L}]\end{aligned} \tag{3.1}$$

where $\mathbf{p}_k = [p_{k,1}\ p_{k,2}\ \cdots\ p_{k,L}]$ is the average power profile of the channel and $\alpha_k[i] = [\alpha_{k,1}[i]\ \alpha_{k,2}[i]\ \cdots\ \alpha_{k,L}[i]]$ are independent Rayleigh distributed intersymbol complex fading coefficients generated in accordance with Clarke's model where 20 scatterers are assumed. These complex coefficients include the Doppler effect where the Doppler shift and symbol period are denoted by f_d and $T_s = NT_c$, respectively [79] and are specified for each simulation.

Short PR spreading codes which maintain cyclostationarity are repeated from symbol to symbol and allow conventional adaptive techniques to be utilised. The use of long codes eliminates the cyclostationarity required for the use of standard adaptive direct detection techniques and alternative channel estimation based methods are required [80, 81]. However, the investigation into MUD and equalisation in long code DS-CDMA is beyond the scope of this work. The M-dimensional received signal $\mathbf{r}[i]$ at the base station after chip-pulse matched filtering and sampling at the chip rate is given by

$$\mathbf{r}[i] = A_1 b_1[i]\mathbf{H}_1[i]\mathbf{c}_1[i] + \underbrace{\sum_{k=2}^{K} A_k b_k[i]\mathbf{H}_k[i]\mathbf{c}_k[i]}_{\text{MUI}} + \boldsymbol{\eta}[i] + \mathbf{n}[i], \tag{3.2}$$

where $M = N+L-1$ and $\mathbf{n}[i] = [n_1[i]\ \ldots\ n_M[i]]^T$ is the complex Gaussian noise vector with zero mean and autocorrelation matrix $E\left[\mathbf{n}[i]\mathbf{n}^H[i]\right] = \sigma_n^2\mathbf{I}$. The notation $E[\cdot]$ stands for expected value and the k^{th} user's symbol is $b_k[i]$ and assumed to have been drawn from a general QPSK constellation normalised to unit power. The amplitude of user k is A_k and $\boldsymbol{\eta}[i]$ is the ISI vector resulting from the multipath channel. The $M\times N$ convolution channel matrix, $\mathbf{H}_k[i]$, contains one-chip shifted versions of the zero padded channel vector, $\mathbf{h}_k[i]$, and the $N\times 1$ vector $\mathbf{c}_k[i]$ is the spreading code of user k. The structures

can be described by

$$\mathbf{H}_k[i] = \begin{bmatrix} h_{k,1}[i] & & \mathbf{0} \\ \vdots & \ddots & h_{k,1}[i] \\ h_{k,L}[i] & & \vdots \\ \mathbf{0} & \ddots & h_{k,L}[i] \end{bmatrix}, \mathbf{c}_k[i] = \begin{bmatrix} c_k^1[i] \\ \vdots \\ c_k^N[i] \end{bmatrix}. \tag{3.3}$$

In this model, the ISI span and contribution $\boldsymbol{\eta}_k[i]$ are functions of the processing gain, N, and channel length, L. If $1 < L \leq N$, 3 symbols would interfere in total: the current, the previous and the successive symbol. In the case of $N < L \leq 2N$, 5 symbols would interfere: the current one, the 2 previous and the 2 successive ones. In most practical DS-CDMA systems $1 < L \leq N$; therefore only 3 symbols are usually affected [78].

Training-based adaptive multiuser linear receivers of the sort considered in this chapter are tasked with suppression of the interference in (3.2). However, these do not require knowledge of the system spreading codes and are therefore well suited to scenarios where it is not possible or practical to obtain the spreading codes of the user of interest or interfering users. The design of such receivers corresponds to determining an FIR filter $\mathbf{w}_k[i] = [w_{k,1}[i]\ w_{k,2}[i]\ \ldots\ w_{k,M}]^T$ with M coefficients which provides an estimate of the desired symbol, as given by

$$\begin{aligned} \hat{b}_k[i] &= \mathrm{Q}(z_k[i]) \\ &= \tfrac{1}{\sqrt{2}}\mathrm{sgn}(\Re[z_k[i]]) + \tfrac{1}{\sqrt{2}}\mathrm{sgn}(\Im[z_k[i]])j \\ &= \tfrac{1}{\sqrt{2}}\mathrm{sgn}(\Re[\mathbf{w}_k^H[i]\mathbf{r}[i]]) + \tfrac{1}{\sqrt{2}}\mathrm{sgn}(\Im[\mathbf{w}_k^H[i]\mathbf{r}[i]])j, \end{aligned} \tag{3.4}$$

where $\Re(\cdot)$ and $\Im(\cdot)$ denote the real and imaginary parts respectively, $j = \sqrt{-1}$, Q is a QPSK slicer, sgn$(\cdot)$ is the signum function and the system of interest uses unity normalised QPSK modulation. The quantity $z_k[i] = \mathbf{w}_k^H[i]\mathbf{r}[i]$ is the output of the adaptive receiver $\mathbf{w}_k[i]$ for user k at the i^{th} time instant where $\mathbf{w}_k$ is optimised according to a chosen criterion. However, the $M \times 1$ dimensionality of $\mathbf{w}[i]$ can become large in highly spread systems, leading to computationally intensive implementations and slow conver-

gence when full-rank adaptive algorithms are used. Reduced-rank and SM techniques offer solutions to these problems.

3.3 Set-Membership Reduced-Rank Framework

Reduced-rank techniques for communications achieve dimensionality reduction by projecting the $M \times 1$ received vector $\mathbf{r}[i]$ onto a reduced-rank signal subspace, for example, the Krylov subspace for the MSWF and the AVF with orthogonal auxiliary vectors. The tasks of interference suppression, symbol estimation and detection can then be performed in the lower dimensionality signal subspace with a standard reduced length adaptive filter. For user k in a multiuser system, this is mathematically expressed as

$$\hat{b}_k[i] = \mathrm{Q}([\tilde{\mathbf{w}}_k^H[i]\mathbf{S}_{D_k}^H[i]\mathbf{r}[i]]) = \mathrm{Q}([\tilde{\mathbf{w}}_k^H[i]\tilde{\mathbf{r}}_k[i]]) \tag{3.5}$$

where $\tilde{\mathbf{r}}_k[i] = \mathbf{S}_{D_k}^H[i]\mathbf{r}[i]$ and the $M \times D$ projection matrix $\mathbf{S}_{D_k}$ performs the dimensionality reduction. The $D \times 1$ vector $\tilde{\mathbf{w}}[i]$ performs the linear interference suppression where D is the rank of signal subspace and therefore the dimensionality of the filter where $D \ll M$. However, the majority of techniques prior to the proposition of JIO of adaptive filters relied in some part on SVD or a similarly complex task to generate the projection matrix $\mathbf{S}_{D_k}$ [39], [12].

Reduced-rank adaptive filtering based on JIO circumvents these complex tasks by considering the projection matrix and reduced-rank filter as adaptive structures and placing them in a joint optimisation function. These two structures are then jointly and iteratively adapted to reach a solution. Expressing this as a conventional optimisation problem yields

$$[\mathbf{S}_{D,opt}[i], \tilde{\mathbf{w}}_{opt}[i]] = \arg\min_{\mathbf{S}_D, \tilde{\mathbf{w}}} E[|b[i] - \tilde{\mathbf{w}}^H[i]\mathbf{S}_D^H[i]\mathbf{r}[i]|^2], \tag{3.6}$$

where the user index k has been omitted and user 1 is assumed; a feature that will

continue for the remainder of this chapter. The MMSE expressions for these structures are then derived by fixing $\tilde{\mathbf{w}}[i]$ and $\mathbf{S}_D[i]$ in turn and minimising with respect to the other, resulting in the following expressions

$$\tilde{\mathbf{w}}_{opt}[i] = \tilde{\mathbf{R}}^{-1}[i]\tilde{\mathbf{p}}[i] \tag{3.7}$$

and

$$\mathbf{S}_{D,opt}[i] = \mathbf{R}^{-1}[i]\mathbf{P}_D[i]\mathbf{R}_w^{-1}[i], \tag{3.8}$$

where $\tilde{\mathbf{R}}[i] = E[\tilde{\mathbf{r}}_{opt}[i]\tilde{\mathbf{r}}_{opt}^H[i]]$, $\tilde{\mathbf{p}}[i] = E[b^*[i]\tilde{\mathbf{r}}_{opt}[i]]$, $\mathbf{R}[i] = E[\mathbf{r}[i]\mathbf{r}^H[i]]$ and $\mathbf{R}_\mathbf{w}[i] = E[\tilde{\mathbf{w}}_{opt}[i]\tilde{\mathbf{w}}_{opt}^H[i]]$ are the reduced-rank and full-rank input signal autocorrelation matrices, and reduced-rank filter autocorrelation matrix respectively. In addition to this, $\mathbf{P}_D[i] = E[b^*[i]\mathbf{r}[i]\tilde{\mathbf{w}}_{opt}^H[i]]$ is the reduced-rank cross-correlation matrix. The interdependency between $\tilde{\mathbf{w}}_{opt}[i]$ and $\mathbf{S}_{D,opt}[i]$ prohibits a closed form solution, however, solutions can be reached by iterating (3.7) and (3.8) after suitable initialisation which does not annihilate the signal or de-stabilise the iterative process. The MMSE can then be obtained, as given by

$$\text{MMSE} = \sigma_b^2 - \tilde{\mathbf{p}}^H[i]\tilde{\mathbf{R}}^{-1}[i]\tilde{\mathbf{p}}[i] \tag{3.9}$$

where $\sigma_b^2 = E[|b[i]|^2]$. The joint optimisation structure of the MMSE function given by (3.6) opens up the possibility of a non-convex error-surface. However, this is considered in [12] and although multiple solutions exist, there are no local minima when implemented iteratively and therefore the adaptive process is not sensitive to initialisation[2]. The purely adaptive nature of JIO and its previous implementation with NLMS and RLS algorithms suits it well to integration with SM techniques. Additionally, the process of integration is also far less involved and problematic, and more complete than previous methods that use alternative reduced-rank techniques [71]. This is due to the well defined SM framework that already exists for the algorithms used to implement the JIO schemes.

[2]Provided the signal is not annihilated

The generation of the JIO-SM framework resembles that of a standard SM scheme, however, two solution sets are required at each iteration. To create the JIO-SM framework, firstly an expression for the soft symbol estimate and the two error bounds have to be defined;

$$z[i] = \tilde{\mathbf{w}}^H[i-1]\mathbf{S}_D^H[i-1]\mathbf{r}[i], \tag{3.10}$$

and

$$\begin{aligned} &\mid b[i] - \tilde{\mathbf{w}}^H[i]\mathbf{S}_D^H[i-1]\mathbf{r}[i] \mid^2 \leq \gamma_{\tilde{w}}^2 \\ \text{and} \quad &\mid b[i] - \tilde{\mathbf{w}}^H[i-1]\mathbf{S}_D^H[i]\mathbf{r}[i] \mid^2 \leq \gamma_S^2 \end{aligned} \tag{3.11}$$

where γ_S and $\gamma_{\tilde{w}}$ are the error bounds for the projection matrix and reduced-rank filter, respectively. The structures $\tilde{\mathbf{w}}[i-1]$ and $\mathbf{S}_D[i-1]$ refer to the previous estimate of the reduced-rank filter and projection matrix, respectively, in an iterative estimation procedure.

Following this, defining a sample space χ that contains all possible data pairs b and $\mathbf{r}$ enables the definition of the feasibility sets $\Theta_{\tilde{\mathbf{w}}}$ and $\Theta_{\mathbf{S}_D}$ as subsets of χ, which contain the values that fulfil each error bound in (3.11). These sets for the reduced-rank filter and the projection matrix are expressed as

$$\begin{aligned} \Theta_{\tilde{w}} &\triangleq \bigcap_{(b,\mathbf{r})\in\chi} \tilde{\mathbf{w}} \in \mathbb{C}^D :\mid b - \tilde{\mathbf{w}}^H\mathbf{S}_D^H\mathbf{r} \mid^2 \leq \gamma_{\tilde{w}}^2 \\ \text{and} \quad \Theta_{\mathbf{S}} &\triangleq \bigcap_{(b,\mathbf{r})\in\chi} \mathbf{S}_D \in \mathbb{C}^{M\times D} :\mid b - \tilde{\mathbf{w}}^H\mathbf{S}_D^H\mathbf{r} \mid^2 \leq \gamma_S^2, \end{aligned} \tag{3.12}$$

respectively, where the alternative adaptive structure is assumed fixed in each.

The final step in the development requires the application of the feasibility sets to a time-varying scenario to ensure they contain all estimates which fulfil the respective error criterion at the i^{th} time instant. These sets are termed the constraint sets and are given by

$$\begin{aligned} \mathcal{H}_{\tilde{w}}[i] &= \{\tilde{\mathbf{w}}[i] \in \mathbb{C}^D : |b[i] - \tilde{\mathbf{w}}^H[i]\mathbf{S}_D^H[i-1]\mathbf{r}[i]| \leq \gamma_{\tilde{w}}\} \\ \text{and} \quad \mathcal{H}_S[i] &= \{\mathbf{S}_D[i] \in \mathbb{C}^{M\times D} : |b[i] - \tilde{\mathbf{w}}^H[i-1]\mathbf{S}_D^H[i]\mathbf{r}[i]| \leq \gamma_S\}. \end{aligned} \tag{3.13}$$

Presuming the error bounds are chosen to ensure that the constraint sets are non-empty ($\mathcal{H}_{\tilde{w}}[i], \mathcal{H}_S[i] \neq \emptyset$), every point within each set is a valid estimate of the structure. The objective of a SM algorithm is to then select a point which lies in the appropriate constraint set at each time instant.

With the set-theory foundation set-out, it is now possible to construct the optimisation functions that form the starting point of the algorithms' derivations. For both the SG and LS based schemes, their derivation begins with a constrained optimisation problem formed on the principle of minimal disturbance [82]. This corresponds to minimising the disturbance to the projection matrix and interference suppression filter at each update instant. Accordingly, the distance traversed across the sample space at each time instant to reach the current constraint set is to be minimised. A natural progression from this is that if the previous estimate lies in the current constraint set, it remains a valid estimate and therefore no update is required to satisfy the conditions of the optimisation function. The result is a sparsely updating algorithm which effectively discards data if it will not result in a sufficient level of innovation.

3.4 Proposed Algorithms

In this section the theory set out in Section 3.3 is interpreted as two optimisation problems, leading to the formation of MSE and LS cost functions. Solving these optimisation functions results in two algorithms termed the JIO-SM-NLMS and JIO-BEACON.

3.4.1 Set-Membership Reduced-Rank NLMS Algorithm

To derive the JIO-SM-NLMS, the following constrained optimisation problem is considered

$$
\begin{aligned}
[\mathbf{S}_D[i], \tilde{\mathbf{w}}[i]] = \quad & \underset{\mathbf{S}_D, \tilde{\mathbf{w}}}{\arg\min} \quad && \| \tilde{\mathbf{w}}[i] - \tilde{\mathbf{w}}[i-1] \|^2 + \\
& && \| \mathbf{S}_D[i] - \mathbf{S}_D[i-1] \|^2 \\
& \text{subject to} \quad && b[i] - \tilde{\mathbf{w}}^H[i]\mathbf{S}_D^H[i-1]\mathbf{r}[i] = \gamma_{\tilde{w}} \\
& && b[i] - \tilde{\mathbf{w}}^H[i-1]\mathbf{S}_D^H[i]\mathbf{r}[i] = \gamma_S,
\end{aligned} \tag{3.14}
$$

where the objective is to minimise the disturbance to the projection matrix and reduced-rank filter while satisfying the bounds imposed on the estimation error. In order to recast (3.14) as a more readily solvable unconstrained optimisation problem, the method of Lagrange multipliers is used, yielding

$$
\begin{aligned}
\mathcal{L} = \quad & \| \tilde{\mathbf{w}}[i] - \tilde{\mathbf{w}}[i-1] \|^2 + \| \mathbf{S}_D[i] - \mathbf{S}_D[i-1] \|^2 \\
& + \lambda_1 (b[i] - \tilde{\mathbf{w}}^H[i]\mathbf{S}_D^H[i-1]\mathbf{r}[i] - \gamma_{\tilde{w}}) \\
& + \lambda_2 (b[i] - \tilde{\mathbf{w}}^H[i-1]\mathbf{S}_D^H[i]\mathbf{r}[i] - \gamma_S).
\end{aligned} \tag{3.15}
$$

Taking the gradient with respect to the two adaptive structures and equating to zero, the following system of equations is reached

$$
\nabla_{\tilde{w}[i]} = 2(\tilde{\mathbf{w}}[i] - \tilde{\mathbf{w}}[i-1]) - \mathbf{S}_D^H[i-1]\mathbf{r}[i]\lambda_1 = 0, \tag{3.16}
$$

$$
\nabla_{S_D[i]} = 2(\mathbf{S}_D[i] - \mathbf{S}_D[i-1]) - \mathbf{r}[i]\tilde{\mathbf{w}}^H[i-1]\lambda_2 = 0. \tag{3.17}
$$

Further manipulations then allow us to arrive at expressions for the reduced-rank filter, projection matrix and Lagrange multipliers, given by

$$
\lambda_1 = \frac{2(b[i] - \tilde{\mathbf{w}}^H[i-1]\mathbf{S}_D^H[i-1]\mathbf{r}[i] - \gamma_{\tilde{w}})^*}{\mathbf{r}^H[i]\mathbf{S}_D[i-1]\mathbf{S}_D^H[i-1]\mathbf{r}[i]}, \tag{3.18}
$$

$$
\lambda_2 = \frac{2(b[i] - \mathbf{w}^H[i-1]\mathbf{S}_D^H[i-1]\mathbf{r}[i] - \gamma_S)^*}{\mathbf{r}^H[i]\mathbf{r}[i]\tilde{\mathbf{w}}^H[i-1]\tilde{\mathbf{w}}[i-1]}, \tag{3.19}
$$

$$\tilde{\mathbf{w}}[i] = \tilde{\mathbf{w}}[i-1] + \underbrace{\frac{(e[i] - \gamma_{\tilde{w}})^*}{\mathbf{r}^H[i]\mathbf{S}_D[i-1]\mathbf{S}_D^H[i-1]\mathbf{r}[i]}}_{\bar{\mu}[i]} \mathbf{S}_D^H[i-1]\mathbf{r}[i] \tag{3.20}$$

and

$$\mathbf{S}_D[i] = \mathbf{S}_D[i-1] + \underbrace{\frac{(e[i] - \gamma_S)^*}{\mathbf{r}^H[i]\mathbf{r}[i]\tilde{\mathbf{w}}^H[i-1]\tilde{\mathbf{w}}[i-1]}}_{\bar{\eta}[i]} \mathbf{r}[i]\tilde{\mathbf{w}}^H[i-1] \tag{3.21}$$

where the *a priori* error $e[i]$ is given by

$$e[i] = b[i] - \tilde{\mathbf{w}}^H[i-1]\mathbf{S}_D^H[i-1]\mathbf{r}[i]. \tag{3.22}$$

For the reduced-rank interference suppression filter, but equally applicable to the projection matrix, the update term $\bar{\mu}$ will attempt to find the shortest path from $\tilde{\mathbf{w}}[i-1]$ to the bounding hyperplane of $\mathcal{H}_{\tilde{w}}[i]$ in accordance with the principle of minimal disturbance, as in Figure 3.2. However, if $\tilde{\mathbf{w}}[i-1] \in \mathcal{H}_{\tilde{w}}[i]$, it is clear that the error bound constraint

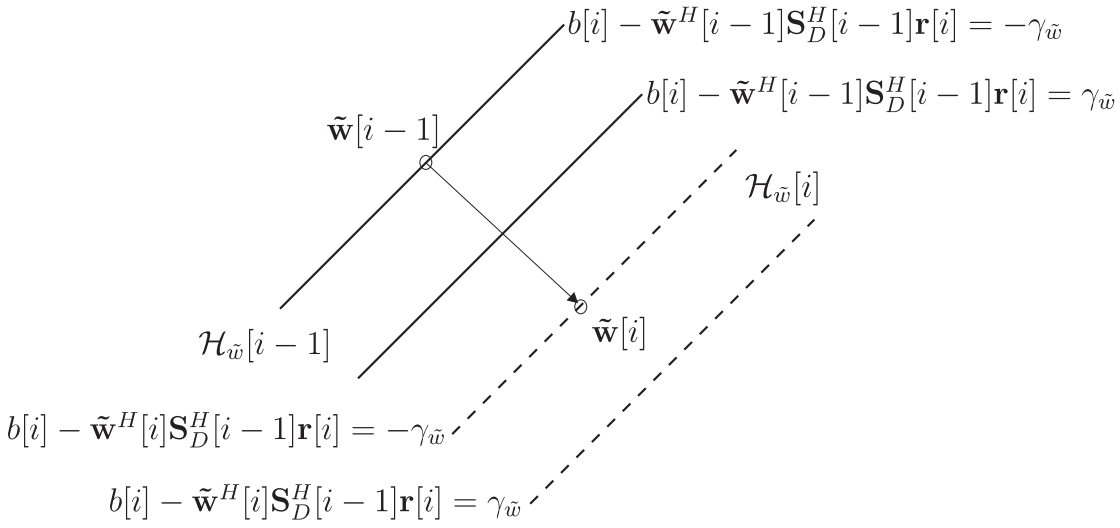

Figure 3.2: Geometric interpretation of JIO-SM-NLMS reduced-rank filter update.

is satisfied, therefore no update is necessary and $\tilde{\mathbf{w}}[i] = \tilde{\mathbf{w}}[i-1]$. To assess the need for an update a simple innovation check (IC) consisting of an '*if*' statement comparing the *a priori* error to the bound is used. The update terms are then set to zero if the result

of the conditional statement is found to be negative, effectively removing the update procedure. When placed into the familiar NLMS structure, the following expressions for the adaptation of the reduced-rank interference suppression filter are reached

$$\tilde{\mathbf{w}}[i] = \tilde{\mathbf{w}}[i-1] + \mu[i]e^*[i]\mathbf{S}_D^H[i-1]\mathbf{r}[i] \tag{3.23}$$

where

$$\mu[i] = \begin{cases} \frac{1}{\mathbf{r}^H[i]\mathbf{S}_D[i-1]\mathbf{S}_D^H[i-1]\mathbf{r}[i]}\left(1 - \frac{\gamma_{\tilde{w}}}{|e^*[i]|}\right) & \text{if } |e^*[i]| \leq \gamma_{\tilde{w}} \\ 0 & \text{otherwise.} \end{cases} \tag{3.24}$$

Similarly, for the projection matrix,

$$\mathbf{S}_D[i] = \mathbf{S}_D[i-1] + \eta[i]e^*[i]\mathbf{r}[i]\tilde{\mathbf{w}}^H[i-1] \tag{3.25}$$

where

$$\eta[i] = \begin{cases} \frac{1}{\mathbf{r}^H[i]\mathbf{r}[i]\tilde{\mathbf{w}}^H[i-1]\tilde{\mathbf{w}}[i-1]}\left(1 - \frac{\gamma_S}{|e^*[i]|}\right) & \text{if } |e^*[i]| \leq \gamma_S \\ 0 & \text{otherwise.} \end{cases} \tag{3.26}$$

The full algorithm is then formed from the update equations of (3.22), (3.23) and (3.25), where the variable step-sizes are given by (3.24) and (3.26). Finally, to prevent instability of the algorithm during the transient, an upper bound, μ^+, is placed upon the reduced-rank filter step-size when the projection matrix has been updated during the current time instant.

3.4.2 Reduced-Rank BEACON Algorithm

The BEACON algorithm operates by defining the constraint set as a degenerate ellipsoid specified by (3.11) at each time instant. An additional set denoted as the membership set can then be defined as the intersection of every constraint set up to the current time instant ($\cap_{l=1}^{i}\mathcal{H}[i]$) [9]. An OBE algorithm is then used to outer bound the membership set with the centroid of this ellipsoid able to be taken as a point estimate, i.e. the i^{th} filter value. The definition of the BEACON algorithm in these terms does not initially lend

itself to straightforward integration with JIO, however, in [9] the BEACON is shown to also be the solution to a constrained LS optimisation; an interpretation which enables easier integration with the JIO.

After some initial manipulation, the constrained optimisation problem is given by

$$\begin{aligned}
[\mathbf{S}_D[i], \tilde{\mathbf{w}}[i]] = \quad & \arg\min_{\mathbf{S}_D, \tilde{\mathbf{w}}} \cdots \\
& (\tilde{\mathbf{w}}[i] - \tilde{\mathbf{w}}[i-1])^H \mathbf{P}^{-1}[i](\tilde{\mathbf{w}}[i] - \tilde{\mathbf{w}}[i-1]) + \\
& (\mathbf{S}_D[i] - \mathbf{S}_D[i-1])^H \mathbf{C}^{-1}[i](\mathbf{S}_D[i] - \mathbf{S}_D[i-1]) \\
\text{subject to} \quad & \mid b[i] - \tilde{\mathbf{w}}^H[i]\mathbf{S}_D^H[i-1]\mathbf{r}[i] \mid^2 \leq \gamma_{\tilde{w}}^2 \\
& \mid b[i] - \tilde{\mathbf{w}}^H[i-1]\mathbf{S}_D^H[i]\mathbf{r}[i] \mid^2 \leq \gamma_S^2
\end{aligned} \tag{3.27}$$

where

$$\mathbf{P}[i] = \mathbf{P}[i-1] - \frac{\lambda_{\tilde{w}}[i]\mathbf{P}[i-1]\mathbf{S}_D^H[i-1]\mathbf{r}[i]\mathbf{r}^H[i]\mathbf{S}_D[i-1]\mathbf{P}[i-1]}{1 + \lambda_{\tilde{w}}[i]G[i]} \tag{3.28}$$

and

$$\mathbf{C}[i] = \mathbf{C}[i-1] - \frac{\lambda_S[i]\mathbf{C}[i-1]\mathbf{r}[i]\tilde{\mathbf{w}}^H[i-1]\tilde{\mathbf{w}}[i-1]\mathbf{r}^H[i]\mathbf{C}[i-1]}{1 + \lambda_S[i]F[i]}. \tag{3.29}$$

To continue with the derivation, (3.27) is recast as an unconstrained optimisation problem with the use of the method of Lagrange multipliers, yielding,

$$\begin{aligned}
\mathcal{L} = \quad & (\tilde{\mathbf{w}}[i] - \tilde{\mathbf{w}}[i-1])^H \mathbf{P}^{-1}[i](\tilde{\mathbf{w}}[i] - \tilde{\mathbf{w}}[i-1]) + \\
& (\mathbf{S}_D[i] - \mathbf{S}_D[i-1])^H \mathbf{C}^{-1}[i](\mathbf{S}_D[i] - \mathbf{S}_D[i-1]) + \\
& \lambda_{\tilde{w}}[i](\mid b[i] - \tilde{\mathbf{w}}^H[i]\mathbf{S}_D^H[i-1]\mathbf{r}[i] \mid^2 - \gamma_{\tilde{w}}^2) + \\
& \lambda_S[i](\mid b[i] - \tilde{\mathbf{w}}^H[i-1]\mathbf{S}_D^H[i]\mathbf{r}[i] \mid^2 - \gamma_S^2).
\end{aligned} \tag{3.30}$$

Forming a system of equations by taking the gradient of (3.30) with respect to the adap-

tive structures results in

$$\begin{aligned}\nabla_{\tilde{w}}[i] =&(\tilde{\mathbf{w}}[i] - \mathbf{w}[i-1])\mathbf{P}^{-1}[i] - \lambda_{\tilde{w}}[i]\mathbf{r}^H[i]\mathbf{S}_D[i-1]... \\ &(b[i] - \tilde{\mathbf{w}}^H[i]\mathbf{S}_D^H[i-1]\mathbf{r}[i]).\end{aligned} \tag{3.31}$$

$$\begin{aligned}\nabla_S[i] =&(\mathbf{S}_D[i] - \mathbf{S}_D[i-1])\mathbf{C}^{-1}[i] - \lambda_S[i]\mathbf{r}[i]\tilde{\mathbf{w}}^H[i-1]... \\ &(d[i] - \tilde{\mathbf{w}}^H[i-1]\mathbf{S}_D^H[i]\mathbf{r}[i]).\end{aligned} \tag{3.32}$$

Further manipulation then allows intermediate expressions for the reduced-rank filter and projection matrix to be reached, respectively

$$\tilde{\mathbf{w}}[i] = \tilde{\mathbf{w}}[i-1] + \frac{\lambda_{\tilde{w}}[i]\mathbf{P}[i]\mathbf{r}^H[i]\mathbf{S}_D[i-1]\delta[i]\gamma_{\tilde{w}}}{\mid \delta[i] \mid}, \tag{3.33}$$

and

$$\mathbf{S}_D[i] = \mathbf{S}_D[i-1] + \frac{\lambda_S[i]\mathbf{C}[i]\mathbf{r}[i]\tilde{\mathbf{w}}^H[i-1]\delta[i]}{1 + \lambda_S[i]F[i]}, \tag{3.34}$$

where

$$\delta[i] = b[i] - \tilde{\mathbf{w}}^H[i-1]\mathbf{S}_D^H[i-1]\mathbf{r}[i]. \tag{3.35}$$

To arrive at a recursive estimation procedure for each structure, $\mathbf{P}[i-1]$ and $\mathbf{C}[i-1]$ are used to calculate the auxiliary scalar variables $G[i]$ and $F[i]$, respectively, where

$$G[i] = \mathbf{r}^H[i]\mathbf{S}_D[i-1]\mathbf{P}[i-1]\mathbf{S}_D^H[i-1]\mathbf{r}[i]. \tag{3.36}$$

$$F[i] = \tilde{\mathbf{w}}^H[i-1]\tilde{\mathbf{w}}[i-1]\mathbf{r}^H[i]\mathbf{C}[i-1]\mathbf{r}[i]. \tag{3.37}$$

Using the relationship

$$1 + \lambda_{\tilde{w}}[i]G[i] = 1 + \frac{1}{G[i]}\left(\frac{\mid \delta[i] \mid}{\gamma_{\tilde{w}}} - 1\right)G[i] = \frac{\mid \delta[i] \mid}{\gamma_{\tilde{w}}} \tag{3.38}$$

the final reduced-rank filter update equations are reached

$$\tilde{\mathbf{w}}[i] = \tilde{\mathbf{w}}[i-1] + \frac{\lambda_{\tilde{w}}[i]\mathbf{P}[i]\mathbf{S}_D^H[i-1]\mathbf{r}[i]\delta[i]}{1+\lambda_{\tilde{w}}[i]G[i]}, \tag{3.39}$$

where

$$\lambda_{\tilde{w}}[i] = \begin{cases} \frac{1}{G[i]}\left(\frac{|\delta[i]|}{\gamma_{\tilde{w}}} - 1\right) & \text{if } \mid \delta[i] \mid \geq \gamma_{\tilde{w}} \\ 0 & \text{otherwise} \end{cases} \tag{3.40}$$

and once again the *if* statement forms the IC. In an analogous manner to step-size in the NLMS variant, the forgetting factor is set to zero thus skipping the update procedure when the *if* statement returns a negative result . Similarly for the projection matrix, the relationship given by

$$1 + \lambda_S[i]F[i] = 1 + \frac{1}{F[i]}\left(\frac{\mid \delta[i] \mid}{\gamma_{\tilde{w}}} - 1\right)F[i] = \frac{\mid \delta[i] \mid}{\gamma_S} \tag{3.41}$$

is used to arrive at the recursive update procedure

$$\mathbf{S}_D[i] = \mathbf{S}_D[i-1] + \frac{\lambda_S[i]\mathbf{C}[i]\mathbf{r}[i]\tilde{\mathbf{w}}^H[i-1]\delta[i]}{1+\lambda_S[i]F[i]}, \tag{3.42}$$

where

$$\lambda_S[i] = \begin{cases} \frac{1}{F[i]}\left(\frac{|\delta[i]|}{\gamma_S} - 1\right) & \text{if } \mid \delta[i] \mid \geq \gamma_S \\ 0 & \text{otherwise} \end{cases} \tag{3.43}$$

The final algorithm then iteratively operates using (3.35), (3.39) and (3.42) where the variable forgetting factors are given by (3.40) and (3.43). As in the JIO-SM-NLMS implementation, an upper bound, $\lambda_{\tilde{w}}^{+}$, is placed upon reduced-rank filter forgetting factor when the projection matrix has been updated during the current time instant. This ensures stability during the initial transient period of the algorithm.

Table 3.1: Computational complexity of proposed and existing algorithms

	Average number of complex operations per iteration
Algorithm	Additions
NLMS	$3M-1$
RLS	$4M^2$
SM-NLMS	$UR_w(2M+4)+M+1$
BEACON	$UR_w(3M^2+M+7)+M+1$
MSWF-NLMS	$M^2(D+2)+M(D+1)-D-2$
MSWF-RLS	$M^2(D+2)+M(D+1)+4D^2-D-1$
JIO-NLMS	$M(2D+1)-3D-4$
JIO-RLS	$3M^2+M(3D-2)+3D^2$
JIO-SM-NLMS	$UR_S(M(D+1)+D-1)+UR_w(2D)+DM+4$
JIO-BEACON	$UR_S(M^2-M+D^2+4D+1)+UR_w(6D^2+2)+DM+1$
	Multiplications
NLMS	$3M+2$
RLS	$5M^2+5M+2$
SM-NLMS	$UR_w(2M)+M+1$
BEACON	$UR_w(2M^2+M)+M+1$
MSWF-NLMS	$M^2(D+2)+M(2D+3)+3D+3$
MSWF-RLS	$M^2(D+2)+M(2D+3)+3D+3$
JIO-NLMS	$M(2D+1)+5D+5$
JIO-RLS	$4M^2+M(2D+1)+8D^2+4D+6$
JIO-SM-NLMS	$UR_S(M(D+1)+2D+5)+UR_w(2D+4)+MD+D$
JIO-BEACON	$UR_S(2M^2D+2MD+D^2+4D+10)+$ $UR_w(6D^2+2D+7)+MD+D+1$

3.4.3 Computational Complexity

The potential complexity reductions made by the proposed algorithms are closely related to the frequency of updates or update rates, denoted UR_S and UR_w for the projection matrix and reduced-rank interference suppression filter, respectively. These terms are defined as the fraction of received symbols which result in an update of their respective structure. Figure 3.3 shows a comparison between the complexity of the conventional full and reduced-rank algorithms and that of the proposed schemes. The results shown in Figure are based on update rates of 10% for all SM schemes and a rank of D=6. The accompanying analytical expressions for the algorithm complexities are given by Table 3.1.

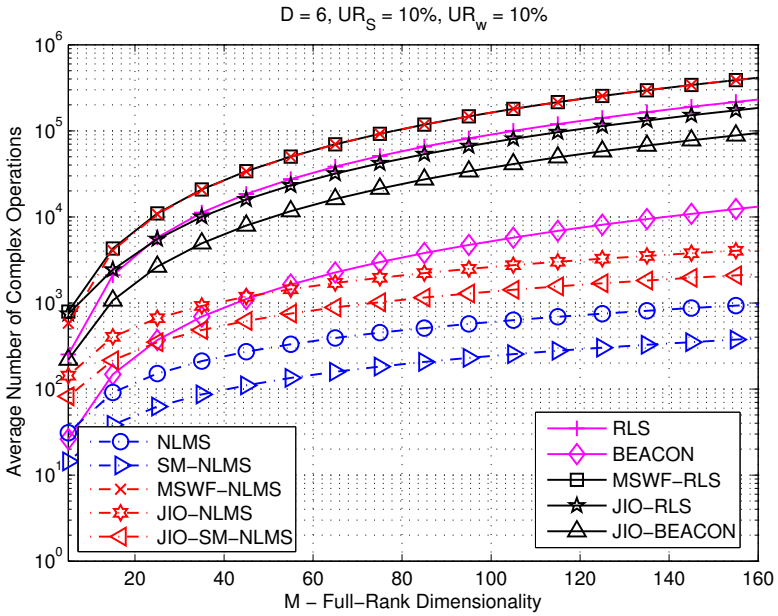

Figure 3.3: Computational complexity of the proposed and existing algorithms.

From Figure 3.3 it is evident that complexity savings of approximately an order of magnitude are possible for the JIO-BEACON and approximately 63% for the JIO-SM-NLMS, both of which are substantial savings with regards to power consumption in mobile and wireless sensor networks. The complexity of the JIO-SM-NLMS is also below that of the full-rank BEACON at all but low values of M at which the overheads of the linear JIO scheme exceed the additional complexity resulting from quadratic com-

plexity of the BEACON scheme.

3.4.4 Rank Adaptation Algorithm

The dimensionality of the subspace of a reduced-rank algorithm has an impact on their performance, in a manner analogous to conventional adaptive filtering. This therefore allows the rank of the proposed schemes to act as an additional optimisation parameter. By adjusting the rank of the subspace depending on the stage of operation, it is possible to obtain performance improvements. In practical scenarios this corresponds to using lower ranks during the convergence of algorithms to aid the convergence, and increased ranks for steady state operation. Such methods have been previously proposed but the application of an automatic rank-selection algorithm to a SM scheme has not featured. The integration of a rank-adaptation feature involves the formulation of a cost-function which allows the optimum rank to be determined. In [13] an exponentially weighted LS *a posteriori* cost function was used and a similar approach shall be used here. However, adaptation of the rank shall only be permitted when the *a priori* error exceeds the appropriate bounds and an update performed. The chosen rank D_{opt} shall be constrained to lie between D_{min} and D_{max} and selected according to the expression

$$D_{opt}[i] = \begin{cases} \underset{D_{min} \leq D \leq D_{max}}{\arg\min} \; \mathcal{R}(\tilde{\mathbf{w}}_D[i], \mathbf{S}_D[i]) & \text{if } \mid e[i] \mid \geq \gamma \\ D[i-1] & \text{otherwise,} \end{cases} \tag{3.44}$$

where

$$\mathcal{R}(\tilde{\mathbf{w}}_D[i], \mathbf{S}_D[i]) = \sum_{l=1}^{i} \beta^{i-l} \mid b[l] - \tilde{\mathbf{w}}_D^H[i]\mathbf{S}_D^H[i]\mathbf{r}[l] \mid^2 \tag{3.45}$$

The values of D_{min} and D_{max} are chosen to offer optimum performance throughout the data record the algorithm is operating over and β is the exponential weighting factor to ensure a smooth transition between subspace ranks. Figure 3.4 displays the relationship between the rank and performance of the NLMS based schemes with optimised parameters. The optimum range of ranks equates to $D_{min} = 2$ and $D_{max} = 10$, and therefore

these bounds shall be used for relevant simulations which feature later in this chapter.

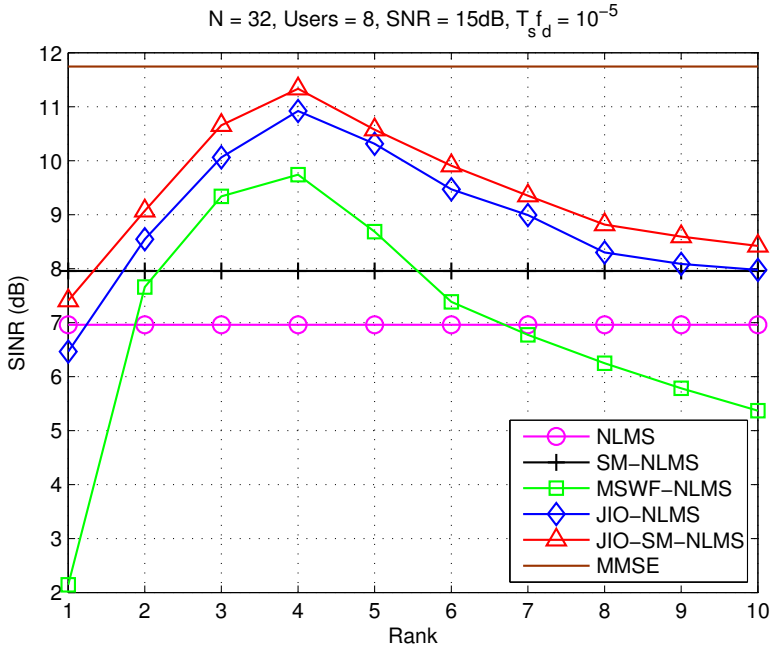

Figure 3.4: NLMS scheme rank comparison with 1000 training symbols.

3.4.5 Adaptive Variable Error Bound

The determination of the error bounds for an SM scheme is a complex task and one which requires knowledge of the parameters of the considered system. Inappropriate error bound selection results in the possibility of under and over bounding, and associated performance degradation and complexity increases [74, 75]. By incorporating selected system parameters into the formulation of a variable bound for the proposed algorithms, it is possible to reduce the probability of encountering bounding problems but also remove the need for an accurate determination of error bounds prior to the operation of the schemes. In this chapter, the implementation of parameter dependent bounds which require knowledge of the projection matrix and reduced-rank filter are considered. For the implementation given here knowledge of the noise variance is also assumed; however, it is readily obtainable via noise estimation algorithms [83, 84]. The

variable error bounds for the projection matrix and reduced-rank filter are given by

$$\gamma_S[i+1] = (1-\beta)\gamma_S[i] + \beta\sqrt{\alpha_S \|\mathbf{S}_D[i]\tilde{\mathbf{w}}[i]\|\hat{\sigma}_n^2[i]} \tag{3.46}$$

and

$$\gamma_{\tilde{w}}[i+1] = (1-\beta)\gamma_{\tilde{w}}[i] + \beta\sqrt{\alpha_{\tilde{w}} \|\mathbf{S}_D[i]\tilde{\mathbf{w}}[i]\|\hat{\sigma}_n^2[i]} \tag{3.47}$$

where β is a forgetting factor and α_S and $\alpha_{\tilde{w}}$ are tuning parameters for the projection matrix and reduced-rank filter bounds, respectively. The motivation behind the formation of the variable bound expressions lies in providing the SM process with information on the noise at the output of the filtering process, an approximation given by the term $\sqrt{\alpha_S \|\mathbf{S}_D[i]\tilde{\mathbf{w}}[i]\|\hat{\sigma}_n^2[i]}$. Time averaging is then performed by β to ensure stable transitions between error bound values and overall stability. For added protection against the risk of over-bounding and inaccurate symbol estimation, a ceiling value is implemented with regards to the bounds. For the power normalised QPSK system considered in this chapter, these ceiling values are set at $\gamma_{S_{max}} = 0.7$ and $\gamma_{\tilde{w}_{max}} = 0.65$ for both the JIO-SM-NLMS and JIO-BEACON schemes.

3.5 Analysis

The MSE analysis of set-membership schemes presents a number of unique and challenging problems when compared to conventional adaptive algorithms. The variable convergence parameters and the sparse updates increase the complexity of the analysis significantly. However, methods to partially take account of these SM features have been previously presented in [85, 86] for system identification. These include a 'probability of update' term which accounts for the sparse adaptation and simplifying assumptions about the variable convergence parameters. The analysis of JIO-SM is substantially more complex than conventional SM analysis, however, the methods above shall still be used to aid the analysis. To begin, the probability of update terms are incorporated into

the recursive equations for the adaptation of the reduced-rank interference suppression filter and the projection matrix, this yields the following expressions

$$\tilde{\mathbf{w}}[i] = \tilde{\mathbf{w}}[i-1] + \mu[i] P_{\tilde{w}_{up}} e^*[i] \mathbf{S}_D^H[i-1] \mathbf{r}[i], \tag{3.48}$$

and

$$\mathbf{S}_D[i] = \mathbf{S}_D[i-1] + \eta[i] P_{S_{up}} e^*[i] \mathbf{r}[i] \tilde{\mathbf{w}}^H[i-1], \tag{3.49}$$

for the JIO-NLMS and

$$\tilde{\mathbf{w}}[i] = \tilde{\mathbf{w}}[i-1] + \frac{\lambda_{\tilde{w}}[i] P_{\tilde{w}_{up}} \mathbf{P}[i] \mathbf{S}_D^H[i-1] \mathbf{r}[i] \delta[i]}{1 + \lambda_{\tilde{w}}[i] G[i]}, \tag{3.50}$$

and

$$\mathbf{S}_D[i] = \mathbf{S}_D[i-1] + \frac{\lambda_S[i] P_{S_{up}} \mathbf{C}[i] \mathbf{r}[i] \tilde{\mathbf{w}}^H[i-1] \delta[i]}{1 + \lambda_S[i] F[i]}, \tag{3.51}$$

for the JIO-BEACON. $P_{S_{up}}$ and $P_{\tilde{w}_{up}}$ are the probability of update terms for the projection matrix and reduced-rank interference suppression filter, respectively, and are the analytical embodiment of the update rates. To increase the accuracy and practicality of analysing the SM schemes, their dependency on the *a priori* error is eliminated by confining the analysis to the excess error under steady-state conditions. This allows more accurate models of the probability of update to be formed as it can be assumed that $P_{S_{up}/\tilde{w}_{up}}$ are constant and reflect the probability of the steady state error exceeding the appropriate bound.

3.5.1 Stability

As with much of the JIO material covered in this chapter, analysis of its application to adaptive interference suppression is limited. However, with methods inspired by beamforming analysis in [87] the stability analysis of the proposed JIO-SM-NLMS algorithm can be approached.

The spectral radius technique can be used for the JIO-SM-NLMS but depends upon

obtaining recursive relationships for the error weight vector and error weight matrix for the reduced-rank filter and projection matrix, respectively. To do this, expanded versions of (3.48) and (3.49), which include $P_{\tilde{w}_{up}}$, $P_{S_{up}}$ and the optimised step-sizes, are substituted into the reduced-rank filter error weight vector $\boldsymbol{\varepsilon}_{\tilde{w}}[i+1] = \tilde{\mathbf{w}}[i+1] - \tilde{\mathbf{w}}_{opt}[i+1]$ and the projection matrix error weight matrix $\boldsymbol{\varepsilon}_{S_D}[i+1] = \mathbf{S}_D[i+1] - \mathbf{S}_{D,opt}[i+1]$ equations, yielding

$$\begin{aligned}\boldsymbol{\varepsilon}_{\tilde{w}}[i+1] =& (\mathbf{I} - \mu[i]P_{\tilde{w}_{up}}\mathbf{S}_D^H[i]\mathbf{r}[i]\mathbf{r}^H[i]\mathbf{S}_D^H[i])\boldsymbol{\varepsilon}_{\tilde{w}}[i] \\ &+ \mu[i]P_{\tilde{w}_{up}}b^*[i]\mathbf{S}_D^H[i]\mathbf{r}[i] \\ &- \mu[i]P_{\tilde{w}_{up}}\mathbf{S}_D^H[i]\mathbf{r}[i]\mathbf{r}^H[i]\mathbf{S}_D^H[i]\tilde{\mathbf{w}}_{opt}\end{aligned} \tag{3.52}$$

and

$$\begin{aligned}\boldsymbol{\varepsilon}_S[i+1] =& \boldsymbol{\varepsilon}_S[i](\mathbf{I} - \eta[i]P_{S_{up}}\mathbf{r}[i]\mathbf{r}^H[i]) \\ &- \eta[i]P_{S_{up}}\mathbf{r}[i]\tilde{\mathbf{w}}^H[i]\mathbf{r}^H[i]\mathbf{S}_D[i]\boldsymbol{\varepsilon}_{\tilde{w}}[i] \\ &- \eta[i]P_{S_{up}}\mathbf{r}[i]\tilde{\mathbf{w}}^H[i]\mathbf{r}^H[i]\mathbf{S}_D[i]\tilde{\mathbf{w}}_{opt} \\ &+ \eta[i]P_{S_{up}}b^*[i]\mathbf{r}[i]\tilde{\mathbf{w}}^H[i].\end{aligned} \tag{3.53}$$

The expectations of (3.52) and (3.53) are then taken and a recursive expression reached,

$$\begin{bmatrix} \mathrm{E}(\boldsymbol{\varepsilon}_{\tilde{w}}[i+1]) \\ \mathrm{E}(\boldsymbol{\varepsilon}_S[i+1]) \end{bmatrix} = \mathbf{B}\begin{bmatrix} \mathrm{E}(\boldsymbol{\varepsilon}_{\tilde{w}}[i]) \\ \mathrm{E}(\boldsymbol{\varepsilon}_S[i]) \end{bmatrix} + \mathbf{T} \tag{3.54}$$

where

$$\mathbf{B} = \begin{bmatrix} \mathbf{I} - \mu[i]P_{\tilde{w}_{up}}\tilde{\mathbf{R}} & \mathbf{0} \\ -\eta[i]P_{S_{up}}\mathrm{E}(\mathbf{r}[i]\tilde{\mathbf{w}}^H[i]\mathbf{r}^H[i]\mathbf{S}_D[i]) & I - \mu[i]P_{S_{up}}\mathbf{R} \end{bmatrix}, \tag{3.55}$$

$$\mathbf{T} = \begin{bmatrix} \mu[i]P_{\tilde{w}_{up}}(\tilde{\mathbf{p}} - \tilde{\mathbf{R}}\tilde{\mathbf{w}}_{opt}) \\ \eta[i]P_{S_{up}}\mathbf{p}\tilde{\mathbf{w}}^H[i] - \eta[i]P_{S_{up}}\mathrm{E}(\mathbf{r}[i]\tilde{\mathbf{w}}^H[i]\mathbf{r}^H[i]\mathbf{S}_D[i]) \end{bmatrix}, \tag{3.56}$$

and $\tilde{\mathbf{p}} = \mathrm{E}(b^*[i]\tilde{\mathbf{r}}[i])$ and $\tilde{\mathbf{R}} = \mathrm{E}(\tilde{\mathbf{r}}[i]\tilde{\mathbf{r}}^H[i])$. The stability of the algorithm can then be

determined from the spectral radius of (3.54). For convergence, the eigenvalues of $\mathbf{B}^H\mathbf{B}$ should not exceed 1 at each time instant, a factor which is partly ensured by the variable step-sizes and the reduced-rank filter step-size limits, μ^+ and λ_w^+. Numerical studies can then verify (3.54) and its ability to determine the stability.

3.5.2 Steady State MSE

In this section, the steady state MSE of the proposed schemes is studied and expressions developed that allow the steady state MSE to be more accurately predicted compared to using the *a priori* error bound.

JIO-SM-NLMS

The interdependency of the adaptive structures in JIO poses several problems when approaching the analysis, consequently a semi-analytical steady state error solution is sought. The analysis begins by forming an M-dimensional expression for the MSE where an equivalent M-dimensional low-rank filter is obtained by an inverse mapping of the reduced-rank interference suppression filter, given by

$$\mathbf{w}[i] = \mathbf{S}_D[i]\tilde{\mathbf{w}}[i]. \tag{3.57}$$

The MSE can then be expressed as

$$J[i] = \mathrm{E}[|b[i] - \mathbf{w}^H[i]\mathbf{r}[i]|^2]. \tag{3.58}$$

After straightforward manipulation, the MSE dependency on the full-rank error weight matrix can be obtained

$$J[i] = J_{min}[i] + \mathrm{tr}\left(\mathrm{E}[\boldsymbol{\varepsilon}_w^H[i]\mathbf{r}[i]\mathbf{r}^H[i]\boldsymbol{\varepsilon}_w[i]]\right), \tag{3.59}$$

where $\boldsymbol{\varepsilon}_w[i] = \mathbf{w}[i] - \mathbf{w}_{opt}$ and $J_{min} = E[|b[i] - \mathbf{w}_{opt}^H \mathbf{r}[i]|]$. The second term in (3.59) is equal to the excess MSE and can be rearranged into a form which is appropriate for analysis and the pursuit of an expression for the steady state error,

$$J[i] = J_{min}[i] + \underbrace{\mathrm{tr}\left(\mathrm{E}[\mathbf{r}[i]\mathbf{r}^H[i]\boldsymbol{\varepsilon}_w[i]\boldsymbol{\varepsilon}_w^H[i]]\right)}_{\mathrm{J_{ex}}}. \tag{3.60}$$

The first step is to reach a recursive expression for the full-rank equivalent filter error vector. To do this, (3.23) and (3.25) are substituted into (3.57) and the optimum full-rank equivalent filter subtracted, yielding

$$\begin{aligned}
\boldsymbol{\varepsilon}_w[i+1] = \boldsymbol{\varepsilon}_w[i] & \\
&+ \frac{\mu[i] P_{\tilde{w}_{up}} e^*[i]}{\tilde{\mathbf{r}}[i]\tilde{\mathbf{r}}[i]} \mathbf{S}_D[i]\mathbf{S}_D^H[i]\mathbf{r}[i] \\
&+ \frac{\eta[i] P_{S_{up}} e^*[i]}{\tilde{\mathbf{w}}^H[i]\tilde{\mathbf{w}}[i]\mathbf{r}^H\mathbf{r}[i]} \mathbf{r}[i]\tilde{\mathbf{w}}^H[i]\tilde{\mathbf{w}}[i] \\
&+ \frac{\mu[i]\eta[i] P_{\tilde{w}_{up}} P_{S_{up}} e^*[i] e^*[i]}{\tilde{\mathbf{r}}^H[i]\tilde{\mathbf{r}}^H[i]\tilde{\mathbf{w}}^H[i]\tilde{\mathbf{w}}[i]\mathbf{r}^H\mathbf{r}[i]} \mathbf{r}[i]\tilde{\mathbf{w}}^H[i]\mathbf{S}_D^H[i]\mathbf{r}[i].
\end{aligned} \tag{3.61}$$

At this point in the derivation, in addition to the common independence assumptions associated with convergence analysis [38], a number of simplifying assumptions can be made as a result of the proposed algorithm structure and the small values of the step-sizes at steady-state. These include

$$\begin{aligned}
\mu^2[i]\eta[i] &\approx 0 \\
\mu[i]\eta^2[i] &\approx 0 \quad . \\
\mu^2[i]\eta^2[i] &\approx 0
\end{aligned} \tag{3.62}$$

The next step is to substitute (3.61) into the expression for J_{ex} in (3.60). The convenient manipulation available due to the trace of expectation operators allows a number of terms to be simplified and removed, resulting in a recursive expression for J_{ex}. Then

assuming $P_{S_{up}}[i]$, $P_{\tilde{w}_{up}}[i]$ and $J_{ex}[i]$ are constant under steady-state conditions

$$\begin{aligned} \lim_{i\to\infty} \quad & P_{S_{up}}[i] = P_{S_{up}} \\ & P_{\tilde{w}_{up}}[i] = P_{\tilde{w}_{up}} \\ & J_{ex}[i] = J_{ex} \end{aligned} , \tag{3.63}$$

an expression for the steady-state excess error of the JIO-SM-NLMS algorithm can be reached,

$$J_{ex} = J_{min} \frac{\mu^2 P^2_{\tilde{w}_{up}} + \eta^2 P^2_{S_{up}} + 2\mu\eta P_{\tilde{w}_{up}} P_{S_{up}}}{\mu P_{\tilde{w}_{up}}(2 - \mu P_{\tilde{w}_{up}}) + \eta P_{S_{up}}(2 - \eta P_{S_{up}}) - 2\mu\eta P_{\tilde{w}_{up}} P_{S_{up}}} \tag{3.64}$$

where $\mu = E[\mu[i]]$ and $\eta = E[\eta[i]]$.

Unlike the majority of existing SM analysis [85, 86] which concentrate on system identification, the analysis here is in relation to an interference suppression scenario and therefore certain simplifying assumptions about the properties of the input signal cannot be made. This results in a steady-state error expression which although different, has a similar structure.

It is clear that (3.64) is dependent upon $P_{S_{up}/\tilde{w}_{up}}$ and has to be obtained in order to arrive at an analytical expression. Assuming the additive noise is white and Gaussian, and that the estimation error has reached its steady state value, the variations in J_{ex} can also be assumed to be Gaussian. Therefore the probability of the steady-state error exceeding the bound can be modelled by a complementary Gaussian cumulative distribution or 'Q'function. Ideally (3.64) would be used to obtain an accurate value for the steady-state error and therefore the probability of it exceeding the error bound. However, its dependency on $P_{S_{up}/\tilde{w}_{up}}$ prohibits such an approach. The alternative is to approximate the upper and lower bounds on the probability of update for the projection matrix based on J_{min}, γ_S and σ_n^2. A lower bound can then be approximated by

$$P_{Sup_{min}} = 2Q\left(\frac{\gamma_S}{\sqrt{\sigma_n^2 + J_{min}}}\right) \tag{3.65}$$

and an upper bound by

$$P_{Sup_{max}} = 2Q\left(\frac{\gamma_S}{\sqrt{\sigma_n^2 + \gamma_S^2}}\right) \tag{3.66}$$

where the factor of 2 is to ensure $Q(0) = P_{up} = 1$ for $\gamma_S = 0$. The difference in application from existing SM analysis also impacts here because it is unrealistic to assume that the minimum error is bounded by the noise variance. Consequently, the lower bound is assumed to be the error from the optimum equivalent full-rank filter with the addition of the noise variance. As before the upper bound of the error is approximated by the sum of the SM error bound and the noise variance. However, as will become clear in Section 3.5.2, using γ_S as an upper bound is not a satisfactory approximation of the error for the γ_S of interest and in supporting simulations the update rate is considerably better modelled by (3.65) than (3.66), therefore (3.65) shall be used for the remainder of this chapter. Due to the higher update priority given to the projection matrix, the update characteristics of the reduced-rank filter $P_{\tilde{w}_{up}}$ differ from P_{Sup} and are therefore more suitably modelled using a semi-analytical approach where $P_{\tilde{w}_{up}}$ can be approximated from comparable simulations. Using this approach the divergence of the theory from the simulations is minimised.

The second pair of quantities required for the calculation of (3.64) are the expectation of the step-sizes. In [86] the worst case scenario step size is used and a similar approach shall be taken in this chapter, where the step-size can take any value in the range 0 - 1, but shall be set to $\eta = 1$ and $\mu = 0.1$.

JIO-BEACON

The analysis presented in Section 3.5.2 extends that currently available for SM schemes and shall now be applied to the JIO-BEACON algorithm. The derivation presented here for the JIO-BEACON follows a similar method and begins by forming an expression for the full-rank equivalent filter error weight vector so that J_{ex} can be calculated from (3.60). By substituting (3.33) and (3.34) into (3.57) and again subtracting the optimum

full-rank equivalent filter, a recursive expression for the full-rank equivalent filter error weight vector is reached

$$\begin{aligned}\boldsymbol{\varepsilon}_w[i+1] &= \boldsymbol{\varepsilon}_w[i] \\ &+ \mathbf{S}_D[i]\frac{P_{\tilde{w}_{up}}}{G[i]}\lambda_{\tilde{w}}[i]\mathbf{P}[i]\tilde{\mathbf{r}}[i]e^*[i] \\ &+ \frac{P_{S_{up}}}{1+\lambda_S[i]}\left(\frac{\lambda_S[i]}{F[i]}\mathbf{C}[i]\mathbf{A}[i]\delta^*[i]\right)\tilde{\mathbf{w}}[i] \\ &+ \frac{P_{S_{up}}P_{\tilde{w}_{up}}\lambda_S[i]\lambda_{\tilde{w}}[i]}{(1+\lambda_S[i])G[i]}\left(\frac{\lambda_S[i]}{F[i]}\mathbf{C}[i]\mathbf{A}[i]\delta^*[i]\right)... \\ &\mathbf{P}[i]\tilde{\mathbf{r}}[i]e^*[i],\end{aligned} \tag{3.67}$$

where $\mathbf{A}[i] = \mathbf{r}[i]\tilde{\mathbf{w}}^H[i]$. Using equivalent simplifications to those found in the JIO-SM-NLMS analysis

$$\begin{aligned}\lambda^2_{\tilde{w}}[i]\lambda_S[i] &\approx 0 \\ \lambda_{\tilde{w}}[i]\lambda^2_S[i] &\approx 0 \\ \lambda^2_{\tilde{w}}[i]\lambda^2_S[i] &\approx 0\end{aligned} \cdot \tag{3.68}$$

an expression for the JIO-BEACON steady-state error is obtained

$$J_{ex} = J_{min}\frac{P^2_{\tilde{w}_{up}}\lambda^2_{\tilde{w}} + \frac{P^2_{S_{up}}\lambda^2_S}{(1+\lambda_S)^2} + \frac{2P_{\tilde{w}_{up}}P_{S_{up}}\lambda_{\tilde{w}}\lambda_S}{1+\lambda_S}}{P_{\tilde{w}_{up}}\lambda_{\tilde{w}}(2-P_{\tilde{w}_{up}}\lambda_{\tilde{w}}) + \frac{P_{S_{up}}\lambda^2_S}{1+\lambda_S}(2-\frac{P_{S_{up}}\lambda^2_S}{1+\lambda_S}) - 2\frac{P_{\tilde{w}_{up}}P_{S_{up}}\lambda_{\tilde{w}}\lambda^2_S}{1+\lambda_S}} \tag{3.69}$$

The expressions in (3.67) - (3.69) are included here for mathematical completeness and are similar to the JIO-SM-NLMS. The main differences between (3.69) and (3.64) stem from the fact that the JIO-SM-NLMS uses a variable step-size whereas the JIO-BEACON employs a variable forgetting factor.

3.6 Simulations

In this section, the performance of the algorithms presented in this chapter are compared against existing full-rank and reduced-rank schemes. Comparisons shall be made in terms of convergence and tracking performance using the SINR and BER as metrics.

Throughout all simulations the JIO and MSWF based schemes have a reduced dimensionality subspace of rank of 4 and 6 respectively. Each simulation is averaged over 2000 independent runs and, where the channel is non-stationary, the fading rate is given by the dimensionless normalised fading parameter, $T_s f_d$, which is specified in each plot. All MMSE based filters, full and reduced-rank, are initialised as $w[0] = \delta \times (\mathbf{1})$ and all LS based filters are initialised as $w[0] = (\mathbf{0})$ and $w(1) = 1$. Projection matrices shall be initialised as $S[0] = \zeta \times \begin{bmatrix} \mathbf{I} \\ \mathbf{0} \end{bmatrix}$ where δ and ζ are small positive constants.

3.6.1 Analytical MSE Performance

In this section the analytical expressions and approximations derived in Section 3.5.2 for the JIO-SM-NLMS steady state error are validated via comparison against simulations of the proposed schemes. The JIO-SM-NLMS applied here makes use of a fixed estimation error bound and therefore exhibits a specific MSE performance characteristic where the optimum MSE performance is obtained when the bound is small but non-zero, a value defined here as $\gamma_{S,opt}$. Consequently, two methods of estimating the MSE are required; for small γ_S the MSE expression $J[\infty] \approx J_{min} + J_{ex}$ can be used to provide an accurate lower bound, but for $\gamma_S > \gamma_{S,opt}$, $J[\infty] = \gamma^2$ acts as a increasingly accurate error approximation.

In the following simulations, a lightly loaded system with a spreading gain of 32 is used and operates in a stationary environment with a signal-to-noise ratio of 15dB. The simulated and analytical MSE are plotted against the projection matrix error bound which has been normalised by the noise power σ_n^2, the reduced-rank filter error bound is set to $\gamma_S - 0.05$.

As one can see from Figure 3.5, the analytical MSE provides a lower and significantly more accurate bound on the MSE of the JIO-SM schemes for $\gamma_S < \gamma_{S,opt}$ compared to γ_S^2 where $\gamma_{S,opt}^2/\sigma_n^2 \sim 4$ and therefore verifies the method of analysis presented in this chapter. However, as previously mentioned γ_S^2 acts as more accurate bound for

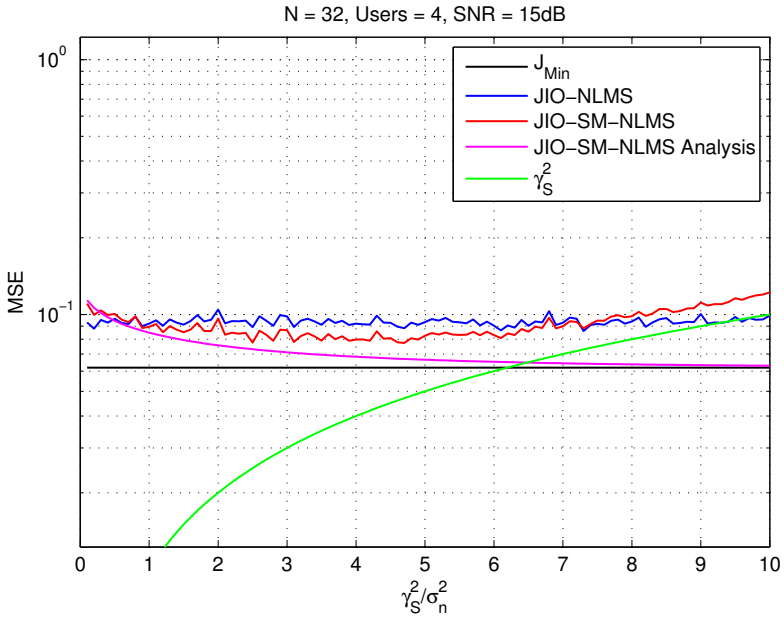

Figure 3.5: Analytical MSE performance.

larger steady state error and therefore the use of either depends upon the relative level of the error bound.

3.6.2 SINR and BER Performance

In the presented simulations, each algorithm has an initial period of training and then switches to decision directed operation. The step-sizes throughout all the simulations were set to $\mu = 0.25$ for the full-rank NLMS and MSWF-NLMS, and $\eta = 0.25$ and $\mu = 0.1$ for the reduced-rank interference suppression filter and projection matrix adaptation for the JIO-NLMS, respectively. The exponential forgetting factor for the LS based schemes is $\lambda = 0.998$ for the convergence, multiuser and SNR performance simulations. The reduced-rank filter step-size and forgetting factor upper bounds, μ^+ and $\lambda_{\bar{w}}^+$, respectively, are set to 0.1 and 0.998 for each simulation.

The performance of the stochastic gradient based schemes is shown in Figure 3.6. The convergence of the proposed scheme can be seen to exceed that of the conventional JIO and MSWF algorithms while having a considerably lower computational complexity. The proposed scheme can also be seen to achieve a comparable steady-

state SINR compared to the conventional implementation whilst achieving a considerable 3dB SINR advantage after 25 iterations.

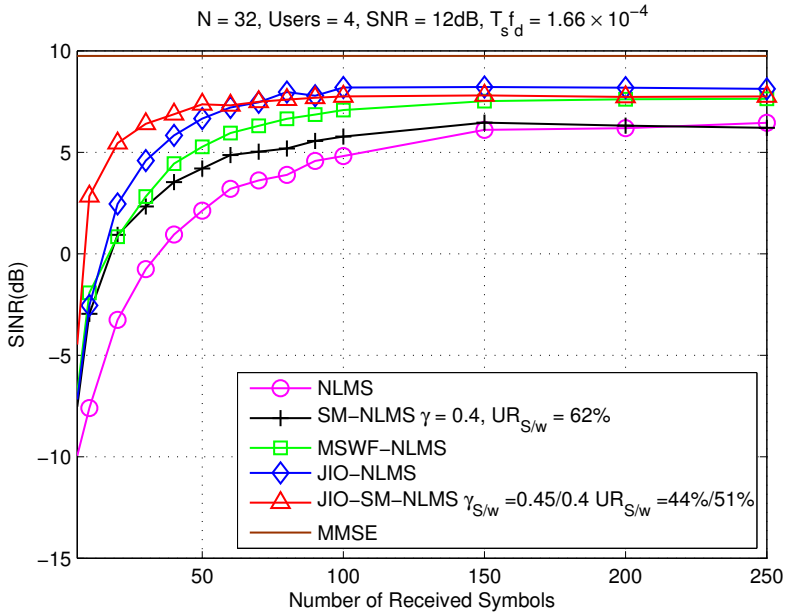

Figure 3.6: SINR performance comparison of MSE algorithms with 150 training symbols.

Figure 3.7 gives the performance of the LS based schemes and shows that the proposed scheme exhibits improved convergence performance compared to the conventional JIO-RLS. It also reaches a maximum SINR close to the MSE while achieving a significant 50% reduction in complexity. In addition to this, the performance after convergence shows that the JIO-BEACON outperforms the SINR of the JIO-RLS by up to 1dB and the full-rank BEACON by up to 2dB, indicating that the reduced-rank SM scheme has maintained the capability to mitigate the effects of a fading channel.

Figure 3.8 gives the performance of the proposed and existing reduced-rank algorithms when the spreading sequence length is increased to 64 and the system is heavily loaded. Both the proposed schemes exhibit improved convergence over the MSWF schemes with the JIO-NLMS also achieving a 3dB SINR gain over the over the conventional JIO-NLMS during convergence. The performance of the BEACON-JIO has dropped in comparison with the JIO-RLS when processing these more highly spread signals but complexity savings are still made.

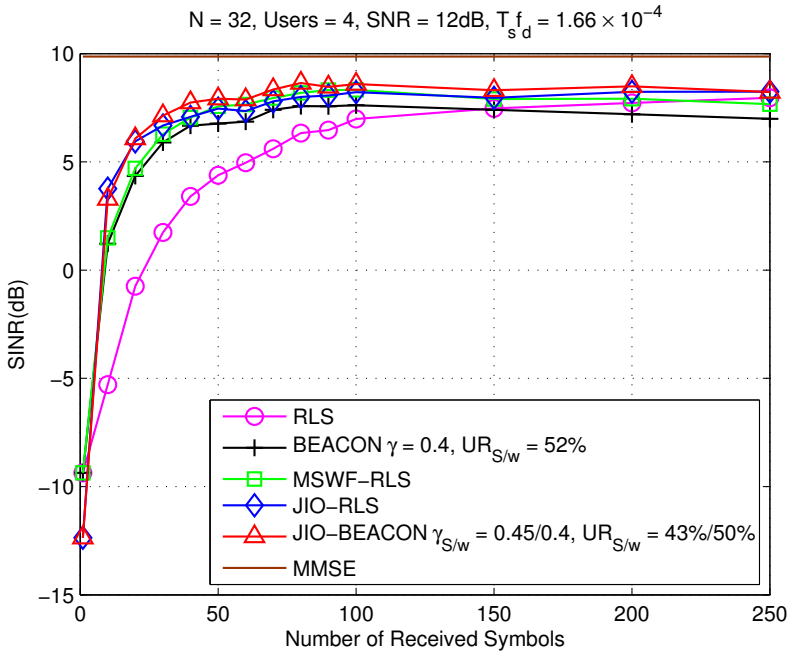

Figure 3.7: SINR performance comparison of LS algorithms with 100 training symbols.

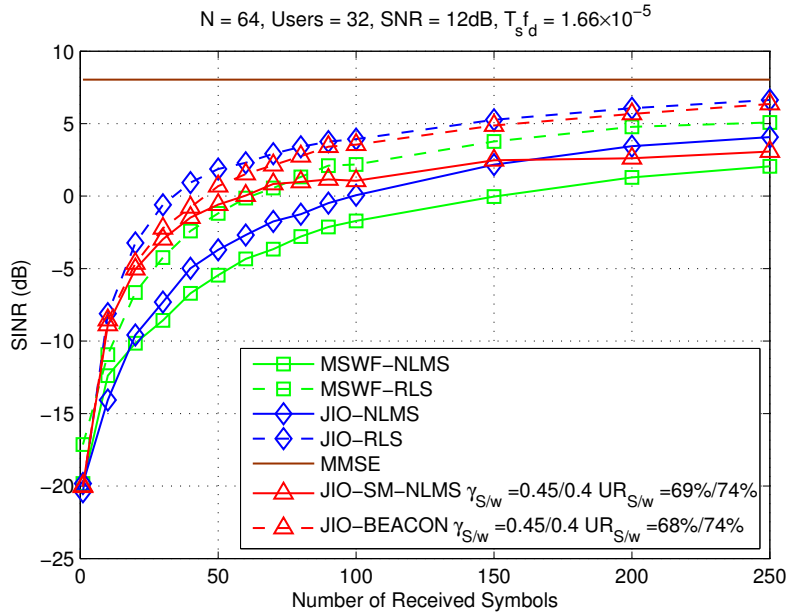

Figure 3.8: SINR performance comparison of LS and MSE algorithms with 250 training symbols and increased length spreading sequences.

Figure 3.9a and 3.9b show the SINR performance of the proposed MSE based scheme versus the system SNR and loading, respectively, for a fading channel after 150 training symbols. The JIO-SM provides an improvement in performance compared to the conventional scheme at moderate SNR whilst achieving a reduction in complex-

ity. At low SNR its performance declines however it maintains an improvement over the full-rank scheme. The performance of the scheme under increasing system loads is good and exceeds that of the conventional scheme at low system loads. Its performance degrades in a similar manner to the MSWF when interference suppression becomes more challenging but maintains a 1-2dB improvement in SINR performance.

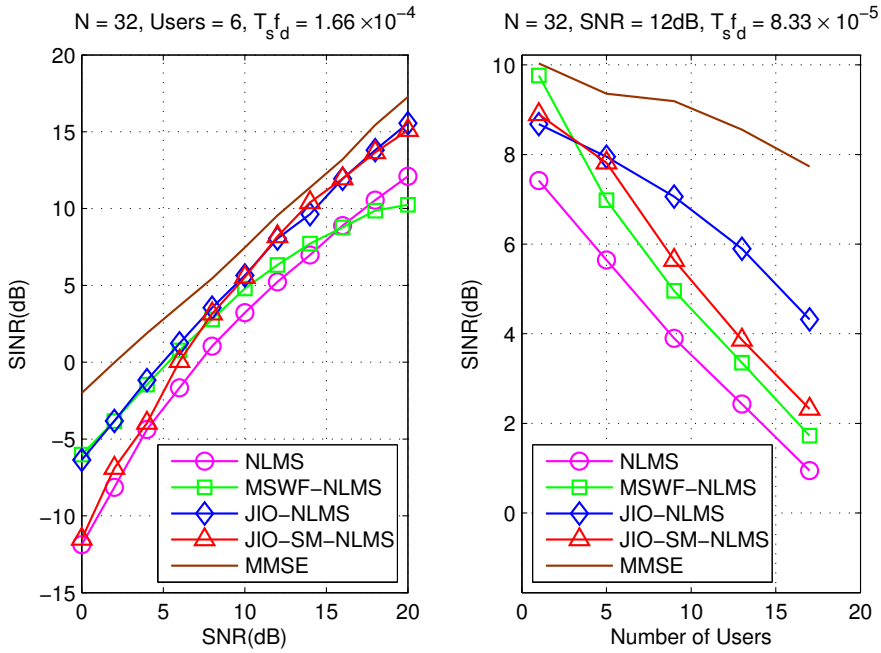

(a) SINR versus SNR

(b) SINR versus system loading

Figure 3.9: MSE schemes - SNR and multiuser performance after 150 training symbols.

The SINR performance versus system SNR and loading for the LS based schemes are shown by Figure 3.10a and 3.10b. Once again, the simulations have been conducted with a fading channel and 100 training symbols. In Figure 3.10a the proposed scheme can be seen to perform well and closely match the performance of the conventional JIO for SNRs of interest and suffers only a 2dB SINR disadvantage at an SNR of 20dB. The performance of the scheme in Figure 3.10b at low system loading is good but does degrade at higher loading levels compared with the conventional JIO-RLS. However, as the system approaches a state of overloading, Figure 3.10b indicates that although performance of the proposed scheme will degrade it will significantly outperform the

MSWF and full-rank RLS.

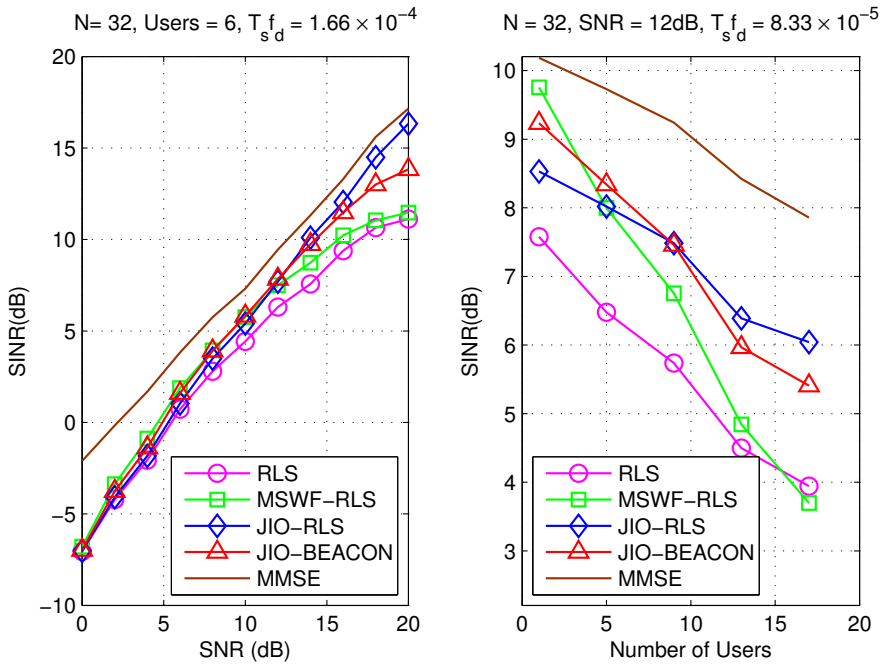

(a) SINR versus system SNR (b) SINR versus system loading

Figure 3.10: LS schemes - SNR and multiuser performance after 100 training symbols.

The SINR plot in Figure 3.11, shows the performance gains that are possible when the automatic rank-selection feature from Section 3.4.4 is incorporated into the proposed algorithms. The automatic rank-selection improves steady-state SINR performance whilst also exceeding the convergence performance of the fixed-rank algorithms. The update rates associated with the schemes in Figure 3.11 differ from those of the previous simulations because of the larger gap between the error bounds placed on the adaptive structures. In this simulation the projection matrix and reduced-rank filter bounds are $\gamma_S = 0.6$ and $\gamma_w = 0.3$ respectively; therefore, an increase in the probability of the reduced-rank filter updating results.

The performance and complexity improvements brought about the introduction of an adaptive variable error bound are illustrated by Figure 3.12. Improvements in the complexity of both schemes result whilst preserving performance. Accordingly, the performance of the variable bound schemes can be improved above that of the fixed

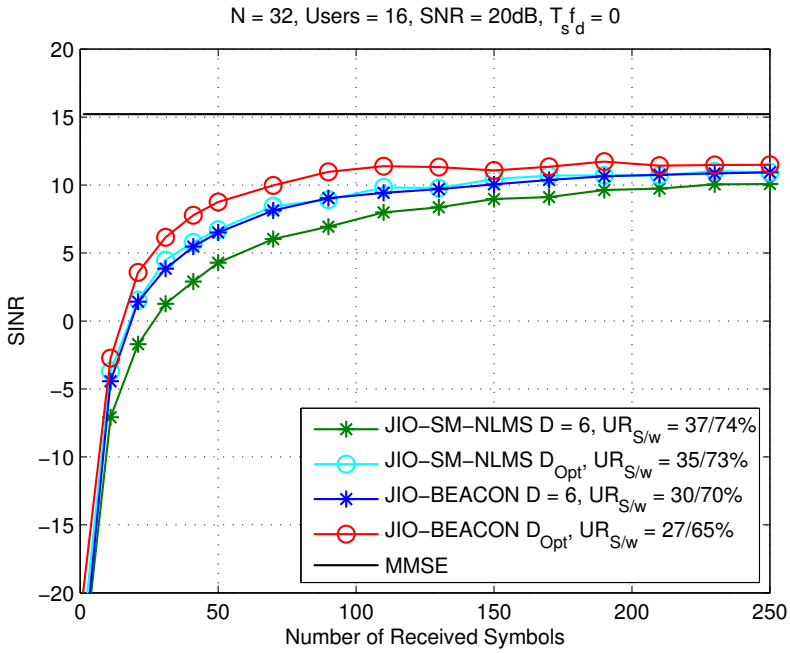

Figure 3.11: Performance comparison of automatic rank-selection algorithms.

schemes whilst maintaining complexity savings.

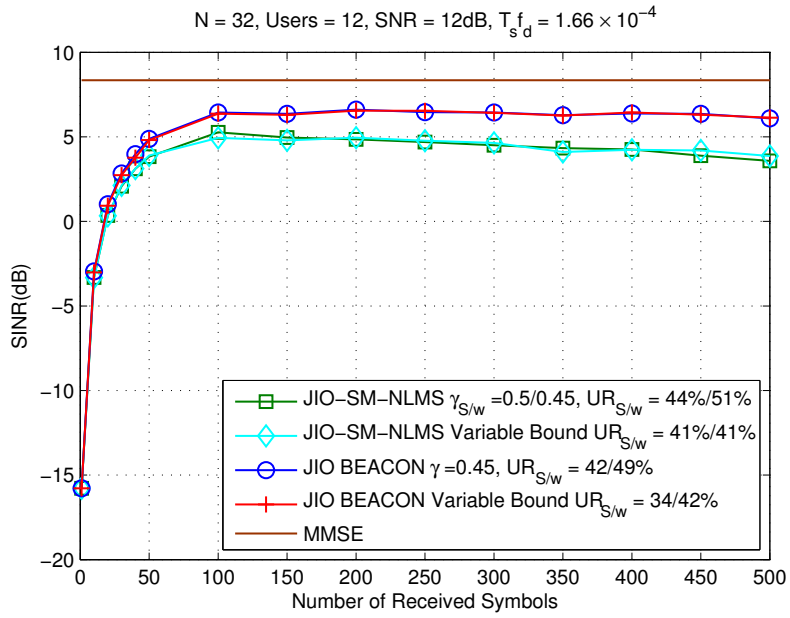

Figure 3.12: SINR performance of proposed JIO-SM-NLMS and JIO-BEACON algorithms with variable γ_S and $\gamma_{\tilde{w}}$ where $\alpha_S = 5$ and $\alpha_{\tilde{w}} = 4$, and a training sequence of 100 symbols.

Figure 3.13 shows the uncoded BER performance of the proposed schemes and existing reduced-rank schemes along with the two most common full-rank schemes. The

schemes are trained with 500 symbols and then switched to decision directed operation. Both the SM reduced-rank algorithms exceed the convergence of the MSWF schemes and reach a lower steady-state error; however, as has been previously documented, the MSWF-NLMS fails to tridiagonalise its autocorrelation matrix and therefore struggles in this scenario. The JIO-BEACON exhibits excellence performance and, along with the NLMS implementation, achieves significant complexity savings which increase with the SNR.

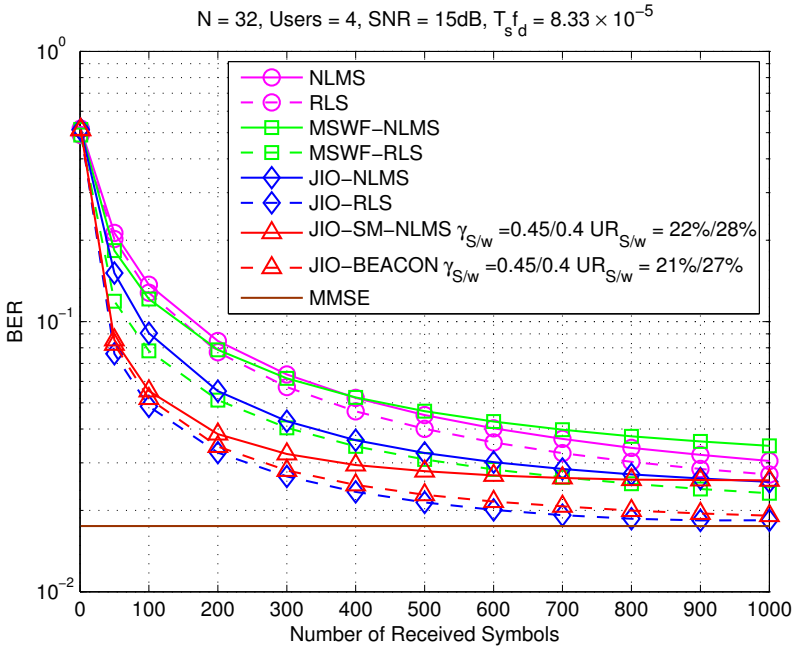

Figure 3.13: BER performance comparison.

3.7 Summary

This chapter presented an SM reduced-rank framework based on joint iterative optimisation of receive parameters. The sparse updates and optimised convergence parameters associated with SM schemes were brought to the adaptation of the subspace estimating projection matrix and the reduced-rank interference suppression filter. Least squares, stochastic gradient, automatic rank-adaptation and adaptive error bound algorithms were presented along with their application to interference suppression in the

uplink of a time-varying multiuser DS-CDMA system. Novel analysis of the proposed schemes has been given along with the limitations of applying existing SM analysis techniques to the proposed algorithms. Simulations have then been presented and illustrate that the performance of the proposed schemes closely matches that of the existing reduced-rank schemes while achieving a significant reduction in computational complexity.

This chapter has addressed the need for low-complexity high-performance interference suppression in the DS-CDMA systems currently used in the third generation of mobile networks; however, the capacity and infrastructure cost of DS-CDMA is envisaged to be unsuitable for the next generation of mobile systems. Consequently, cooperative MIMO systems have been proposed for next generation networks and are the system that the forthcoming chapter focuses upon.

Chapter 4

Joint Discrete and Continuous Algorithms for Resource Allocation and Interference Suppression in Cooperative MIMO Networks

Contents

4.1 Introduction

Cooperative MIMO networks have received significant attention in the recent research literature due to their spatial diversity gain, multiplexing gain, robustness, low power and high capacity. These characteristics suit cooperative MIMO to future mobile networks that require extended coverage, increased data rates and enhanced quality of service whilst minimising infrastructure investment. Consequently, cooperative MIMO techniques have been incorporated into future mobile protocols [22–25, 88–91]. Although still in their infancy, promising results and techniques for cooperative MIMO systems have been published, predominantly focussing on cooperation protocols, routing, information theoretic limits and diversity maximisation [88]. The common protocols of DF and AF both offer added degrees of freedom, which when effectively exploited, can lead to significant performance gains. Cooperative MIMO systems also enable the use of transmit diversity TDS, power allocation and relay optimisation to improve performance and reduce the number of relays burdened with retransmission of the signal [92, 93]. TDS and RS can be interpreted as sub-optimal variants of beamforming and power allocation where transmit powers are constrained to discrete values of 1 and 0. However, a trade-off exists between this sub-optimality and the reduced feedback requirements resulting from the 1 bit quantisation [3, 94]. The multiplexing gain resulting from MIMO systems is an attractive feature and one that is already exploited in a range of systems; however, there is an associated increase in interference from the multi-stream transmission. When channel state information (CSI) is available at the transmitter, this interference can be mitigated by the use of SIC and equivalent techniques such as the Vertical Bell-Labs Layered Space-Time (V-BLAST) and multi-branch implementations [95–98]. If CSI is unavailable, adaptive interference suppression, reception and power allocation provide alternative means to mitigate this interference at significantly lower computational expense [99, 100].

Previous works that addressed antenna selection and RS have chosen several different approaches in an attempt to obtain increased performance and lower complex-

ity. In [101], an iterative method is presented that determines the antenna selection by assessing the MMSE impact of adding antenna pairs to the transmit antenna pattern. However, this work assumes full CSI in an AF system and does not guarantee convergence to the exhaustive solution. In [3], an SNR based approach is taken where the transmit antennas at the source and relay are chosen to maximise the post-processing SNR. An SNR based approach is also taken in [102] and [103] where antennas are chosen based on their instantaneous SNR and maximisation of the SNR after maximal-ratio combining. Once again though, full CSI is assumed and the application has not been extended to cooperative systems with a non-negligible direct path. The mutual information/capacity of MIMO systems is also an important consideration and in [104] sum-rate maximisation is performed via receive antenna selection for a non-cooperative system.

When the suppression of multiple access interference is also taken into consideration, the task of establishing optimal TDS and RS in terms of capacity, BER performance and diversity takes on an added degree of complexity. SIC reception in a cooperative MIMO system has previously been considered in [28,105] to address this. However, these concentrate on single relay AF systems which present a less challenging environment to implement cooperative SIC reception and subsequent optimisation. To further address interference mitigation, adaptive interference suppression techniques for MIMO networks have been proposed. These have shown good performance but encounter the problems of limited applicability to cooperative MIMO systems, and undiscerning use of system channels and relays [99, 100].

Progressing beyond TDS leads to continuous power allocation. Although extensive literature has been published on power allocation in wireless networks [63, 93, 99, 100, 106, 107], optimisation in multirelay cooperative MIMO networks has not been considered. The high number of antennas places an increased complexity and feedback burden on the system and limits the use of optimal techniques. Iterative techniques and coarse quantisation can help alleviate this burden but come at the cost of degraded performance and extended convergence periods. In addition, conventional MSE power

allocation procedures do not take into account the performance of preceding phases; therefore, potentially, optimising the transmission of erroneous data.

In this chapter, the problem of low complexity optimisation of TDS and continuous power allocation is addressed for a cooperative MIMO system. A range of MMSE reception techniques are utilised and their integration with low-complexity TDS considered. The combinatorial nature of TDS results in a discrete optimisation problem where conventional continuous iterative methods are unsuitable. Although solvable with an exhaustive search, this constitutes a highly complex solution and is inappropriate for practical implementation. Consequently, a discrete stochastic procedure first proposed in [14] is introduced as an alternative low-complexity method to arrive at the optimum transmit diversity. However, convergence is dependent upon the cardinality of the solution set and this therefore acts as a limiting factor on the performance of an algorithm. Furthermore, the potential for inaccurate reception at the relays leads to complications and performance implications for the relaying protocol. To address these issues, a technique termed RS is introduced. This eliminates a number of the most poorly performing relays from consideration and leads to a reduction in the cardinality and increase in quality of the solution set. To formalise this approach, a joint TDS and RS framework is developed and a number of discrete iterative algorithms based on MSE and mutual information optimality criteria presented. Discrete iterative RS is extended to continuous power allocation to restrict its operation to an optimised set of relays. This constrains the transmission power of the poorly performing relays to zero, in a manner not possible with power allocation alone, but also allows the performance of the preceding stage to influence the subsequent optimisation. Furthermore, the reduction in the number of considered relays improves the convergence performance of iterative techniques thus increasing their suitability to application in cooperative MIMO systems.

TDS and RS schemes are shown to converge to the exhaustive solution at low computational expense and also operate effectively when recursive least squares channel estimation is introduced to provide CSI. To illustrate the versatility of the proposed al-

gorithms and their ability to jointly operate with continuous algorithms, they are also applied to low-complexity continuous adaptive interference suppression. The computational complexity, convergence, and diversity gains of the proposed algorithms are analysed and are then implemented in a multi-relay cooperative MIMO system. Comparisons are drawn against the optimal exhaustive solutions and standard cooperative implementations.

This chapter is organised as follows: Sections 4.2 and 4.3 give the system, data models and reception techniques used throughout this chapter. Sections 4.4, 4.5 detail the problems that face multi-relay cooperative MIMO systems, the corresponding linear and non-linear MMSE, mutual information optimisation problems and the framework for their solution. The proposed discrete iterative and continuous algorithms are given in Section 4.6 along with a channel estimation procedure. Section 4.7 presents the analysis of and an investigation into the computational complexity, convergence, diversity and feedback properties of the proposed algorithms. The performance of the proposed algorithms, along with comparisons against standard cooperative and non-cooperative methods are given in Section 4.8. The chapter is drawn to a close by the concluding remarks of Section 4.9.

4.2 System and Data Model

The cooperative network considered is a two-phase, QPSK system where the direct path is non-negligible and no ISI is assumed. All relays are half-duplex, and MMSE interference suppression and symbol estimation is performed at decoding all nodes. Single source and destination nodes are separated by N_{r} intermediate relay nodes where the source and relay nodes are anticipated to represent mobile stations and the destination node a fixed base station. The channel of each antenna pair is represented by a complex gain and the direct path has a gain which is a fraction of the indirect paths in order to reflect the increased geographical distance and shadowing involved. The source and

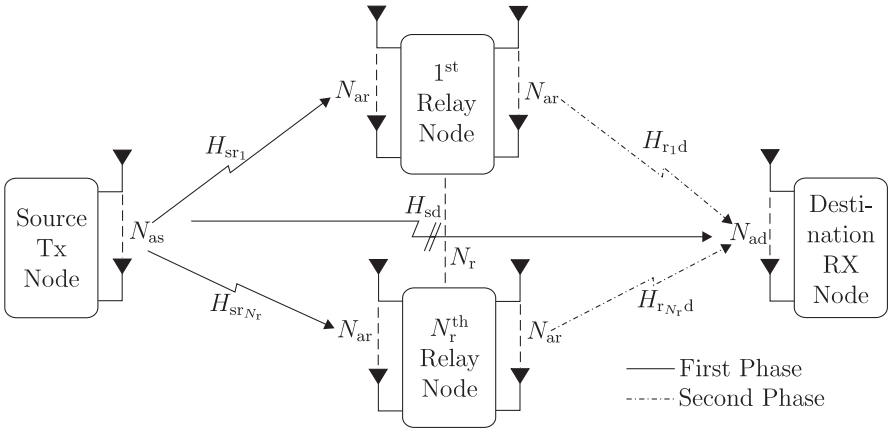

Figure 4.1: MIMO multi-relay system model.

destination nodes each have N_{as} forward and N_{ad} backward antennas respectively, and the relay nodes have N_{ar} forward and backward antennas. N_{as} data streams are transmitted in the system and each is allocated to the correspondingly numbered antenna at the source node. Data are transmitted in packets of N symbols where during the first phase packets are transmitted from the source to the relay and destination nodes. The second phase then consists of decoding, power normalisation and forwarding for the DF protocol and simply power normalisation and retransmission for the AF protocol. All channels are assumed uncorrelated, unless otherwise specified, with frequency flat block fading where the coherence time is equal to the N symbol packet. The total average transmit power in each phase is maintained at unity and equally distributed between the active antennas. The maximum spatial multiplexing gain and diversity advantage simultaneously available in the system are $r^* = N_{as}$ and $d^* = N_{ad}(1 + (N_r N_{ar}/N_{as}))$, respectively [4, 108]. An outline system model is given in Figure 4.1.

4.2.1 Decode-and-Forward

The received signals of the first phase at the destination and n^{th} relay for the i^{th} symbol are given by

$$\mathbf{r}_{sd}[i] = \mathbf{H}_{sd}[i]\mathbf{A}_s[i]\mathbf{T}_s[i]\mathbf{b}[i] + \boldsymbol{\eta}_{sd}[i] \tag{4.1}$$

and

$$\mathbf{r}_{\mathrm{sr}_n}[i] = \mathbf{H}_{\mathrm{sr}_n}[i]\mathbf{A}_{\mathrm{s}}[i]\mathbf{T}_{\mathrm{s}}[i]\mathbf{b}[i] + \boldsymbol{\eta}_{\mathrm{sr}_n}[i], \tag{4.2}$$

respectively. The structures $\mathbf{H}_{\mathrm{sd}}$ and $\mathbf{H}_{\mathrm{sr}_n}$ are the $N_{\mathrm{as}} \times N_{\mathrm{ad}}$ source - destination and $N_{\mathrm{as}} \times N_{\mathrm{ar}}$ source - n^{th} relay channel matrices, respectively. The quantities $\boldsymbol{\eta}_{\mathrm{sd}}$ and $\boldsymbol{\eta}_{\mathrm{sr}_n}$ are the $N_{\mathrm{ad}} \times 1$ and $N_{\mathrm{ar}} \times 1$ vectors of zero mean additive white Gaussian noise at the destination and n^{th} relay, respectively, whose variances are σ^2_{sd} and $\sigma^2_{\mathrm{sr}_n}$ and autocorrelation matrices $\sigma^2_{\mathrm{sd}}\mathbf{I}_{\mathrm{N_{ad}}}$ and $\sigma^2_{\mathrm{sr}_n}\mathbf{I}_{\mathrm{N_{sr_n}}}$. The source's $N_{\mathrm{as}} \times 1$ transmit data vector is denoted by $\mathbf{b}$ and $\mathbf{A}_{\mathrm{s}}$ is the diagonal source transmit power allocation matrix that normalises the average total transmit power of the first phase to unity, assuming that the modulation scheme is also power normalised to 1. Lastly, $\mathbf{T}_{\mathrm{s}}$ is a diagonal $N_{\mathrm{as}} \times N_{\mathrm{as}}$ source TDS matrix, where elements of the main diagonal specify whether the correspondingly numbered antenna is active. Accordingly, to maintain maximum multiplexing gain under the described protocol all source antennas are required, therefore, $\mathbf{T}_{\mathrm{s}}[i] = \mathbf{I}_{N_{\mathrm{as}}}$.

At the n^{th} relay, the output of the reception procedure is denoted $\mathbf{z}_{\mathrm{r}_n}[i]$ and the decoded symbol vector is given by

$$\begin{aligned} \hat{\mathbf{b}}_{\mathrm{r}_n}[i] &= \mathrm{Q}(\mathbf{z}_{\mathrm{r}_n}[i]) \\ &= \tfrac{1}{\sqrt{2}}\left[\mathrm{sgn}(\Re[\mathbf{z}_{\mathrm{r}_n}[i]]) + \mathrm{sgn}(\Im[\mathbf{z}_{\mathrm{r}_n}[i]])\right] \end{aligned} \tag{4.3}$$

where $\mathrm{Q}(\cdot)$ is the QPSK slicer, $\Re(\cdot)$ and $\Im(\cdot)$ denote the real and imaginary parts, respectively and $\mathrm{sgn}(\cdot)$ is the signum function.

The $N_{\mathrm{ad}} \times 1$ second phase received signal at the destination is the summation of the N_{r} relayed signals, yielding

$$\mathbf{r}_{\mathrm{rd}}[i] = \sum_{n=1}^{N_{\mathrm{r}}} \mathbf{H}_{\mathrm{r}_n\mathrm{d}}[i]\mathbf{A}_{\mathrm{r}_n}[i]\mathbf{T}_{\mathrm{r}_n}[i]\hat{\mathbf{b}}_{\mathrm{r}_n}[i] + \boldsymbol{\eta}_{\mathrm{rd}}[i], \tag{4.4}$$

where $\mathbf{H}_{\mathrm{r}_n\mathrm{d}}$ is the n^{th} relay - destination channel matrix and $\mathbf{A}_{\mathrm{r}_n}[i]$ is the n^{th} relay transmit power allocation matrix that ensures the total transmit power of the second phase is unity. $\mathbf{T}_{\mathrm{r}_n}$ is the TDS matrix of the n^{th} relay and specifies which of its N_{ar} antennas are

active. The summation of (4.4) can be expressed in a more compact form, given by

$$\mathbf{r}_{\mathrm{rd}}[i] = \boldsymbol{\mathcal{H}}_{\mathrm{rd}}[i]\boldsymbol{\mathcal{A}}_{\mathrm{r}}[i]\boldsymbol{\mathcal{T}}_{\mathrm{r}}[i]\hat{\tilde{\mathbf{b}}}[i] + \boldsymbol{\eta}_{\mathrm{rd}}[i] \tag{4.5}$$

where $\boldsymbol{\mathcal{T}}_{\mathrm{r}}[i] = \mathrm{diag}\left[\mathbf{T}_{\mathrm{r}_1}[i]\ \mathbf{T}_{\mathrm{r}_2}[i]...\mathbf{T}_{\mathrm{r}_{N_\mathrm{r}}}[i]\right]$ is the $N_{\mathrm{ar}}N_{\mathrm{r}} \times N_{\mathrm{ar}}N_{\mathrm{r}}$ compound relay TDS matrix, $\hat{\tilde{\mathbf{b}}}[i] = \left[\hat{\mathbf{b}}^T_{\mathrm{r}_1}[i]\ \hat{\mathbf{b}}^T_{\mathrm{r}_2}[i]\ ...\ \hat{\mathbf{b}}^T_{\mathrm{r}_{N_\mathrm{r}}}[i]\right]^T$, $\boldsymbol{\mathcal{H}}_{\mathrm{rd}}[i] = \left[\mathbf{H}_{\mathrm{r}_1\mathrm{d}}[i]\ \mathbf{H}_{\mathrm{r}_2\mathrm{d}}[i]\ ...\ \mathbf{H}_{\mathrm{r}_{N_\mathrm{r}}\mathrm{d}}[i]\right]$ is the $N_{\mathrm{ad}} \times N_{\mathrm{ar}}N_{\mathrm{r}}$ compound channel matrix and $\boldsymbol{\mathcal{A}}_{\mathrm{r}}[i] = \mathrm{diag}\left[\mathbf{A}_{\mathrm{r}_1}[i]\ \mathbf{A}_{\mathrm{r}_2}[i]...\mathbf{A}_{\mathrm{r}_{N_\mathrm{r}}}[i]\right]$ is the compound power allocation matrix where $\mathrm{trace}(\boldsymbol{\mathcal{A}}^H_{\mathrm{r}}[i]\boldsymbol{\mathcal{A}}_{\mathrm{r}}[i]) = 1$. The final received signal at the destination is formed by stacking the received signals from the relay and source nodes to give

$$\mathbf{r}_{\mathrm{d}}[i] = \begin{bmatrix} \mathbf{r}_{\mathrm{sd}}[i] \\ \\ \mathbf{r}_{\mathrm{rd}}[i] \end{bmatrix}. \tag{4.6}$$

4.2.2 Amplify-and-Forward

For the AF protocol, the common approach of compounding the first and second phase signals and channels is used [3]. The resulting expression for the destination's second phase received signal is given by

$$\mathbf{r}_{\mathrm{rd}}[i] = \boldsymbol{\mathcal{H}}_{\mathrm{rd}}[i]\boldsymbol{\mathcal{A}}_{\mathrm{r}}[i]\boldsymbol{\mathcal{T}}_{\mathrm{r}}[i]\bar{\mathbf{r}}_{\mathrm{sr}}[i] + \boldsymbol{\eta}_{\mathrm{rd}}, \tag{4.7}$$

where $\bar{\mathbf{r}}_{\mathrm{sr}}[i]$ can be interpreted as the AF equivalent of $\hat{\mathbf{s}}[i]$. Expanding (4.7) yields

$$\begin{aligned} \mathbf{r}_{\mathrm{rd}}[i] \ = \ & \boldsymbol{\mathcal{H}}_{\mathrm{rd}}[i]\boldsymbol{\mathcal{A}}_{\mathrm{r}}[i]\boldsymbol{\mathcal{T}}_{\mathrm{r}}[i]\boldsymbol{\mathcal{H}}_{\mathrm{sr}}[i]\mathbf{A}_{\mathrm{s}}[i]\mathbf{T}_{\mathrm{s}}[i]\mathbf{b}[i] \\ & + \boldsymbol{\mathcal{H}}_{\mathrm{rd}}[i]\boldsymbol{\mathcal{A}}_{\mathrm{r}}[i]\boldsymbol{\mathcal{T}}_{\mathrm{r}}[i]\bar{\boldsymbol{\eta}}_{sr} \\ & + \boldsymbol{\eta}_{\mathrm{rd}} \end{aligned} , \tag{4.8}$$

where $\bar{\mathbf{r}}_{\mathrm{sr}}[i] = \left[\mathbf{r}^T_{\mathrm{sr}_1}[i]\ \mathbf{r}^T_{\mathrm{sr}_2}[i]\ ...\ \mathbf{r}^T_{\mathrm{sr}_{N_\mathrm{r}}}[i]\right]^T$, $\boldsymbol{\mathcal{H}}_{\mathrm{sr}}[i] = \left[\mathbf{H}^T_{\mathrm{sr}_1}[i]\ \mathbf{H}^T_{\mathrm{sr}_2}[i]\ ...\ \mathbf{H}^T_{\mathrm{sr}_{N_\mathrm{r}}}[i]\right]^T$ and $\boldsymbol{\mathcal{A}}_{\mathrm{r}}[i]$ normalises the average transmit power of the second phase based on the each relay's receive power. The received signals of the first and second phases can then be stacked

as in (4.6) to give $\mathbf{r}_{\mathrm{d}}[i]$.

4.3 MMSE Reception

In cooperative MIMO networks, signal detection and interference suppression is required for the signals given by (4.2) and (4.6). This chapter focuses on MMSE based reception techniques at the relays and destination due to their simplicity, versatility and the ease of extracting performance metrics. The primarily concentration is on the DF protocol but expressions for reception at the destination node are easily transferred to AF.

4.3.1 Optimal Linear MMSE

Linear MMSE reception can be achieved with the use of the Wiener filter. The optimisation functions for the Wiener filter at the n^{th} relay and the destination are given by

$$\mathbf{W}_{\mathrm{r}_n}^{\mathrm{opt}} = \arg\min_{\mathbf{W}_{\mathrm{r}_n}[i]} E\Big\|\mathbf{b}[i] - \underbrace{\mathbf{W}_{\mathrm{r}_n}^{H}[i]\mathbf{r}_{\mathrm{sr}_n}[i]}_{\mathbf{z}_{\mathrm{r}_n}[i]}\Big\|^2 \tag{4.9}$$

and

$$\mathbf{W}_{\mathrm{d}}^{\mathrm{opt}} = \arg\min_{\mathbf{W}_{\mathrm{d}}[i]} E\Big\|\mathbf{b}[i] - \underbrace{\mathbf{W}_{\mathrm{d}}^{H}[i]\mathbf{r}_{\mathrm{d}}[i]}_{\mathbf{z}_{\mathrm{d}}[i]}\Big\|^2 \tag{4.10}$$

whose dimensions are $N_{\mathrm{ar}} \times N_{\mathrm{as}}$ and $2N_{\mathrm{ad}} \times N_{\mathrm{as}}$, respectively. These expressions yield the following filters

$$\mathbf{W}_{\mathrm{sr}_n} = \mathbf{R}_{\mathrm{sr}_n}^{-1}\mathbf{P}_{\mathrm{sr}_n} \tag{4.11}$$

and

$$\mathbf{W}_{\mathrm{d}} = \mathbf{R}_{\mathrm{d}}^{-1}\mathbf{P}_{\mathrm{d}} \tag{4.12}$$

where $\mathbf{R}_{\mathrm{sr}_n} = E\left[\mathbf{r}_{\mathrm{sr}_n}[i]\mathbf{r}^H_{\mathrm{sr}_n}[i]\right]$, $\mathbf{P}_{\mathrm{sr}_n} = E\left[\mathbf{r}_{\mathrm{sr}_n}[i]\mathbf{b}^H[i]\right]$, $\mathbf{R}_{\mathrm{d}} = E\left[\mathbf{r}_{\mathrm{d}}[i]\mathbf{r}^H_{\mathrm{d}}[i]\right]$ and $\mathbf{P}_{\mathrm{d}} = E\left[\mathbf{r}_{\mathrm{d}}[i]\mathbf{b}^H[i]\right]$. The MSE at the destination and n^{th} relay can then be given by

$$\sigma^2_{\mathbf{s}} - \mathrm{trace}\left(\mathbf{P}^H_{\mathrm{d}}\mathbf{R}^{-1}_{\mathrm{d}}\mathbf{P}_{\mathrm{d}}\right) \tag{4.13}$$

and

$$\sigma^2_{\mathbf{b}} - \mathrm{trace}\left(\mathbf{P}^H_{\mathrm{sr}_n}\mathbf{R}^{-1}_{\mathrm{sr}_n}\mathbf{P}_{\mathrm{sr}_n}\right), \tag{4.14}$$

respectively, where $\sigma^2_{\mathbf{b}} = E\left[\mathbf{b}^H[i]\mathbf{b}[i]\right]$.

4.3.2 Optimal MMSE SIC

Non-linear reception offers performance advantages in MIMO systems by assisting in the mitigation of the multi-antenna interference; however, this is at the cost of increased complexity. By using MMSE SIC, advantages can be obtained whilst avoiding the complexity associated with other non-linear methods such as sphere and full maximum likelihood decoding. The implementation of SIC in MIMO systems has been addressed in previous works but cooperative DF MIMO systems add an additional layer of complexity to the process due to two reception phases and the multiple, independent nodes transmitting simultaneously [97, 98].

To perform SIC at the destination a modified destination received vector with the contribution of the $l^{\mathrm{th}} - 1$ data streams removed for the l^{th} layer of decoding is required

$$\mathbf{r}^l_{\mathrm{d}}[i] = \begin{bmatrix} \mathbf{r}^l_{\mathrm{sd}}[i] \\ \mathbf{r}^l_{\mathrm{rd}}[i] \end{bmatrix}, \tag{4.15}$$

where

$$\mathbf{r}^l_{\mathrm{rd}}[i] = \mathbf{r}_{\mathrm{rd}}[i] - \boldsymbol{\mathcal{H}}_{\mathrm{rd}}[i]\boldsymbol{\mathcal{A}}_{\mathrm{r}}[i]\boldsymbol{\mathcal{T}}_{\mathrm{r}}[i]\hat{\tilde{\mathbf{b}}}^{l-1}_{\mathrm{d}}[i] \tag{4.16}$$

and

$$\mathbf{r}^l_{\mathrm{sd}}[i] = \mathbf{r}_{\mathrm{sd}}[i] - \mathbf{H}_{\mathrm{sd}}[i]\mathbf{A}_{\mathrm{s}}[i]\mathbf{T}_{\mathrm{s}}[i]\hat{\mathbf{b}}^{l-1}_{\mathrm{d}}[i]. \tag{4.17}$$

The detection and estimation of the l^{th} data stream at the destination is performed using the relayed and direct signals. Interference cancelation is then implemented in a batch process where the detection order can be optimised in accordance with a selected criterion. In the cooperative system considered here, a single destination symbol estimate is used to generate the cancelation terms for all the relevant source and relay antennas, thus the implicit assumption that all relays transmit the identical data is made. The $N_{\text{ar}}N_{\text{r}} \times 1$ estimated symbol interference cancelation vector is given by

$$\hat{\tilde{\mathbf{b}}}_{\text{d}}^{l}[i] = \begin{bmatrix} \hat{\mathbf{b}}_{\text{d}}^{l}[i] \\ \vdots \\ \hat{\mathbf{b}}_{\text{d}}^{l}[i] \end{bmatrix} \tag{4.18}$$

where

$$\underset{l=0}{\hat{\mathbf{b}}_{\text{d}}^{0}[i]} = \begin{bmatrix} 0 \\ \vdots \\ 0 \end{bmatrix} \quad \underset{l=1\cdots N_{\text{as}}-1}{\hat{\mathbf{b}}_{\text{d}}^{l}[i]} = \begin{bmatrix} \hat{b}_{\text{d}}^{1}[i] \\ \vdots \\ \hat{b}_{\text{d}}^{l}[i] \\ \mathbf{0}_{(N_{\text{as}}-l)\times 1} \end{bmatrix}. \tag{4.19}$$

are $N_{\text{ar}} \times 1$ estimated symbols vectors. The destination Wiener filter for the l^{th} layer is then given by

$$\mathbf{w}_{\text{d}}^{l} = \mathbf{R}_{\text{d}}^{l\,-1}\mathbf{p}_{\text{d}}^{l}, \tag{4.20}$$

where $\mathbf{R}_{\text{d}}^{l}$ and $\mathbf{p}_{\text{d}}^{l}$ are the associated correlation matrices. MMSE SIC is also undertaken at each relay and the modified received signal for the l^{th} layer of decoding at the n^{th} relay is given by

$$\mathbf{r}_{\text{sr}_n}^{l}[i] = \mathbf{r}_{\text{sr}_n}[i] - \mathbf{H}_{\text{sr}_n}[i]\mathbf{A}_{\text{s}}[i]\mathbf{T}_{\text{s}}[i]\hat{\mathbf{b}}_{\text{r}_n}^{l-1}[i] \tag{4.21}$$

where

$$\underset{l=0}{\hat{\mathbf{b}}^{0}_{\mathrm{r}_n}}[i] = \begin{bmatrix} 0 \\ \vdots \\ 0 \end{bmatrix} \qquad \text{and} \qquad \underset{l=1\cdots N_{\mathrm{as}}-1}{\hat{\mathbf{b}}^{l}_{\mathrm{r}_n}}[i] = \begin{bmatrix} \hat{b}^{1}_{\mathrm{r}_n}[i] \\ \vdots \\ \hat{b}^{l}_{\mathrm{r}_n}[i] \\ \mathbf{0}_{(N_{\mathrm{as}}-l)\times 1}. \end{bmatrix} \tag{4.22}$$

have a dimensionality of $N_{\mathrm{as}} \times 1$ and form the estimated symbol interference cancelation vector. The associated Wiener filter is given by

$$\mathbf{w}^{l}_{\mathrm{r}_n} = \mathbf{R}^{l\ -1}_{\mathrm{r}_n}\mathbf{p}^{l}_{\mathrm{r}_n}, \tag{4.23}$$

where $\mathbf{R}^{l}_{\mathrm{r}_n}$ and $\mathbf{p}^{l}_{\mathrm{r}_n}$ are the required correlation matrices. The MSE resulting from SIC at the relays and destination are given by

$$\mathrm{MSE}_{\mathrm{r}_n} = \sigma^2_{\mathbf{s}} - \sum_{j=1}^{N_{\mathrm{as}}} \left(\mathbf{P}^{j\ H}_{\mathrm{r}_n} \mathbf{R}^{j\ -1}_{\mathrm{r}_n} \mathbf{P}^{j}_{\mathrm{r}_n} \right) \tag{4.24}$$

$$\mathrm{MSE}_{\mathrm{d}} = \sigma^2_{\mathbf{s}} - \sum_{j=1}^{N_{\mathrm{as}}} \left(\mathbf{P}^{j\ H}_{\mathrm{d}} \mathbf{R}^{j\ -1}_{\mathrm{d}} \mathbf{P}^{j}_{\mathrm{d}} \right), \tag{4.25}$$

respectively.

4.3.3 Iterative Adaptive Linear MMSE

Adaptive reception and interference suppression presents a low-complexity and practical alternative to the two previous techniques. By iteratively converging towards the optimal estimation and interference suppression filter the computational expense can be significantly reduced. Derivation of such an approach begins as in Section 4.3.1 with an MSE optimisation problem given by

$$\mathbf{W}^{\mathrm{opt}}_{\mathrm{d}}[i] = \underset{\mathbf{W}_{\mathrm{d}}[i]}{\arg\min}\ E\left[\left\| \mathbf{b}[i] - \mathbf{W}^{H}_{\mathrm{d}}[i]\mathbf{r}_{\mathrm{d}}[i] \right\|^2 \right]. \tag{4.26}$$

However, instead of solving optimally, a stochastic gradient approach is chosen and the gradient taken with respect to the filter $\mathbf{W}_{\mathrm{d}}$. A recursive LMS update equation can then be formed with the aid of a step-size μ, resulting in

$$\mathbf{W}_{\mathrm{d}}[i+1] = \mathbf{W}_{\mathrm{d}}[i] + \mu_{\mathbf{d}}\mathbf{r}_{\mathrm{d}}[i]\mathbf{e}_{\mathrm{d}}^{H}[i], \tag{4.27}$$

where

$$\mathbf{e}_{\mathrm{d}}[i] = \mathbf{s}[i] - \mathbf{W}_{\mathrm{d}}^{H}[i]\mathbf{r}_{\mathrm{d}}[i] \tag{4.28}$$

and $\mathbf{b}[i]$ is provided by a known training sequence or in a decision directed manner. A similar approach is also taken for reception at the relay nodes, resulting in the following LMS update equation

$$\mathbf{W}_{\mathrm{r}_n}[i+1] = \mathbf{W}_{\mathrm{d}}[i] + \mu_{\mathrm{r}}\mathbf{r}_{\mathrm{r}_n}[i]\mathbf{e}_{\mathrm{r}_n}^{H}[i], \tag{4.29}$$

where

$$\mathbf{e}_{\mathrm{r}_n}[i] = \mathbf{b}[i] - \mathbf{W}_{\mathrm{r}_n}^{H}[i]\mathbf{r}_{\mathrm{r}_n}[i]. \tag{4.30}$$

4.3.4 MMSE Power Allocation and Interference Suppression

To enhance the performance of a cooperative MIMO system, the relay power allocation can be optimised. This allows increased transmit power to be dedicated to the relay-destination channels that have advantageous transmission characteristics. Due to the MMSE reception techniques utilised in this chapter, the focus is on MMSE power allocation optimisation. This allows full integration between the reception and power allocation procedures but also does not burden the system with additional metric calculations. However, the received signal first requires reformulating to enable optimisation of the transmit power allocation vector,

$$\mathbf{r}_{\mathrm{rd}}[i] = \boldsymbol{\mathcal{H}}_{\mathrm{rd}}[i]\hat{\bar{\mathbf{B}}}[i]\bar{\boldsymbol{a}}_{\mathrm{r}}[i] + \boldsymbol{\eta}_{\mathrm{rd}}[i] \tag{4.31}$$

where $\hat{\bar{\mathbf{B}}}[i] = \text{diag}\left[\hat{\bar{\mathbf{b}}}[i]\right]$ is the $N_{\text{ar}}N_{\text{r}} \times N_{\text{ar}}N_{\text{r}}$ compound relay estimated data matrix and the $N_{\text{ad}}N_{\text{r}} \times 1$ compound power allocation vector, $\bar{\mathbf{a}}_{\text{r}}[i]$, is given by the diagonal elements of $\mathcal{A}_{\text{r}}[i]$, where $\bar{\boldsymbol{a}}_{\text{r}}^{H}[i]\bar{\boldsymbol{a}}_{\text{r}}[i] = 1$.

Forming a joint power allocation and receive filter optimisation function yields

$$\left[\mathbf{W}_{\text{d}}^{\text{opt}}[i], \bar{\boldsymbol{a}}_{\text{r}}^{\text{opt}}[i]\right] = \underset{\mathbf{W}_{\text{d}}[i], \bar{\boldsymbol{a}}_{\text{r}}[i]}{\arg\min}\, E\left[\left\|\mathbf{b}[i] - \mathbf{W}_{\text{d}}^{H}[i]\mathbf{r}_{\text{d}}[i]\right\|^2\right] \tag{4.32}$$

$$\text{subject to } \bar{\boldsymbol{a}}_{r}^{H}[i]\bar{\boldsymbol{a}}_{r}[i] = 1.$$

To solve optimally, the method of Lagrange multipliers is used to transform (4.32) into an unconstrained optimisation problem, yielding

$$\mathcal{L} = E\left[\left\|\mathbf{b}[i] - \mathbf{W}_{\text{d}}^{H}[i]\mathbf{r}_{\text{d}}[i]\right\|^2\right] + \lambda(\bar{\boldsymbol{a}}_{r}^{H}[i]\bar{\boldsymbol{a}}_{r}[i] - 1), \tag{4.33}$$

where λ is the Lagrange multiplier [63]. By fixing $\mathbf{W}_{\text{d}}$ and taking the gradient with respect to $\bar{\boldsymbol{a}}_{r}$, an optimum expression for the power allocation vector is reached

$$\bar{\boldsymbol{a}}_{r}[i] = (\mathbf{R}_{\bar{\mathbf{a}}} + \lambda\mathbf{I})^{-1}\mathbf{p}_{\bar{\mathbf{a}}}, \tag{4.34}$$

where $\mathbf{R}_{\bar{\mathbf{a}}} = E\left[\bar{\mathbf{B}}^{H}[i]\boldsymbol{\mathcal{H}}_{\text{rd}}^{H}[i]\tilde{\mathbf{W}}_{\text{d}}[i]\mathbf{W}_{\text{d}}^{H}[i]\boldsymbol{\mathcal{H}}_{\text{rd}}[i]\bar{\mathbf{B}}[i]\right]$, $\mathbf{p}_{\bar{\mathbf{a}}} = E\left[\bar{\mathbf{B}}^{H}[i]\boldsymbol{\mathcal{H}}_{\text{rd}}^{H}[i]\tilde{\mathbf{W}}_{\text{d}}[i]\mathbf{b}[i]\right]$ and $\tilde{\mathbf{W}}_{\text{d}}[i]$ contains rows $N_{\text{ad}} + 1$ to $2N_{\text{ad}}$ of $\mathbf{W}_{\text{d}}[i]$. The optimal $\mathbf{W}_{\text{d}}[i]$ can then be derived in a similar fashion to that of Section 4.3.1.

Once again, this optimal MMSE procedure can be implemented in an iterative fashion. This is done by taking the gradient of (4.32) with respect to $\mathbf{W}_{\text{d}}^{H}[i]$ whilst fixing $\bar{\boldsymbol{a}}_{\text{r}}[i]$, and vice versa. The LMS update expressions for the linear receive filter and power allocation vector can then be formed

$$\mathbf{W}_{\text{d}}[i+1] = \mathbf{W}_{\text{d}}[i] + \mu\mathbf{r}_{\text{d}}[i]\mathbf{e}_{\text{d}}^{H}[i] \tag{4.35}$$

and

$$\bar{\boldsymbol{a}}_{\mathrm{r}}[i+1] = \bar{\boldsymbol{a}}_{\mathrm{r}}[i] + \nu \bar{\mathbf{B}}^{H}[i] \boldsymbol{\mathcal{H}}_{\mathrm{rd}}^{H}[i] \tilde{\mathbf{W}}_{\mathrm{d}}[i] \mathbf{e}_{\mathrm{d}}[i] \tag{4.36}$$

where

$$\mathbf{e}_{\mathrm{d}}[i] = \mathbf{b}[i] - \mathbf{W}_{\mathrm{d}}^{H}[i] \mathbf{r}_{\mathrm{d}}[i] \tag{4.37}$$

and μ and ν are manually set step-sizes. At each iteration, (4.35) and (4.36) are performed followed by enforcement of the power constraint of (4.32). However, if enforcement of the power constraint is sought via the Lagrangian multiplier of (4.33), the solution of a complex quadratic problem is required [63]. To avoid the complexity associated with this, the following alternative power normalisation is performed at each time instant

$$\bar{\boldsymbol{a}}_{\mathrm{r}}[i+1] = \frac{\bar{\boldsymbol{a}}_{\mathrm{r}}[i+1]}{\sqrt{\bar{\boldsymbol{a}}_{\mathrm{r}}^{H}[i+1] \bar{\boldsymbol{a}}_{\mathrm{r}}[i+1]}}. \tag{4.38}$$

4.4 Transmit Diversity Optimisation

The added spatial diversity and multiplexing that cooperative MIMO achieves compared to single antenna systems make it an attractive transmission methodology. However, undiscerning use of the available channels when a number may have poor transmission characteristics leads to performance degradation, a loss of achievable diversity and capacity, and increased interference. These problems can be alleviated by the intelligent selection of transmit antennas of each phase in a process termed here as TDS. The requirement to maintain maximum multiplexing gain in the system prohibits selection at the source node and therefore selection at the relays using $\boldsymbol{\mathcal{T}}_{\mathrm{r}}[i]$ is concentrated upon. By optimising the selection of $\boldsymbol{\mathcal{T}}_{\mathrm{r}}[i]$ it is possible to optimise the performance of the system as a whole. The limited number of relay antennas and the finite number of possible states of each (on/off) makes the selection of $\boldsymbol{\mathcal{T}}_{\mathrm{r}}[i]$ a discrete and permutation based task. Therefore the selection task for each reception technique is formed as a discrete optimisation problem.

4.4.1 Optimal Linear MMSE

The availability of MSE information from reception of second phase makes TDS optimisation based on this metric an attractive and low-cost procedure. To begin the optimisation a discrete cost function is first required, given by

$$\begin{aligned} \boldsymbol{\mathcal{T}}_{\mathrm{r}}^{\mathrm{opt}} &= \underset{\boldsymbol{\mathcal{T}}_{\mathrm{r}}[i]\in\Omega_{\mathrm{T}}}{\arg\min}\, C\left[i, \boldsymbol{\mathcal{T}}_{\mathrm{r}}[i]\right] \\ &= \underset{\boldsymbol{\mathcal{T}}_{\mathrm{r}}[i]\in\Omega_{\mathrm{T}}}{\arg\min}\, E\left[\left\|\mathbf{b}[i] - \mathbf{W}_{\mathrm{d}}\left[i, \boldsymbol{\mathcal{T}}_{\mathrm{r}}[i]\right]\mathbf{r}_{\mathrm{d}}\left[i, \boldsymbol{\mathcal{T}}_{\mathrm{r}}[i]\right]\right\|^2\right] \end{aligned} \tag{4.39}$$

where the TDS matrix is chosen from a finite set of candidates denoted by Ω_{T}. The solution to (4.39) can be found by searching the set been generated from the permutations of active antennas over all the relays, Ω_{T}. However, the cardinality of such a set, $\#\Omega_{\mathrm{T}}$, is extremely large even at modest numbers of relays and antennas. When all antennas are active and inter-relay communication is assumed $\#\Omega_{\mathrm{T}} = (N_{\mathrm{ar}} \times N_{\mathrm{r}})!$ and rises further when not all antennas are required to be active. Searching of such a set is clearly impractical and therefore methods to reduce $\#\Omega_{\mathrm{T}}$ are required. Initially the problem is transformed from a permutation based to a combinatorial one by prohibiting inter-relay communications and restricting the allocation of data streams to antennas. The distance between relays and the additional computational expense of inter-relay communication leads us to the realistic and common assumption of no inter-relay communication. This restricts relays to only forward data that has been decoded locally. In addition to this, if $N_{\mathrm{ar}} = N_{\mathrm{as}}$ at each relay, it is possible to pre-allocate data streams to transmit antennas and therefore remove complexity from the relaying process whilst reducing $\#\Omega_{\mathrm{T}}$ without bias towards certain data streams. To do this data streams pre-allocated such that each stream is transmitted from its correspondingly numbered antenna at each relay. The final condition placed on the selection of transmit antennas is to specify the size of the subset of active antennas, a value denoted $N_{\mathrm{a_{sub}}}$ where $1 < N_{\mathrm{a_{sub}}} < N_{\mathrm{r}}$. This constraint ensures that a minimum level of achievable diversity is available whilst ensuring increased robustness by preventing the use of poor quality channels. The combined effect of these

conditions and restrictions is a reduced set Ω_{T} which has a cardinality

$$\#\Omega_{\mathrm{T}} = \binom{N_{\mathrm{ar}} N_{\mathrm{r}}}{N_{\mathrm{a_{sub}}}}, \tag{4.40}$$

where $\mathrm{trace}(\boldsymbol{\mathcal{T}}_{\mathrm{r}}[i]) = N_{\mathrm{a_{sub}}}$ when TDS is employed. This updated candidate set of TDS matrices can now be inserted into the MSE cost function given by (4.39), and the equations of (4.13) and (4.14) used to provide the necessary MSE information to solve (4.39).

4.4.2 Optimal MMSE SIC

The process of TDS can be extended to SIC and offers the prospect of performance advantages over that of standard SIC. As previously set out, the process of TDS is a discrete optimisation task whose performance and complexity is heavily dependent on the cardinality of the candidate set of solutions. Consequently, the considered set of solutions will be refined as it has been for in Section 4.4 for optimal linear MMSE reception. This refined set can then be placed in a TDS SIC optimisation function, giving

$$\begin{aligned} \boldsymbol{\mathcal{T}}_{\mathrm{r}}^{\mathrm{opt}} &= \underset{\boldsymbol{\mathcal{T}}_{\mathrm{r}}[i] \in \Omega_{\mathrm{T}}}{\arg\min}\, C^{\mathrm{sic}}\left[i, \boldsymbol{\mathcal{T}}_{\mathrm{r}}[i]\right] \\ &= \underset{\boldsymbol{\mathcal{T}}_{\mathrm{r}}[i] \in \Omega_{\mathrm{T}}}{\arg\min} \sum_{l=1}^{N_{\mathrm{as}}} E\left[\left\| b^{l}[i] - \mathbf{w}_{\mathrm{d}}^{l}\left[i, \boldsymbol{\mathcal{T}}_{\mathrm{r}}[i]\right] \mathbf{r}_{\mathrm{d}}^{l}\left[i, \boldsymbol{\mathcal{T}}_{\mathrm{r}}[i]\right] \right\|^{2}\right]. \end{aligned} \tag{4.41}$$

As before, the task is to then select the optimal TDS matrix from the set Ω_{T} with respect to MSE performance.

4.4.3 Mutual Information and Capacity Maximisation

Maximisation of the enhanced capacity and sum-rate that cooperative MIMO networks offer leads to a second optimisation criterion based on the mutual information of the system. Once again the concentration shall be on the second phase due to the lack of antenna redundancy at the source node. The optimisation framework given in Section 4.4 will be used but the optimality of each selection will be determined by its effect on

the mutual information.

In [18, 109] the formulation of the mutual information of a conventional MIMO system is studied. Treating the cooperative system considered in this work in a similar manner it is possible to arrive at an expression for the mutual information of the second phase. Fundamentally, the mutual information of the second phase is given by the difference between the differential and the conditional differential entropy of the received signal when the transmit data are known. This can be expressed as

$$I_{\mathrm{d}}\left(\mathbf{b};\mathbf{r}_{\mathrm{rd}}\right) = H(\mathbf{r}_{\mathrm{rd}}) - H(\mathbf{r}_{\mathrm{rd}}|\mathbf{b}). \tag{4.42}$$

With further manipulation presented in [18, 109], the mutual information of the second phase can be expressed as

$$I_{\mathrm{T}}\left(\mathbf{b};\mathbf{r}_{\mathrm{rd}},i,\boldsymbol{\mathcal{T}}_{\mathrm{r}}[i]\right) = \log_2\mathrm{det}\left(\mathbf{I}_{N_{\mathrm{a}}} + \frac{1}{N_{\mathrm{a_{sub}}}\sigma_{\eta}^2}E\left[\boldsymbol{\mathcal{H}}_{\mathrm{rd}}[i]\boldsymbol{\mathcal{T}}_{\mathrm{r}}[i]\hat{\tilde{\mathbf{b}}}[i]\hat{\tilde{\mathbf{b}}}^{H}[i]\boldsymbol{\mathcal{T}}_{\mathrm{r}}^{H}[i]\boldsymbol{\mathcal{H}}_{\mathrm{rd}}^{H}[i]\right]\right). \tag{4.43}$$

By transforming the TDS framework given in Section 4.4 into a maximisation procedure and inserting (4.43), the following expression is reached

$$\begin{aligned}\boldsymbol{\mathcal{T}}_{\mathrm{r}}^{\mathrm{opt}} &= \underset{\boldsymbol{\mathcal{T}}_{\mathrm{r}}[i]\in\Omega_{\mathrm{T}}}{\arg\max} I_{\mathrm{T}}\left(\mathbf{b};\mathbf{r}_{\mathrm{rd}},i,\boldsymbol{\mathcal{T}}_{\mathrm{r}}[i]\right)\\ &= \underset{\boldsymbol{\mathcal{T}}_{\mathrm{r}}[i]\in\Omega_{\mathrm{T}}}{\arg\max}\ \log_2\mathrm{det}\Big(\mathbf{I}_{N_{\mathrm{a}}}+\\ &\qquad \frac{1}{N_{\mathrm{a_{sub}}}\sigma_{\eta_{\mathrm{rd}}}^2}\boldsymbol{\mathcal{H}}_{\mathrm{rd}}[i]\boldsymbol{\mathcal{T}}_{\mathrm{r}}[i]\mathbf{R}_{\hat{\tilde{\mathbf{s}}}}\boldsymbol{\mathcal{T}}_{\mathrm{r}}^{H}[i]\boldsymbol{\mathcal{H}}_{\mathrm{rd}}^{H}[i]\Big),\end{aligned} \tag{4.44}$$

where the autocorrelation matrix of the transmitted relay data is given by

$$\mathbf{R}_{\hat{\tilde{\mathbf{b}}}} = E\left[\hat{\tilde{\mathbf{b}}}[i]\hat{\tilde{\mathbf{b}}}^{H}[i]\right] = \begin{bmatrix}\mathbf{I}_{N_{\mathrm{a}}} & \cdots & \mathbf{I}_{N_{\mathrm{a}}}\\ \vdots_{N_{\mathrm{r}}} & \ddots & \vdots\\ \mathbf{I}_{N_{\mathrm{a}}} & \underset{N_{\mathrm{r}}}{\cdots} & \mathbf{I}_{N_{\mathrm{a}}}\end{bmatrix}. \tag{4.45}$$

Once again, the optimisation problem posed by (4.45) is a discrete combinational prob-

lem where the finite set Ω_{T} contains the potential solutions and is required to be searched for a solution to be found.

4.4.4 Iterative Adaptive Linear MMSE

Here an optimisation problem based on low-complexity continuous iterative adaptive linear MMSE reception and the discrete TDS is posed. This is a joint optimisation problem but the solution to (4.10) is iteratively found as opposed to that optimally calculated in Section 4.3.1. Placing into a single continuous-discrete hybrid optimisation function yields

$$\begin{aligned}\left[\mathbf{W}_{\mathrm{d}}^{\mathrm{opt}}[i], \boldsymbol{\mathcal{T}}_{\mathrm{r}}^{\mathrm{opt}}[i]\right] &= \underset{\mathbf{W}_{\mathrm{d}}[i], \boldsymbol{\mathcal{T}}_{\mathrm{r}}[i] \in \Omega_{\mathrm{T}}}{\arg\min} \; C^{\mathrm{ad}}\left[i, \boldsymbol{\mathcal{T}}_{\mathrm{r}}[i], \mathbf{W}_{\mathrm{d}}[i]\right] \\ &= \underset{\mathbf{W}_{\mathrm{d}}[i], \boldsymbol{\mathcal{T}}_{\mathrm{r}}[i] \in \Omega_{\mathrm{T}}}{\arg\min} \; E\Big[\|\mathbf{b}[i] - \\ &\qquad \mathbf{W}_{\mathrm{d}}\left[i, \boldsymbol{\mathcal{T}}_{\mathrm{r}}[i]\right] \mathbf{r}_{\mathrm{d}}\left[i, \boldsymbol{\mathcal{T}}_{\mathrm{r}}[i]\right]\|^2 \Big] \end{aligned} . \tag{4.46}$$

However, due to the use of an LMS algorithm to arrive at $\mathbf{W}_{\mathrm{d}}[i]$, ideal MSE information is not available. Consequently, the expectation is required to be replaced with an ensemble average using the destination's squared instantaneous estimation error given by (4.28). This results in an updated expression for C^{ad} given by

$$C^{\mathrm{ad}}\left[i, \boldsymbol{\mathcal{T}}_{\mathrm{r}}[i], \mathbf{W}_{\mathrm{d}}[i]\right] = \frac{1}{i} \sum_{k=1}^{i} \|\mathbf{b}[k] - \mathbf{W}_{\mathrm{d}}\left[k, \boldsymbol{\mathcal{T}}_{\mathrm{r}}[i]\right] \mathbf{r}_{\mathrm{d}}\left[k, \boldsymbol{\mathcal{T}}_{\mathrm{r}}[i]\right]\|^2 . \tag{4.47}$$

Additional complexity savings are possible through the use of a recursive averaging procedure instead of the summation in (4.47). However, reducing the complexity further by using the unaveraged instantaneous error is not practical due to the AWGN and the unreliable estimates of $\boldsymbol{\mathcal{T}}_{\mathrm{r}}[i]$ even at high values of i.

4.5 Relay Selection

In Section 4.4, optimisation of the system is considered through the process of TDS. However, due to the separation between the two phases, the advantages available are restricted by the performance of the first phase. The primary problem which exists for MMSE reception with TDS is the possibility of pairing a high quality second phase channel with a poor quality first phase channel, a problem arising from the lack of consideration of first phase channels conditions in the TDS process. This can be alleviated through optimisation of channel pairing. A second aspect of the discrete TDS optimisation and methods to solve it, is its dependence on the cardinality of the set Ω_{T}; therefore reducing this further is desirable. However, first phase performance metrics are not directly available at the destination, inter-relay communication is prohibited and there is no antenna redundancy at the source. Consequently, direct optimisation of the first phase is not possible. To address these issues it is proposed to transfer the burden of first phase optimisation onto the destination by performing a joint optimisation procedure where the TDS set is optimised based on performance metrics from the relays. This is done by forwarding the available MSE and mutual information of each relay to the destination and then removing members of the set Ω_{T} based on the first phase performance of their relays. By removing TDS matrices from Ω_{T} that transmit from the relay(s) with the highest MSE/lowest mutual information, it is possible to reduce the probability of a mismatch between the first and second phase channels whilst reducing the size of the TDS set. This process of selecting relays to remove allows TDS optimisation to operate on a set which has been shaped by the relay metrics whilst not overly restricting the subsequent optimisation and the number of second phase channels available; a scenario which would lead to an increased chance of channel mismatch.

4.5.1 Optimal Linear MMSE

The task of RS is a discrete combinatorial problem and can be expressed as an optimisation function. The selection of the poorest performing relay based on its MSE performance under optimal linear reception can be expressed as

$$\begin{aligned} r^{\text{opt}} &= \arg \max_{r[i] \in \Omega_{\text{R}}} \mathcal{F}\left[i, r[i]\right] \\ &= \arg \max_{r[i] \in \Omega_{\text{R}}} E\left[\left\| \mathbf{b}[i] - \mathbf{w}_{\text{sr}_{r[i]}}^{H}[i]\, \mathbf{r}_{\text{sr}_{r[i]}}[i] \right\|^2 \right], \end{aligned} \tag{4.48}$$

where the set Ω_{R} contains the candidate relays.

For the selection of multiple or N_{rem} relays, the MSE of relay subsets is required. This is obtained by populating Ω_{R} with vectors of dimensionality $N_{\text{rem}} \times 1$ that contain all possible length N_{rem} combinations of relay indices such that

$$|\Omega_{\text{R}}| = \binom{N_{\text{r}}}{N_{\text{rem}}} \tag{4.49}$$

or equivalently, all possible relay subsets of cardinality N_{rem}. When placed into an optimisation framework this yields

$$\begin{aligned} \boldsymbol{r}^{\text{opt}} &= \arg \max_{\boldsymbol{r}[i] \in \Omega_{\text{R}}} \sum_{j=1}^{N_{\text{rem}}} \mathcal{F}\left[i, \boldsymbol{r}_j[i]\right] \\ &= \arg \max_{\boldsymbol{r}[i] \in \Omega_{\text{R}}} \sum_{j=1}^{N_{\text{rem}}} E\left[\left\| \mathbf{b}[i] - \mathbf{w}_{\text{sr}_{\boldsymbol{r}_j[i]}}^{H}[i]\, \mathbf{r}_{\text{sr}_{\boldsymbol{r}_j[i]}}[i] \right\|^2 \right], \end{aligned} \tag{4.50}$$

where $\mathbf{r}_j$ represents the j^{th} element of the vector $\mathbf{r}$. Following the solution of (4.48) or (4.50), set reduction can commence. This is where the TDS matrices which involve transmission from the relay(s) contained within $r^{\text{opt}}/\mathbf{r}^{\text{opt}}$ are removed from Ω_{T}. This reduced TDS set is termed $\bar{\Omega}_{\text{T}}$ and its cardinality is given by

$$\#\bar{\Omega}_{\text{T}} = \binom{N_{\text{ar}}(N_{\text{r}} - N_{\text{rem}})}{N_{\text{a}_{\text{sub}}}}. \tag{4.51}$$

The TDS optimisation given by (4.39) then operates over this set. As can be seen from (4.51), increasing N_{rem} leads to a decrease in $\#\bar{\Omega}_{\text{T}}$ and the complexity of the optimisation process. However, high values of N_{rem} greatly restricts the choice of TDS matrices and therefore second phase channels, leading to an increased probability of a first and second phase channel mismatch. Consequently, there is a balance to be struck between system performance and optimisation complexity when choosing N_{rem}. In general, N_{rem} should remain low in comparison with N_{r}, however, finer adjustment depends on the variance of the qualities of the first and second phase channels.

4.5.2 Optimal MMSE SIC

The SIC receiver when implemented in MIMO networks has the ability to offer considerable advantages over linear reception techniques. However, when applied to DF cooperative networks the separation of the first and second phases can lead to performance degradation and the effective operation of SIC breaking down. In the SIC framework set out in Sections 4.3.2 and 4.4.2, the estimated relay transmit data are formed from a single estimate based on the receive signals from the relayed and direct transmissions. This method operates on the assumption that identical symbol estimates are obtained at each relay for every time instant and that this also occurs at the destination node. However, this assumption is liable to breakdown. RS can help mitigate this problem by identifying and removing the relay(s) most likely to break the identical relay symbol estimate assumption and then refining the TDS set accordingly.

This is achieved by identifying the relay(s) with the highest MSE as for the optimal linear reception. The discrete MSE optimisation function to identify the highest MSE relay(s) are given by

$$\begin{aligned} r^{\text{opt}} &= \arg \max_{r[i] \in \Omega_{\text{R}}} \mathcal{F}^{\text{sic}}\left[i, r[i]\right] \\ &= \arg \max_{r[i] \in \Omega_{\text{R}}} \sum_{l=1}^{N_{\text{as}}} E\left[\left\| b^{l}[i] - \mathbf{w}_{\text{sr}_{r[i]}}^{H}[i]\, \mathbf{r}_{\text{sr}_{r[i]}}^{l}[i] \right\|^{2}\right] \end{aligned} \tag{4.52}$$

for the single relay case. Extending RS to multiple relays yields

$$\begin{aligned} \boldsymbol{r}^{\text{opt}} &= \arg \max_{\boldsymbol{r}[i]\in\Omega_{\text{R}}} \sum_{j=1}^{N_{\text{rem}}} \mathcal{F}^{\text{sic}}\left[i, \boldsymbol{r}_j[i]\right] \\ &= \arg \max_{\boldsymbol{r}[i]\in\Omega_{\text{R}}} \sum_{j=1}^{N_{\text{rem}}} \sum_{l=1}^{N_{\text{as}}} E\left[\left\| b^l[i] - \mathbf{w}^H_{\text{sr}_{\boldsymbol{r}_j[i]}}[i]\, \mathbf{r}^l_{\text{sr}_{\boldsymbol{r}_j[i]}}[i]\right\|^2\right]. \end{aligned} \tag{4.53}$$

The selected relay(s) are then removed from the candidate TDS set to form $\bar{\Omega}_{\text{T}}$, which (4.41) then operates over.

4.5.3 Mutual Information and Capacity Maximisation

Next the introduction of RS and its effect on the performance and complexity of the mutual information TDS process is addressed. The expression of (4.44) does not directly take account of the performance of the source-relay transmission and therefore there is a likelihood of $I_{\text{sr}_n} < I_{\text{r}_n d}$. To address this, it is proposed that the relay(s) with the lowest mutual information between the transmitted data $\mathbf{s}$ and its received signal $\mathbf{r}_{\text{sr}_n}$ are removed from consideration. This can be achieved by the discrete combinatorial optimisation problem given by

$$\begin{aligned} \boldsymbol{r}^{opt} &= \arg \min_{\boldsymbol{r}[i]\in\Omega_{\text{R}}} \sum_{j=1}^{N_{\text{rem}}} I_{\text{R}}\left(\mathbf{b}; \mathbf{r}_{\text{sr}_{\boldsymbol{r}_j[i]}}, i, \boldsymbol{r}_j[i]\right) \\ &= \arg \min_{\boldsymbol{r}[i]\in\Omega_{\text{R}}} \sum_{j=1}^{N_{\text{rem}}} \log_2 \det\left(\mathbf{I}_{N_{\text{a}}} + \frac{1}{N_{\text{a}}\sigma^2_{\eta_{\text{sr}}}} \mathbf{H}_{\text{sr}_{\boldsymbol{r}_j[i]}}[i] \mathbf{R}_{\mathbf{s}} \mathbf{H}^H_{\text{sr}_{\boldsymbol{r}_j[i]}}[i]\right) \end{aligned}, \tag{4.54}$$

where the autocorrelation matrix of the transmitted data is given by

$$\mathbf{R}_{\mathbf{b}} = E\left[\mathbf{b}[i]\mathbf{b}^H[i]\right] = \mathbf{I}_{N_{\mathbf{a}}}. \tag{4.55}$$

As before, the removal of a relay reduces the cardinality of the set over which TDS is performed and therefore improves the speed and/or complexity of the corresponding optimisation.

4.5.4 Iterative Adaptive Linear MMSE

To further illustrate the use of discrete approaches RS is now applied to adaptive linear reception. As for optimal linear reception, the optimal relay(s) shall be selected in accordance with optimisation problem given by

$$\begin{aligned} \boldsymbol{r}^{\text{opt}} &= \arg \max_{\boldsymbol{r}[i] \in \Omega_{\text{R}}} \sum_{j=1}^{N_{\text{rem}}} \mathcal{F}^{\text{ad}} \left[i, \boldsymbol{r}_j[i] \right] \\ &= \arg \max_{\boldsymbol{r}[i] \in \Omega_{\text{R}}} \sum_{j=1}^{N_{\text{rem}}} E \left[\left\| \mathbf{b}[i] - \mathbf{w}_{\text{sr}_{\boldsymbol{r}_j[i]}}^{H} [i] \, \mathbf{r}_{\text{sr}_{\boldsymbol{r}_j[i]}}[i] \right\|^2 \right]. \end{aligned} \tag{4.56}$$

However, the LMS adaptation does not perform the expectation and the MSE is replaced with an ensemble average based on the instantaneous squared relay estimation error given by (4.30). Reformulating $\mathcal{F}^{\text{ad}}$ accordingly, yields

$$\mathcal{F}^{\text{ad}} \left[i, \boldsymbol{r}_j[i] \right] = \frac{1}{i} \sum_{k=1}^{i} \left[\left\| \mathbf{b}[k] - \mathbf{w}_{\text{sr}_{\boldsymbol{r}_j[k]}}^{H} [i] \, \mathbf{r}_{\text{sr}_{\boldsymbol{r}_j[i]}}[k] \right\|^2 \right]. \tag{4.57}$$

4.5.5 MMSE Power Allocation and Interference Suppression

The structure and optimisation criteria of the optimal and iterative solutions to the joint power allocation and interference supersession optimisation, (4.32), and the standard MMSE (4.10) problem are similar. Consequently, the same RS functions as given in Sections 4.5.1 and 4.5.4 can be used when applying RS to the optimisation problems of Section 4.3.4. Once RS is complete at each time instant, the power allocation and interference suppression optimisation procedure operates over the remaining relays and antennas.

4.5.6 Extension to Amplify-and-Forward

Due to the lack of decoding at each relay in an AF system, MSE information is not available and a secondary optimisation criterion is required. Here the end-to-end SNR of each relay branch is chosen and RS based on the branch(es) with the lowest SNR

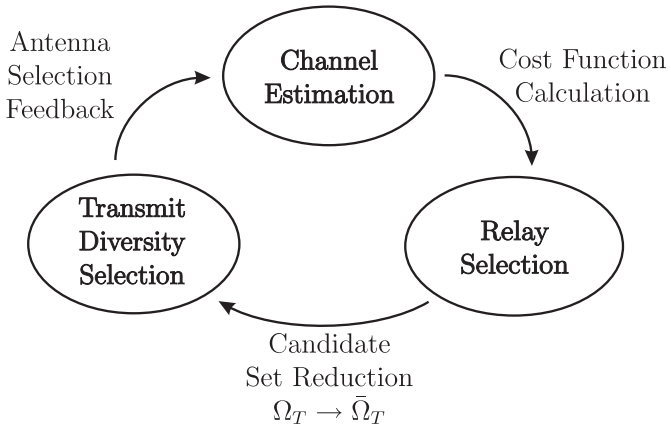

Figure 4.2: Algorithm flow diagram.

performed. Interpreting this in the multiple RS framework yields

$$\boldsymbol{r}^{\text{opt}} = \arg \min_{\boldsymbol{r}[i] \in \Omega_{\text{R}}} \sum_{j=1}^{N_{\text{rem}}} \mathcal{K}\left[i, \boldsymbol{r}_j[i]\right] \tag{4.58}$$

where

$$\mathcal{K}\left[i, \boldsymbol{r}_j[i]\right] = \frac{\text{trace}(\mathbf{H}_{\text{r}_{\boldsymbol{r}_j[i]}\text{d}}[i]\mathbf{A}_{\text{r}_{\boldsymbol{r}_j}\text{d}}[i]\mathbf{H}_{\text{sr}_{\boldsymbol{r}_j[i]}}[i]\mathbf{A}_{\text{s}}[i]\mathbf{A}_{\text{s}}^{H}[i]\mathbf{H}_{\text{sr}_{\boldsymbol{r}_j[i]}}^{H}[i]\mathbf{A}_{\text{r}_{\boldsymbol{r}_j[i]}\text{d}}^{H}[i]\mathbf{H}_{\text{r}_{\boldsymbol{r}_j[i]}\text{d}}^{H}[i])}{\text{trace}(\mathbf{H}_{\text{r}_{\boldsymbol{r}_j[i]}\text{d}}[i]\mathbf{A}_{\text{r}_{\boldsymbol{r}_j}\text{d}}[i]\sigma_{\text{sr}}^2\mathbf{I}_{N_{\text{a}}}\mathbf{A}_{\text{r}_{\boldsymbol{r}_j[i]}\text{d}}^{H}[i]\mathbf{H}_{\text{r}_{\boldsymbol{r}_j[i]}\text{d}}^{H}[i]+\sigma_{\text{rd}}^2\mathbf{I}_{N_{\text{a}}})}. \tag{4.59}$$

4.6 Proposed Algorithms

In this section, algorithms to solve the optimisation problems of Sections 4.4 and 4.5 are presented and the practicalities of their implementation addressed.

4.6.1 Transmit Diversity Selection and Relay Selection

It is proposed that the TDS and RS schemes operate in a joint and cyclic fashion where RS constantly refines the set that TDS operates over. However, to obtain solutions to the optimisation functions, backward CSI is required at the relays and destination. Due to the cyclic nature of the proposed optimisation framework it is possible to insert channel estimation without interrupting the process, a flow diagram given by Figure 4.2 shows this.

Table 4.1: Proposed discrete stochastic TDS algorithm for linear MMSE reception

Step
1. Initialisation
choose $\mathcal{T}[1] \in \Omega_{\mathrm{T}}, \mathcal{T}^{\mathrm{W}}[1] \in \Omega_{\mathrm{T}}, \boldsymbol{\pi}_{\mathrm{T}}[1, \mathcal{T}[1]] = 1,$
$\boldsymbol{\pi}_{\mathrm{T}}[1, \tilde{\mathcal{T}}] = 0$ for $\tilde{\mathcal{T}} \neq \mathcal{T}[1]$
2. For the time index $i = 1, 2, ..., N$
choose $\mathcal{T}^{\mathrm{C}}[i] \in \Omega_{\mathrm{T}}$
3. Comparison and update of the worst performing relay
if $C[i, \mathcal{T}^{\mathrm{C}}[i]] < C[i, \mathcal{T}^{\mathrm{W}}[i]]$ then $\mathcal{T}^{\mathrm{W}}[i+1] = \mathcal{T}^{\mathrm{C}}[i]$
otherwise $\mathcal{T}^{\mathrm{W}}[i+1] = \mathcal{T}^{\mathrm{W}}[i]$
4. State occupation probability (SOP) vector update
$\boldsymbol{\pi}_{\mathrm{T}}[i+1] = \boldsymbol{\pi}_{\mathrm{T}}[i] + \mu[i+1](\mathbf{v}_{\mathcal{T}^{\mathrm{W}}[i+1]} - \boldsymbol{\pi}_{\mathrm{T}}[i])$ where $\mu[i] = 1/i$
5. Determine the largest SOP vector element and select the optimum TDS matrix
if $\boldsymbol{\pi}_{\mathrm{T}}[i+1, \mathcal{T}^{\mathrm{W}}[i+1]] > \boldsymbol{\pi}_{\mathrm{T}}[i+1, \mathcal{T}[i]]$ then $\mathcal{T}[i+1] = \mathcal{T}^{\mathrm{W}}[i+1]$
otherwise $\mathcal{T}[i+1] = \mathcal{T}[i]$

The optimal but most complex method to obtain solutions to the range of TDS and RS optimisation problems is to perform an exhaustive search of the respective sets at each time instant. However, due to the power consumption and complexity constraints on nodes within the system such an approach is not possible, although it can act as a lower bound on performance. Iterative methods which converge to the optimal solution present an alternative low complexity approach and it is these that shall be used in this chapter. Conventional iterative algorithms such as the LMS and RLS are unsuitable for discrete problems and therefore a low-complexity DSA first presented in [14] and later used [91] is selected. Each set of optimisation problems can then be jointly and iteratively solved at little additional computational cost above that of the reception and decoding process.

For the optimisation problems of Sections 4.4 and 4.5, a low-complexity DSA that jointly optimises RS and TDS in accordance with: (4.39) and (4.48), (4.41) and(4.52), (4.54) and (4.45), and (4.46) and (4.56), and converges to the optimal exhaustive solution is proposed. Firstly, in Table 4.1, the TDS segment of the algorithm that performs MMSE optimisation of the TDS matrix $\boldsymbol{\mathcal{T}}_{\mathrm{r}}$ is presented. At each iteration, the MSE of a randomly chosen candidate TDS matrix ($\boldsymbol{\mathcal{T}}_{\mathrm{r}}^{\mathrm{C}}$) (step 2) and that of the best performing TDS matrix currently known ($\boldsymbol{\mathcal{T}}_{\mathrm{r}}^{\mathrm{B}}$) are calculated (step 3). Via a comparison, the lower

Table 4.2: Proposed discrete stochastic RS algorithm for linear MMSE reception

Step
1. Initialisation
choose $r[1] \in \Omega_{\mathrm{R}}, r^{\mathrm{W}}[1] \in \Omega_{\mathrm{R}}, \boldsymbol{\pi}_{\mathrm{R}}[1, r[1]] = 1,$
$\boldsymbol{\pi}_{\mathrm{R}}[1, \tilde{r}] = 0$ for $\tilde{r} \neq r[1]$
2. For the time index $i = 1, 2, ..., N$
choose $r^{\mathrm{C}}[i] \in \Omega_{\mathrm{R}}$
3. Comparison and update of the worst performing relay
if $\mathcal{F}[i, r^{\mathrm{C}}[i]] > \mathcal{F}[i, r^{\mathrm{W}}[i]]$ then $r^{\mathrm{W}}[i+1] = r^{\mathrm{C}}[i]$
otherwise $r^{\mathrm{W}}[i+1] = r^{\mathrm{W}}[i]$
4. State occupation probability (SOP) vector update
$\boldsymbol{\pi}_{\mathrm{R}}[i+1] = \boldsymbol{\pi}_{\mathrm{R}}[i] + \mu[i+1](\mathbf{v}_{r^{\mathrm{W}}[i+1]} - \boldsymbol{\pi}_{\mathrm{R}}[i])$ where $\mu[i] = 1/i$
5. Determine the largest SOP vector element and select the optimum relay
if $\boldsymbol{\pi}_{\mathrm{R}}[i+1, r^{\mathrm{W}}[i+1]] > \boldsymbol{\pi}_{\mathrm{R}}[i+1, r[i]]$ then $r[i+1] = r^{\mathrm{W}}[i+1]$
otherwise $r[i+1] = r[i]$
6. TDS Set Reduction
remove members of Ω_{T} which utilise $r[i+1]$ $(\Omega_{\mathrm{T}} \rightarrow \bar{\Omega}_{\mathrm{T}})$

MSE TDS matrix is designated $\boldsymbol{\mathcal{T}}_{\mathrm{r}}^{\mathrm{B}}$ for the next iteration (step 3). The current solution and TDS matrix chosen for transmission ($\boldsymbol{\mathcal{T}}_{\mathrm{r}}$) is denoted as the current optimum and is the TDS matrix which has occupied $\boldsymbol{\mathcal{T}}_{\mathrm{r}}^{\mathrm{B}}$ most frequently over the course of the packet up to the i^{th} time instant; effectively an average of the occupiers of $\boldsymbol{\mathcal{T}}_{\mathrm{r}}^{\mathrm{B}}$. This averaging/selection process is performed by allocating each member of Ω_{T} a $|\Omega_{\mathrm{T}}| \times 1$ unit vector, $\mathbf{v}_l$, that has a one in its corresponding position in Ω_{T} i.e. $\mathbf{v}_{\boldsymbol{\mathcal{T}}_{\mathrm{r}}^{\mathrm{B}}}[i]$ is the label of the best performing TDS matrix at the i^{th} iteration. The current optimum is then chosen and tracked by means of a $\#\Omega_{\mathrm{T}} \times 1$ state occupation probability (SOP) vector, $\boldsymbol{\pi}_{\mathrm{T}}$. This vector is updated at each iteration by adding $\mathbf{v}_{\boldsymbol{\mathcal{T}}_{\mathrm{r}}^{\mathrm{B}}}[i+i]$ and subtracting the previous value of $\boldsymbol{\pi}_{\mathrm{T}}$ (step 4). The current optimum is then determined by selecting the largest element in $\boldsymbol{\pi}_{\mathrm{T}}$ and its corresponding entry in Ω_{T} (step 5). Through this process, the current optimum converges towards and tracks the exhaustive solution [14]. An alternative interpretation of the proposed algorithm is to view the transitions, $\boldsymbol{\mathcal{T}}_{\mathrm{r}}^{\mathrm{B}}[i] \rightarrow \boldsymbol{\mathcal{T}}_{\mathrm{r}}^{\mathrm{B}}[i+1]$, as a Markov chain and the members of Ω_{T} as the possible transition states. The current optimum can then be defined as the most visited state.

Table 4.2 presents the discrete stochastic RS algorithm which provides the algorithm of Table 4.1 with a refined TDS set $(\Omega_{\mathrm{T}} \rightarrow \bar{\Omega}_{\mathrm{T}})$ in accordance with (4.48). The operation

Table 4.3: TDS Algorithm Alterations

	TDS Step 3
Linear MMSE	if $C[i,\boldsymbol{\mathcal{T}}^{\mathrm{C}}[i]] < C[i,\boldsymbol{\mathcal{T}}^{\mathrm{W}}[i]]$
SIC	if $C^{\mathrm{sic}}[i,\boldsymbol{\mathcal{T}}^{\mathrm{C}}[i]] < C^{\mathrm{sic}}[i,\boldsymbol{\mathcal{T}}^{\mathrm{W}}[i]]$
MI	if $I_{\mathrm{T}}(\mathbf{b};\mathbf{r}_{\mathrm{rd}},i,\boldsymbol{\mathcal{T}}^{\mathrm{C}}[i]) > I_{\mathrm{T}}(\mathbf{b};\mathbf{r}_{\mathrm{rd}},i,\boldsymbol{\mathcal{T}}^{\mathrm{W}}[i])$
Linear Adaptive	if $C^{\mathrm{ad}}\left[i,\boldsymbol{\mathcal{T}}^{\mathbf{C}}[i],\mathbf{W}_{\mathrm{d}}[i]\right] < C^{\mathrm{ad}}\left[i,\boldsymbol{\mathcal{T}}^{\mathbf{W}}[i],\mathbf{W}_{\mathrm{d}}[i]\right]$
AF - Linear MMSE and SNR	if $C[i,\boldsymbol{\mathcal{T}}^{\mathrm{C}}[i]] < C[i,\boldsymbol{\mathcal{T}}^{\mathrm{W}}[i]]$

Table 4.4: RS Algorithm Alterations

	RS Step 3
Linear MMSE	if $\sum_{j=1}^{N_{\mathrm{rem}}}\mathcal{F}\left[i,\boldsymbol{r}_j^{\mathbf{C}}[i]\right] > \sum_{j=1}^{N_{\mathrm{rem}}}\mathcal{F}\left[i,\boldsymbol{r}_j^{\mathbf{W}}[i]\right]$
SIC	if $\sum_{j=1}^{N_{\mathrm{rem}}}\mathcal{F}^{\mathrm{sic}}\left[i,\boldsymbol{r}_j^{\mathbf{C}}[i]\right] > \sum_{j=1}^{N_{\mathrm{rem}}}\mathcal{F}^{\mathrm{sic}}\left[i,\boldsymbol{r}_j^{\mathbf{W}}[i]\right]$
MI	if $\sum_{j=1}^{N_{\mathrm{rem}}} I_{\mathrm{R}}(\mathbf{b};\mathbf{r}_{\mathrm{rd}},i,\boldsymbol{r}_j^{\mathrm{C}}[i]) < \sum_{j=1}^{N_{\mathrm{rem}}} I_{\mathrm{R}}(\mathbf{b};\mathbf{r}_{\mathrm{rd}},i,\boldsymbol{r}_j^{\mathrm{W}}[i])$
Linear Adaptive	if $\sum_{j=1}^{N_{\mathrm{rem}}}\mathcal{F}^{\mathrm{ad}}\left[i,\boldsymbol{r}_j^{\mathbf{C}}[i]\right] > \sum_{j=1}^{N_{\mathrm{rem}}}\mathcal{F}^{\mathrm{ad}}\left[i,\boldsymbol{r}_j^{\mathbf{W}}[i]\right]$
AF - Linear MMSE and SNR	if $\sum_{j=1}^{N_{\mathrm{rem}}}\mathcal{K}\left[i,\boldsymbol{r}_j^{\mathrm{C}}[i]\right] < \sum_{j=1}^{N_{\mathrm{rem}}}\mathcal{K}\left[i,\boldsymbol{r}_j^{\mathrm{W}}[i]\right]$

of the RS algorithm in Table 4.2 is similar to that of the TDS algorithm but with a reversed inequality of step 3, enabling convergence to the highest MSE relay(s), and the addition of Step 6 that performs set reduction as described in Section 4.5. In Table 4.2 a single relay is selected but extension to the selection of multiple relays is straightforward and involves replacing R with the vector form $\boldsymbol{r}$ and using the MSE calculation of (4.50).

In order to adapt the algorithms of Table 4.1 and 4.2 for use with SIC reception, MI optimisation and adaptive reception, a number of alterations are required. These include reversing the inequality of step 3 for MI optimisation and replacing the metric calculation functions, also of step 3, for all schemes. Details of the required changes are given in Tables 4.3 and 4.4, for TDS and RS, respectively, where alterations with respect to RS are for the selection of multiple relays.

Due to the purely adaptive nature of the schemes when iterative adaptive reception is used, a number of further alterations and clarifications are required for correct oper-

Table 4.5: Power Allocation Auxiliary Variable Dimensionality

Structure	Dimensionality
$^{\dagger}\bar{\mathbf{B}}[i]$	$N_{\mathrm{a}}(N_{\mathrm{r}}-N_{\mathrm{rem}})\times N_{\mathrm{a}}(N_{\mathrm{r}}-N_{\mathrm{rem}})$
$^{\dagger}\boldsymbol{\mathcal{H}}_{\mathrm{rd}}[i]$	$N_{\mathrm{a}}\times N_{\mathrm{a}}(N_{\mathrm{r}}-N_{\mathrm{rem}})$
$^{\dagger}\bar{\boldsymbol{a}}_{\mathrm{r}}[i]$	$N_{\mathrm{a}}(N_{\mathrm{r}}-N_{\mathrm{rem}})\times 1$

ation. Firstly, updating of the receive filter at the destination for each TDS matrix and the accompanying error calculation occurs only when its corresponding TDS matrix is selected as either $\boldsymbol{\mathcal{T}}$,$\boldsymbol{\mathcal{T}}^{\mathrm{C}}$ or $\boldsymbol{\mathcal{T}}^{\mathrm{W}}$. Secondly, due to the parallel convergence of the relay filters, destination filters, TDS and RS, an extended convergence period is expected. Consequently, the step-size of step 4 ($\mu[i]$) is not suitable since it more heavily weights early samples. To avoid this, a fixed step-size is implemented which equally weights all samples and assists convergence at large values of i.

4.6.2 Relay Selection and Continuous Power Allocation

For implementation of continuous power allocation with RS, the algorithm alterations given for linear MMSE and linear adaptive reception are used. At each time instant, the entries corresponding to the relay(s) selected by the algorithm of Table 4.2 are removed from the power allocation vector along with the entries in the relay-destination channel matrix when optimal MMSE techniques are used. This reduces the dimensionality of the structures required for power allocation, therefore improving complexity and convergence. The dimensionality of these modified structures are given in Table 4.5 where $^{\dagger}(\cdot)$ represents a modified structure.

After RS, a reformulated relay-destination received vector is given by

$$\mathbf{r}_{\mathrm{rd}}[i] = {}^{\dagger}\boldsymbol{\mathcal{H}}_{\mathrm{rd}}[i]^{\dagger}\hat{\bar{\mathbf{B}}}[i]^{\dagger}\bar{\boldsymbol{a}}_{\mathrm{r}}[i] + \boldsymbol{\eta}_{\mathrm{rd}}[i], \tag{4.60}$$

which can then be introduced into the optimisation functions of Section 4.3.4 via the compound destination vector $\mathbf{r}_{\mathrm{d}}$.

4.6.3 Correlated Channels

In practical cooperative MIMO systems, the channels between antennas pairs are spatially correlated due to the close proximity of the antennas at transmitting and receiving nodes. The most straightforward approach to addressing the problem of correlated channels is to increase antennas spacing at the nodes and control the angle spread (AS) and angle of arrival (AoA) of the incoming signal power. However, these are often not practical solutions due to the size of the nodes relative to the system wavelength and the fact that AS and AoA are functions of the environment and the type of node i.e. base station or mobile station. Correlation between the channels of a system leads to performance degradation due to the challenges correlated signals pose for interference suppression procedures. Consequently, assessing the operation of transmission schemes in the presence of correlated channels is vitally important.

Generation of the correlated channels in this work is performed using the intelligent multi-element transmit and receive antennas(I-METRA) model in combination with a power azimuth spectrum model [18, 110]. Spatial correlation matrices are generated for each antenna array of the base station ($\mathbf{R}_{\text{BS}}$) and mobile station ($\mathbf{R}_{\text{MS}}$), and the overall correlation matrices for the uplink and downlink are given by

$$\begin{aligned} \mathbf{R}_{\text{UP}} &= \mathbf{R}_{\text{MS}} \otimes \mathbf{R}_{\text{BS}} \\ \mathbf{R}_{\text{DN}} &= \mathbf{R}_{\text{BS}} \otimes \mathbf{R}_{\text{MS}} \end{aligned} \tag{4.61}$$

respectively, where $\otimes$ represents the Kronecker product. The proposed schemes are applied to a macrocell environment where the PAS is given by a truncated Laplacian distribution with AS = 5° and AS = 10° for the mobile stations (source and relays) and base station respectively (destination). A single arrival cluster is assumed for all nodes and the AoA for the mobile and base station are given by 67.5° and 20° respectively. The antenna spacing at all nodes is 0.5λ where λ denotes the system wavelength.

4.6.4 RLS Channel Estimation

The operation of the proposed optimal MMSE algorithms require knowledge of the channel, however, an assumption of full CSI is unrealistic and therefore channel estimation is required. Due to the discrete stochastic algorithm used in this work, tracking of a solution is possible and also a strength of the proposed schemes. Consequently, iterative RLS channel estimation is chosen for its relatively low complexity, fast convergence and ability to jointly operate with the proposed iterative algorithms. Channel estimation shall take place at the relays and destination for the first phase and at the destination for the second phase, with no feedback of CSI required in either phase. Standard training based estimation shall be performed for $\mathbf{H}_{\mathrm{sr}_n}$ and $\mathbf{H}_{\mathrm{sd}}$ but this is not possible for $\boldsymbol{\mathcal{H}}_{\mathrm{rd}}$ due to the correlated nature of the transmit data from the relays. To perform accurate and reliable estimation of $\boldsymbol{\mathcal{H}}_{\mathrm{rd}}$, the training sequence at each relay is convoluted with an independent pre-shared PR binary sequence, γ_n, which decorrelates the transmit signal from each relay. The modified received signal at the destination is given by

$$\mathbf{r}_{rd}[i] = \boldsymbol{\mathcal{H}}_{\mathrm{rd}}[i]A_r\boldsymbol{\mathcal{T}}_{\mathrm{r}}[i]\Gamma[i]\hat{\bar{\mathbf{b}}}[i] + \boldsymbol{\eta}_{\mathrm{rd}}[i], \tag{4.62}$$

where

$$\Gamma[i] = \mathrm{diag}\left[\gamma_1[\mathrm{i}]_{\mathrm{N_a}}...\gamma_1[\mathrm{i}]_{\mathrm{N_r}}...\gamma_{\mathrm{N_r}}[\mathrm{i}]_{\mathrm{N_a}}...\gamma_{\mathrm{N_r}}[\mathrm{i}]\right], \tag{4.63}$$

and $\gamma[i] = \{-1, 1\}$. The objective function for $\boldsymbol{\mathcal{H}}_{\mathrm{rd}}$ is given by

$$\hat{\boldsymbol{\mathcal{H}}}_{\mathrm{rd}}[i] = \arg\min_{\hat{\boldsymbol{\mathcal{H}}}_{\mathrm{rd}}[i]} \sum_{i=1}^{N} \lambda^{n-i} \left|\mathbf{r}_{\mathrm{rd}}[i] - \hat{\boldsymbol{\mathcal{H}}}_{\mathrm{rd}}[i]A_{\mathrm{r}}\boldsymbol{\mathcal{T}}_{\mathrm{r}}[i]\bar{\mathbf{b}}[i]\right|^2. \tag{4.64}$$

The expressions for the second phase channel estimation are given by (4.65)-(4.68), where λ in an exponential forgetting factor. With straightforward alterations the expressions for estimation of the channels of the first phase can also be obtained.

$$\mathbf{e}_{\boldsymbol{\mathcal{H}}_{\mathrm{rd}}}[i] = \mathbf{r}_{\mathrm{rd}}[i] - \hat{\boldsymbol{\mathcal{H}}}_{\mathrm{rd}}[i]A_{\mathrm{r}}\boldsymbol{\mathcal{T}}_{\mathrm{r}}[i]\Gamma[i]\bar{\mathbf{b}}[i], \tag{4.65}$$

$$P_{\hat{\mathcal{H}}_{\mathrm{rd}}}[i] = \frac{1}{\lambda} P_{\hat{\mathcal{H}}_{\mathrm{rd}}}[i-1] - \frac{1}{\lambda} \Gamma[i] \bar{\mathbf{b}}[i] A_{\mathrm{r}} \boldsymbol{\mathcal{T}}_{\mathrm{r}}[i] K_{\hat{\mathcal{H}}_{\mathrm{rd}}}[i] P_{\hat{\mathcal{H}}_{\mathrm{rd}}}[i-1], \tag{4.66}$$

$$K_{\hat{\mathcal{H}}_{\mathrm{rd}}}[i] = \frac{\Gamma[i] \bar{\mathbf{b}}[i] A_{\mathrm{r}} \boldsymbol{\mathcal{T}}_{\mathrm{r}}[i] P_{\hat{\mathcal{H}}_{\mathrm{rd}}}[i]}{\lambda + \Gamma[i] \bar{\mathbf{b}}^{H}[i] A_{\mathrm{r}} \boldsymbol{\mathcal{T}}_{\mathrm{r}}[i] P_{\hat{\mathcal{H}}_{\mathrm{rd}}}[i] \Gamma[i] \bar{\mathbf{b}}^{H}[i] A_{\mathrm{r}} \boldsymbol{\mathcal{T}}_{\mathrm{r}}[i]} \tag{4.67}$$

and

$$\hat{\boldsymbol{\mathcal{H}}}_{\mathrm{rd}}[i] = \hat{\boldsymbol{\mathcal{H}}}_{\mathrm{rd}}[i-1] + \mathbf{e}_{\mathcal{H}_{\mathrm{rd}}}[i] K_{\hat{\mathcal{H}}_{\mathrm{rd}}}[i]. \tag{4.68}$$

Once CE has concluded, $\Gamma[i]$ may be removed or transformed to an identity matrix and normal transmission resumed.

4.7 Analysis

In this section, analysis and discussion of the four major aspects of the proposed algorithms that encompass their advantages over existing methods is presented. The four areas covered are computational complexity, convergence, diversity gain and feedback requirements.

4.7.1 Complexity

The iterative operation of the TDS algorithms offers a clear complexity advantage over an exhaustive search of the entire set of solutions. These savings result from a significant reduction in the number of calculations at each time instant for each considered set. However, as is often found in mobile systems, complexity benefits are a tradeoff against performance. In contrast to this, performing RS in combination with the TDS algorithm improves both convergence and complexity. This results from the low-complexity of the RS procedure being outweighed by the saving made from the TDS process operating over the lower cardinality set $\bar{\Omega}$. In Figure 4.3 the computational complexity in terms of the total number of complex multiplications and additions is given for the optimal exhaustive methods and the proposed DSA when optimal linear MMSE reception is used. For simplicity and conciseness, in this figure and throughout the remainder of the

chapter, N_{a} is used to refer to the number of antennas at each node, where $N_{\mathrm{a}} = N_{\mathrm{as}} = N_{\mathrm{ar}} = N_{\mathrm{ad}}$.

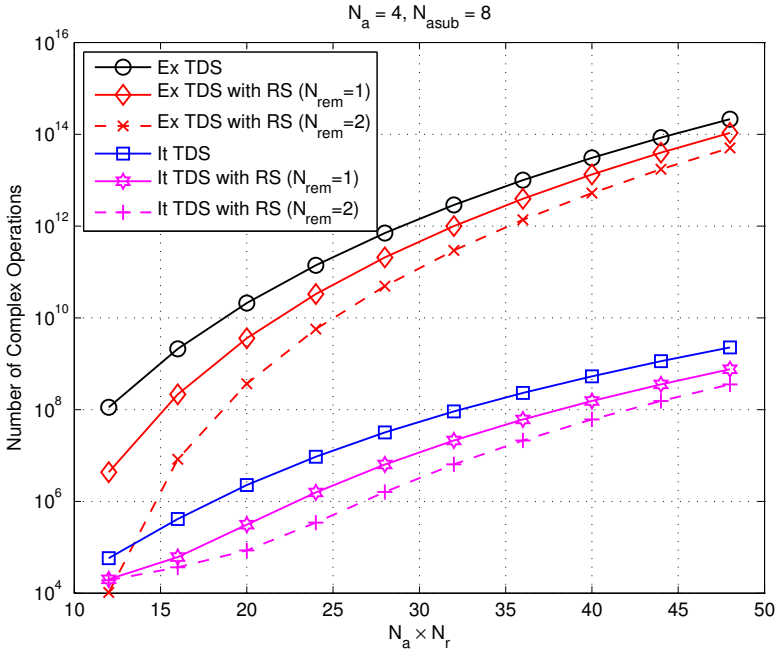

Figure 4.3: Computational complexity of optimal exhaustive (Ex) and proposed iterative (It) MMSE TDS schemes.

There are substantial complexity savings from the use of the proposed algorithms over the exhaustive solutions, savings which increase with the number of relays and total antenna elements in the system. Savings are also achieved from introducing RS into the optimal exhaustive and proposed methods. These savings also increase with system size and confirm that the complexity savings made by RS, due to set reduction, exceed the cost of its implementation. From Figure 4.3 it is evident that the savings also increase with N_{rem}, a feature explained by the following relationship

$$\left(\#\Omega_{R,N_{rem}=2} - \#\Omega_{R,N_{rem}=1}\right) \leq \left(\#\bar{\Omega}_{T,N_{rem}=1} - \#\bar{\Omega}_{T,N_{rem}=2}\right). \tag{4.69}$$

Table 4.6 presents the analytical expressions for the complexity of the linear MMSE based algorithms. The presence of the set cardinality in all expressions accounts for each scheme's complexity dependence on the set over which it operates. Also, the reasons

Table 4.6: Proposed Algorithm Complexity

Algorithm	No. of Complex Additions and Multiplications
Iterative TDS	$3\Big(3(N_aN_r)^3 + 2N_a(N_aN_r)^2 + N_aN_r(6N_a^2 + 4N_a + 5) + \cdots$ $8N_a^3 - N_a^2 + N_a + 1\Big) + 5N_rN_a^3 + N_rN_a + N_r + 3\#\Omega_T$
Iterative TDS with RS	$3\Big(3(N_aN_r)^3 + 2N_a(N_aN_r)^2 + N_aN_r(6N_a^2 + 4N_a + 5) + 8N_a^3 - \cdots$ $N_a^2 + N_a + 1\Big) + 5N_rN_a^3 + N_rN_a + N_r + 6N_a^3 - 3N_a^2 + 2\#\bar{\Omega}_T + 2\#\Omega_R$
Exhaustive TDS	$\#\Omega_T\Big(3(N_aN_r)^3 + 2N_a(N_aN_r)^2 + N_aN_r(6N_a^2 + 4N_a + 5) + \cdots$ $8N_a^3 - N_a^2 + N_a + 1\Big) + 5N_rN_a^3 + N_rN_a + N_r$
Exhaustive TDS with RS	$\#\bar{\Omega}_T\Big(3(N_aN_r)^3 + 2N_a(N_aN_r)^2 + N_aN_r(6N_a^2 + 4N_a + 5) + \cdots$ $8N_a^3 - N_a^2 + N_a + 2\Big) + 7N_rN_a^3 - N_rN_a^2 + N_rN_a + N_r + 2\#\Omega_R$
Adaptive Power Allocation	$3(N_aN_r)^3 + 2N_a(N_aN_r)^2 + N_aN_r(6N_a^2 + 4N_a + 5) + 8N_a^3 - N_a^2 + N_a + 1$ $+2N_a^3N_r + N_a^2N_r + N_aN_r + 4N_a^2$
Adaptive Power Allocation with RS	$3(N_aN_r)^3 + 2N_a(N_aN_r)^2 + N_aN_r(6N_a^2 + 4N_a + 5) + 8N_a^3 - N_a^2 + N_a + 1$ $+2N_a^3(N_r - N_{rem}) + N_a^2(N_r - N_{rem}) + N_a(N_r - N_{rem}) + 4N_a^2 + 2\#\Omega_R$

behind the complexity reduction achieved by the iterative RS algorithm are evident from the expressions for the iterative TDS and iterative TDS with RS. The majority of the savings arise from the difference between $3\#\Omega_T$ and $2\#\bar{\Omega}_T + 2\#\Omega_R$, and by referring back to the set cardinality expressions given by (4.40), (4.51) and (4.49), the characteristics of the lines of Figure 4.3 can be accounted for.

4.7.2 Feedback

A significant advantage of the discrete schemes proposed in this chapter are their low feedback requirements. No precoding is required at the transmitting nodes, TDS operates solely in the second phase, and reception at the receiving node requires only locally available CSI. Consequently, only the feedback of the TDS to the relays is required. For RS, relay MSE information is required to be forwarded. In this work it is assumed perfect, free from the effects of quantisation, and performed during the training period. As covered earlier in this work, TDS can be interpreted as discrete power control with one bit quantisation, where the relative transmit power from each antenna is constrained to either 1 or 0. As a result, N_{ar} feedback bits are required for TDS at each relay node

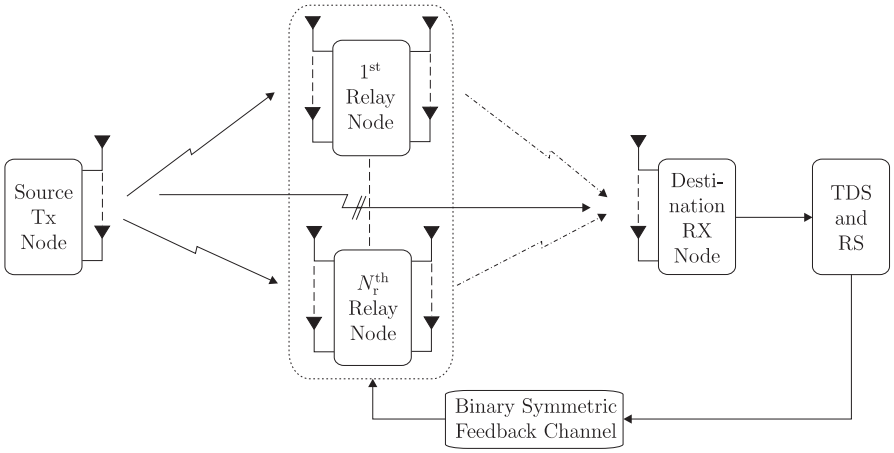

Figure 4.4: Cooperative MIMO system model with feedback model.

and a total of $N_r \times N_{ar}$ bits for the overall system, a figure which grows linearly with the size of the system. This low feedback rate increases the robustness of the TDS and RS optimisation processes and assists in maintaining performance up to significant levels of feedback errors. Additionally, the impact on the capacity of the system is small, as only a brief time slot is required for transmission of the feedback information. As expected, the feedback properties of continuous power allocation are greater and the effect of quantisation more significant. In total $2\log_2(q) \times N_r \times N_{ar}$ bits of feedback are required, where q is the number of quantisation levels and the power allocation vector is imaginary. As well as the capacity impact of the feedback, the higher number of bits also increases bit-error probability and resultant performance degradation.

A binary symmetric channel is used to model the feedback channel, the quality of which is controlled by the probability of error term where $0 \leq p_e \leq 1$. Figure 4.4 gives the system model when a feedback channel is implemented and Figure 4.5 illustrates the structure of the data and feedback packets transmitted in the system when error control coding is not used.

4.7.3 Diversity

A significant benefit of multi-relay MIMO systems is the diversity advantage and spatial multiplexing gains they offer. However, obtaining the full diversity requires complex

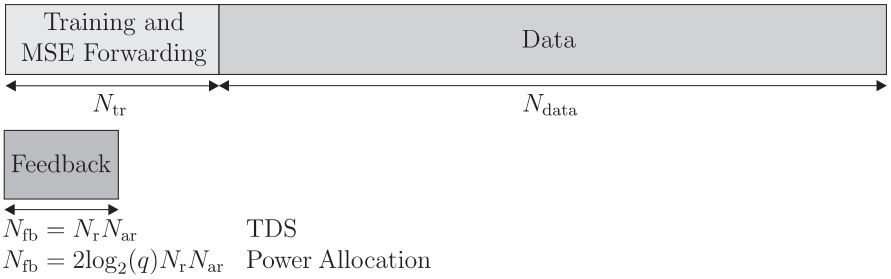

Figure 4.5: Cooperative MIMO packet structure.

optimum non-linear methods such as sphere and maximum likelihood decoding. In this chapter, linear MMSE receivers have been used and therefore it is not possible to obtain the full diversity on offer. Nevertheless, the diversity advantage available to the receivers can be maximised and accompanying interference suppression improved. The proposed methods restrict the number of transmit paths used and therefore lowers the maximum diversity advantage available to the optimum non-linear receivers from $d^* = N_{\text{ad}}(1 + (N_{\text{r}}N_{\text{ar}}/N_{\text{as}}))$ to $d^* = N_{\text{ad}}(N_{\text{asub}}/N_{\text{ar}} + 1)$, when full spatial multiplexing gain is maintained. However, they enable the lower complexity MMSE based techniques to increase their exploitation of the diversity at SNR of interest by removing paths which bring little or no advantage to the cooperative transmissions of the first and second phase, and dedicating increased transmit power over the remaining transmission routes.

4.7.4 Convergence of Discrete Stochastic Algorithm

Here the conditions under which convergence of the proposed discrete algorithms is guaranteed are specified and a discussion on the behavior of the proposed algorithms under non-ideal conditions presented. Considering the combinatorial nature of the problems and algorithms presented in this paper, convergence is judged against the optimal exhaustive solution at each time instant. Due to the application of the proposed schemes in practical communications systems, here and Section 4.8 the primary concentrations is upon BER and squared estimation error as a measure of performance and convergence.

Global convergence of the proposed algorithms is dependent on two assumptions:

the independence between the observations used for the objective function calculations and the satisfaction of

$$Pr\left\{C_T\left[i,t^{opt}\right] > C_T\left[i,t[i]\right]\right\} > Pr\left\{C_T\left[i,t[i]\right] > C_T\left[i,t^{opt}\right]\right\} \tag{4.70}$$

and

$$Pr\left\{C_T\left[i,t^{opt}\right] > C_T\left[i,t^C[i]\right]\right\} > Pr\left\{C_T\left[i,t[i]\right] > C\left[i,t^C[i]\right]\right\} \tag{4.71}$$

for the MMSE TDS and

$$Pr\left\{\mathcal{F}_R\left[i,r^{opt}\right] > \mathcal{F}_R\left[i,r[i]\right]\right\} > Pr\left\{\mathcal{F}_R\left[i,r[i]\right] > \mathcal{F}_R\left[i,r^{opt}\right]\right\} \tag{4.72}$$

and

$$Pr\left\{\mathcal{F}_R\left[i,r^{opt}\right] > C_R\left[i,r^C[i]\right]\right\} > Pr\left\{\mathcal{F}_R\left[i,r[i]\right] > \mathcal{F}_R\left[i,r^C[i]\right]\right\} \tag{4.73}$$

for the MMSE RS . When these conditions are met and independent observations utilised, $t[i] \rightarrow t^{opt}$ and $r[i] \rightarrow r^{opt}$ are guaranteed when operating independently [14, 91]. However, due to the joint of operation of TDS and RS and the practical difficulties of obtaining numerous independent observations under the system model presented in this work, the proof of convergence is intractable and therefore not guaranteed. Nevertheless, throughout the simulations presented in the work and supporting simulations, excellent steady-state convergence performance has been observed, indicating that the lack of independent observations is not a problem for the optimal reception schemes. Further support for this conclusion is presented in [91], where no convergence issues were encountered as a result of the lack of independent observations. However, additional care has to be taken when studying the convergence of the schemes which feature adaptive reception. As previously specified, the step-size of TDS and RS algorithms is fixed for the adaptive MMSE implementation to aid convergence of TDS and RS at large i and avoid becoming trapped in an non-optimal state. Though effective, the rate of convergence will still lag behind the optimal scheme due to the convergence of the LMS

adaptive filter algorithms and the ensemble error, but also the convergence of a plurality of algorithms in parallel for TDS with RS. To aid the convergence of all schemes, $\#\Omega_R << \#\bar{\Omega}_T$ to ensure RS converges significantly before TDS ($\#\Omega_{\mathrm{R}} < \#\bar{\Omega}_{\mathrm{T}}$). This therefore minimises the number of TDS iterations performed on the non-optimal $\bar{\Omega}_{\mathrm{T}}$ set and assists in ensuring that the detrimental convergence effects of a changing $\bar{\Omega}_T$ in the initial transient is outweighed by the benefits of TDS operating over a significantly reduced cardinality set.

4.8 Simulations

In this section, simulations of the proposed algorithms and their various implementations are presented. Comparisons shall be given between the optimal exhaustive (Exhaustive TDS, Exhaustive TDS with RS), the standard cooperative system (No TDS - All relays), non-cooperative transmission (Non-Cooperative), iterative (Iterative TDS, Iterative TDS and RS) and power allocation (PA) based implementations. Optimal MMSE reception is used at the relay and destination nodes unless otherwise stated and equal power allocation shall be maintained in all phases for TDS DF schemes, where $\mathcal{A}_{\mathrm{r}}[i] = 1/\sqrt{N_{\mathrm{asub}}}\mathbf{I}_{N_{\mathrm{ar}}N_{\mathrm{r}}}$ when TDS is employed and $\mathcal{A}_{\mathrm{r}}[i] = 1/\sqrt{N_{\mathrm{ar}}N_{\mathrm{r}}}\mathbf{I}_{N_{\mathrm{ar}}N_{\mathrm{r}}}$ for standard cooperative transmission. For TDS AF, the transmit power of the m^{th} antenna at the n^{th} relay when TDS is employed is given by

$$\mathbf{A}_{\mathrm{r}_n,m}[i]\frac{1}{\sqrt{N_{\mathrm{asub}}}\mathbf{H}_{\mathrm{sr}_n,m}[i]\mathbf{H}_{\mathrm{sr}_n,m}[i] + \sigma^2_{\mathrm{sr}}}, \tag{4.74}$$

thus ensuring $E\left[\mathcal{A}^H_{\mathrm{r}}[i]\mathcal{A}_{\mathrm{r}}[i]\right] = 1$. For standard cooperative transmission N_{asub} is replaced with N_{ar} and CSI is provided by the RLS algorithm of Section 4.6.4. The RLS variables $\mathbf{P}_{\hat{\mathcal{H}}_{\mathrm{rd}}}$, $\mathbf{P}_{\hat{\mathbf{H}}_{\mathrm{sr}_n}}$ and $\mathbf{P}_{\hat{\mathbf{H}}_{\mathrm{sd}}}$ are initialised as identity matrices and λ, the exponential forgetting factor, is 0.9. The initial values of $\hat{\mathcal{H}}_{\mathrm{rd}}$, $\hat{\mathbf{H}}_{\mathrm{sr}_n}$ and $\hat{\mathbf{H}}_{\mathrm{sd}}$ are zero matrices. For adaptive power allocation, the vector $\bar{\mathbf{a}}_{\mathrm{r}}$ is initialised with equal power allocation and all step-sizes for adaptive reception and power allocation are set to 0.1. Throughout all

simulations, $N_{as} = N_{ar} = N_{ad} = N_a$, where N_a is specified in each plot, and $N_{asub} = 4$ unless otherwise stated. and Each simulation is averaged over N_p packets where N_p is specified in each plot.

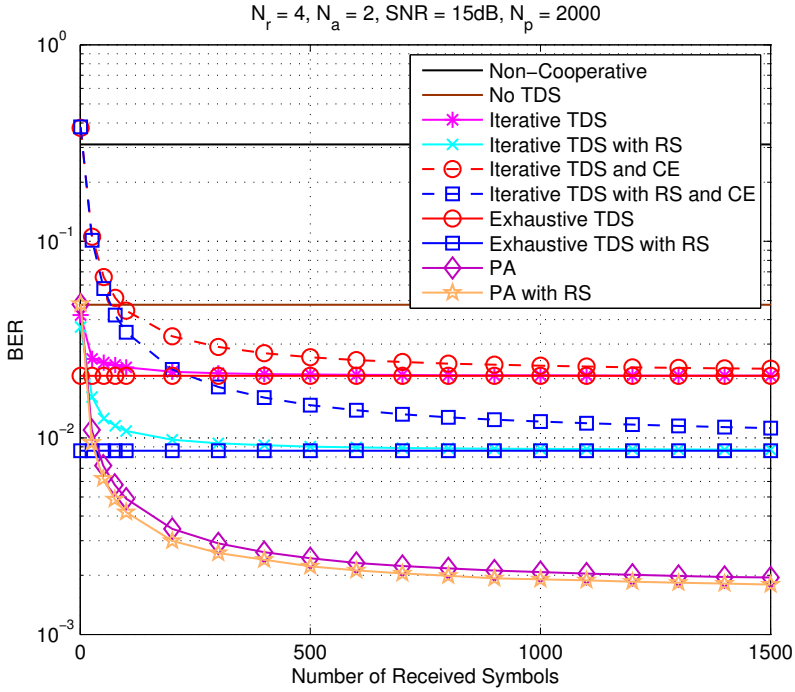

Figure 4.6: BER performance versus the number of received symbols for the proposed schemes with full and estimated CSI, and optimal linear receivers.

Figure 4.6 shows the BER performance versus the number or received symbols for the proposed schemes when a single relay is removed and estimated CSI is used for TDS schemes. The performance of the TDS schemes exceed that of the standard cooperative system and RS improves performance further in terms of convergence and steady-state. This shows that the process of RS decreases the likelihood of channel mismatch between the first and second phases but also confirms the improvement in convergence performance obtained by refining and reducing the cardinality of the set which TDS operates over. The behavior of the CE schemes indicate that TDS, RS and CE jointly operate correctly and allow the convergence to the exhaustive solution if an appropriate value of λ is chosen. Lastly, applying RS to adaptive power allocation improves performance further by constraining relays nodes' transmission power to zeros based on their

first phase performance. This indicates that RS and power allocation operate correctly in parallel but also that the resulting power allocation process considers the attributes of both the first and second phases, an outcome which is not possible with power allocation alone.

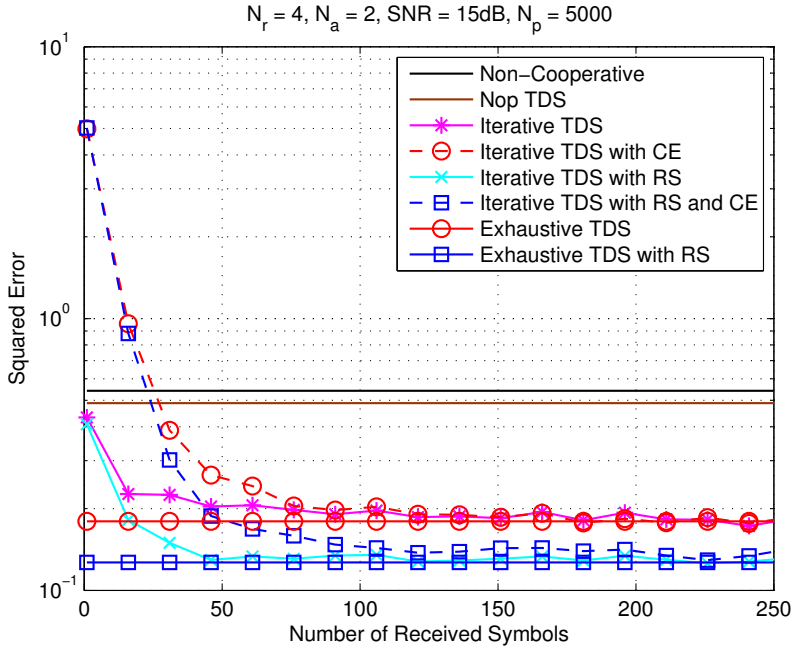

Figure 4.7: Squared error performance versus the number of received symbols for the proposed schemes with full and estimated CSI, and optimal linear receivers.

Figure 4.7 presents the squared error performance of the TDS based schemes presented in Figure 4.6. Once again, the improvement in convergence brought about by $\#\bar{\Omega}_{\mathrm{T}} < \#\Omega_{\mathrm{T}}$ is evident as well as the effective operation of the schemes which use iteratively estimated CSI. The rapid and complete convergence of the iterative TDS and RS also confirms the correct operation of two simultaneous discrete iterative algorithms. A further semi-analytical conclusion can also be drawn, stating that for effective convergence of the TDS with RS scheme when the variable step-size of step 4 is used, $\#\Omega_{\mathrm{R}} < \#\bar{\Omega}_{\mathrm{T}}$. This condition ensures that the RS DSA converges significantly before the TDS DSA and therefore allows TDS to operate on the fully refined TDS set for the majority of the time. This condition also goes someway to ensuring that sufficient

relays/antennas are available for TDS whilst avoiding an increased risk of channel mismatch, i.e. $N_{a_{sub}}/N_a \approx N_r - N_{rem}$.

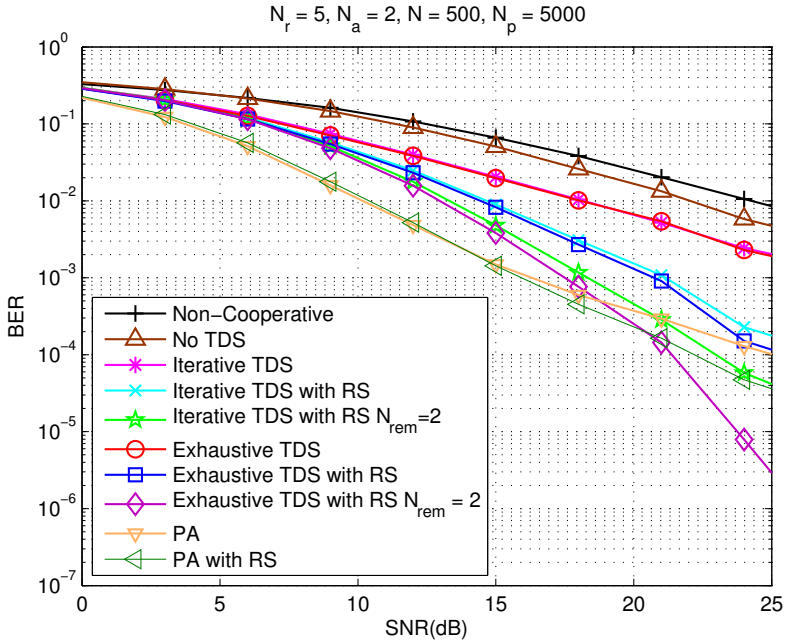

Figure 4.8: BER performance versus SNR for the proposed schemes with optimal linear receivers and $N_{rem} = 1, 2$.

The BER performance versus SNR of the proposed algorithms is shown in Figure 4.8. The steeper gradient of the proposed schemes indicate that increased diversity has been achieved by the RS schemes at the SNR of interest, gains which increase when $N_{rem} = 2$. Improved interference suppression is also obtained as evidenced by the shifting of the plots compared to the standard system, gains which reach 5dB at a BER of 10^{-2}. In general, the BER performance of the discrete iterative scheme closely matches the exhaustive performance; however, there is an increasing discrepancy for the schemes with $N_{rem} = 2$ as the SNR increases. This is partially accounted for by the lower BER but is also explained by the increased size of Ω_R and the increased time the DSA takes to converge to the optimal Ω_R. This results in the TDS portion of the algorithm operating on a suboptimal $\bar{\Omega}_T$ for a significant number of initial iterations, therefore increasing the BER convergence time. Differing rates of convergence are also responsible for the closing of the performance gap at high SNR between the schemes with $N_{rem} = 2$ and those

with adaptive power allocation. At high SNR the power allocation schemes and the iterative scheme with $N_{\text{rem}} = 2$ have not fully converged at $N = 500$ and consequently have not reached their error floor. Although power allocation with RS increases the rate of convergence, the exhaustive scheme with $N_{\text{rem}} = 2$ does not require convergence and therefore at a moderate number of received symbols at high SNR the exhaustive scheme's BER performance exceeds that of the power allocation schemes.

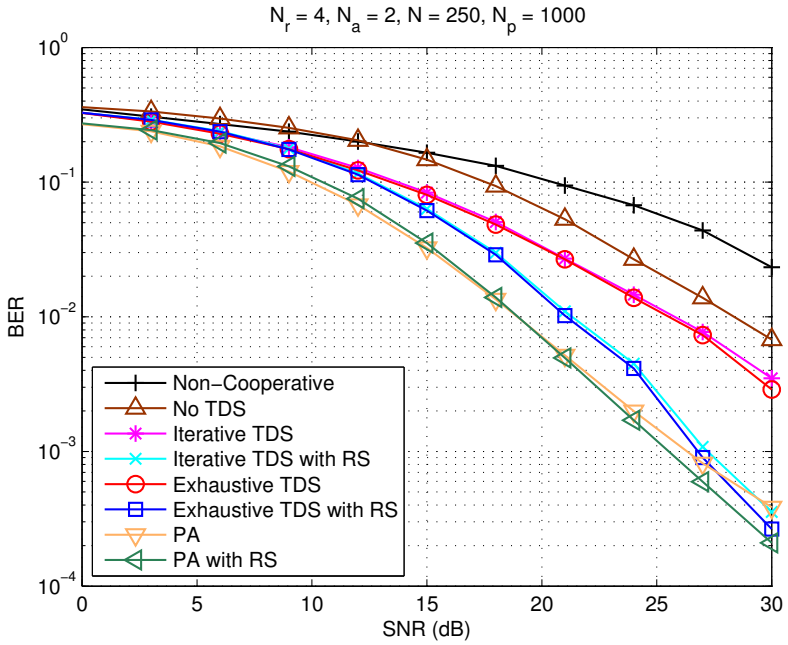

Figure 4.9: BER performance versus SNR for the proposed schemes with optimal linear receivers when operating over correlated channels.

An important aspect of cooperative MIMO systems and transmission strategies is their performance in the presence of correlated channels. Figure 4.9 shows the performance of the schemes over the correlated channels specified in Section 4.6.3. Improved interference suppression and diversity has been achieved by the proposed schemes and no significant convergence problems are evident. The RS schemes also achieve significant gains of 4dB at a BER of 10^{-2} compared to the scheme where only single relay is removed. However, as expected, the performance has been degraded by the correlated channels compared to the results in Figure 4.8. As in Figure 4.8, the BER performance of the power allocation and RS schemes appear to converge; however, this is once again

due to the differing convergence rates of the iterative and exhaustive TDS schemes with RS compared the iterative power allocation schemes.

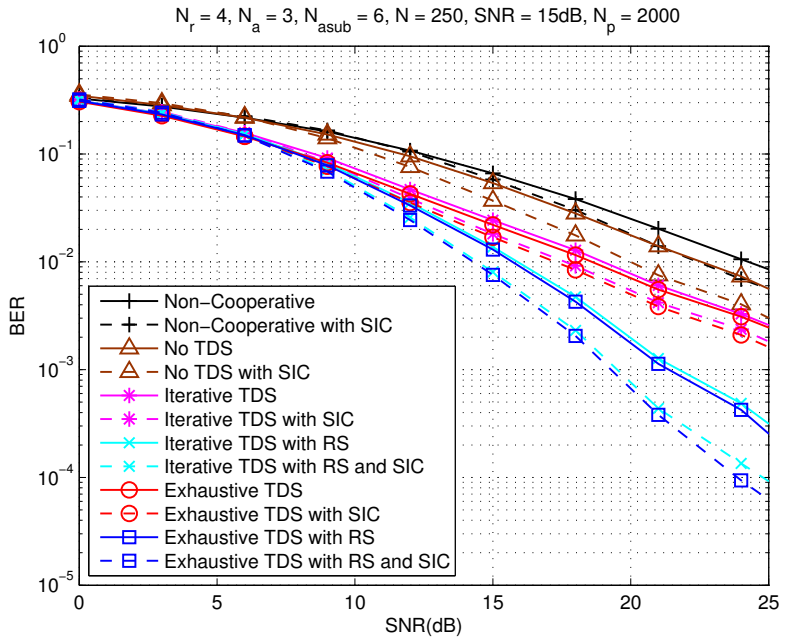

Figure 4.10: BER performance versus SNR for the proposed schemes with SIC.

The effect of introducing SIC to the TDS schemes is illustrated by Figure 4.10. The advantage in interference suppression is evident from the shifted plots but there are also diversity gains when RS is considered. The gains of introducing RS when SIC is utilised are substantial and exceed that of introducing RS when SIC is not used. This can be attributed to the decrease in probability that RS brings about of different symbols being transmitted from the active relays. Thus reducing the likelihood that the identical transmit symbol assumption of Section 4.5.2 is violated.

Figure 4.11 presents the BER performance versus the number of received symbols for TDS and TDS with RS when joint adaptive linear MMSE reception is used at the destination node. Firstly, an interesting feature to note is the performance of the standard cooperative scheme (No TDS) when an adaptive receiver is used. It exceeds the performance of the MMSE filter although no CSI or power allocation information is required. Similar performance of the LMS algorithm has been observed previously [111, 112],

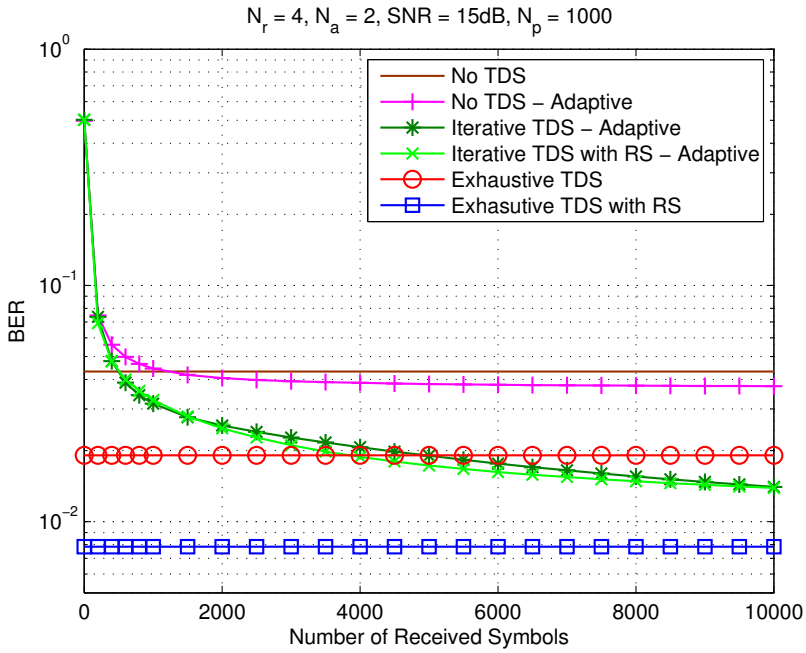

Figure 4.11: BER performance versus the number of received symbols for proposed schemes with joint adaptive linear MMSE receive filters.

however, this have been in the presence of narrow band interference. In this scenario the non-Wiener performance is dependent upon the independence of the reception at the relays nodes. The erroneous symbols transmitted by the relays can be viewed as interference that the LMS receiver is able to suppress to a greater extent than the MMSE receiver because it does not have fixed correlation structures. The rate of convergence of both iterative TDS algorithms has been slowed considerably due to the convergence of the receive filters and their ensemble error but also the challenges of several adaptive schemes operating in parallel. The TDS algorithm exceeds the performance of the optimal filter due to the non-Wiener behaviour but RS does not improve performance further. This can be attributed to the challenges of a number of iterative algorithms operating jointly but also the suboptimal sets that the TDS with RS algorithm will be operating on for a significant number of iterations.

Figure 4.12 presents the BER convergence performance of the proposed power allocation algorithms when joint power allocation and interference suppression is used at

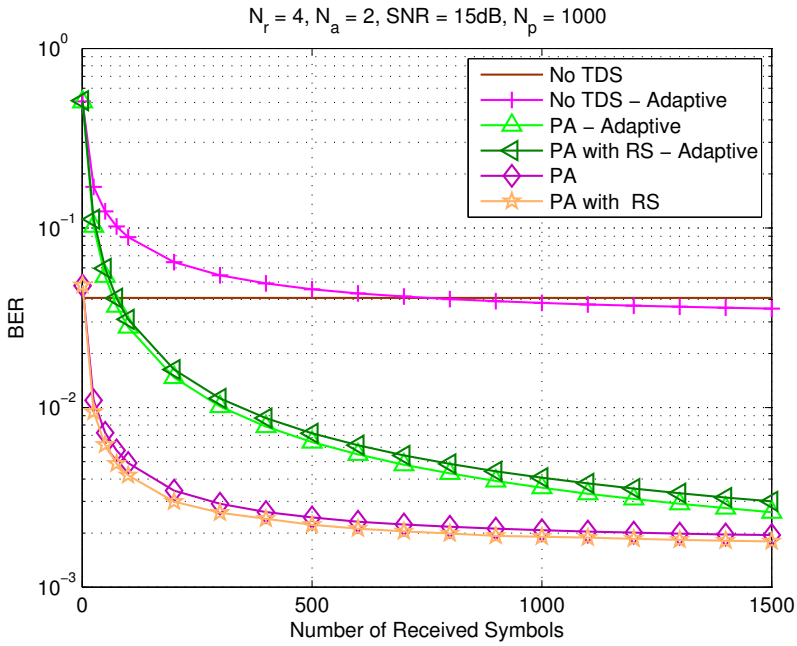

Figure 4.12: BER performance versus the number of received symbols for the proposed PA schemes.

the destination node. The algorithms with adaptive reception converge towards those with MMSE reception but, as has been observed previously, the challenges of the RS, power allocation and interference suppression jointly operating marginally outweigh the benefits that RS brings when optimal, non-iterative reception is used.

Figure 4.13 illustrates the performance of the proposed iterative TDS schemes when implemented in an AF system. Both the iterative schemes converge to their optimal exhaustive counterparts and, as expected, the TDS and RS scheme displays an increased rate of convergence compared to TDS alone. However, RS does not bring about an improvement in steady state performance as in DF systems. This results from the use of branch SNR as secondary RS criteria and the resulting incomplete integration with the MSE based TDS at the destination.

In previous simulations, the feedback channel to each relay is assumed error free. However, in reality this assumption is likely to breakdown. Figure 4.14 gives the BER performance versus the probability of error in each individual feedback bit when no error coding and correction is used. All schemes are compared when optimal linear

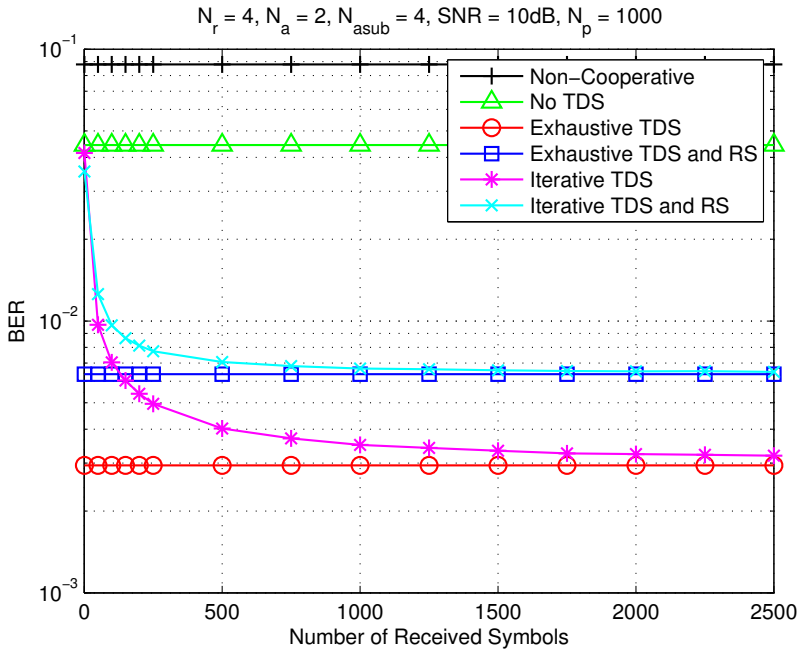

Figure 4.13: BER performance versus the number of received symbols for the proposed schemes in an AF system with optimum linear receivers.

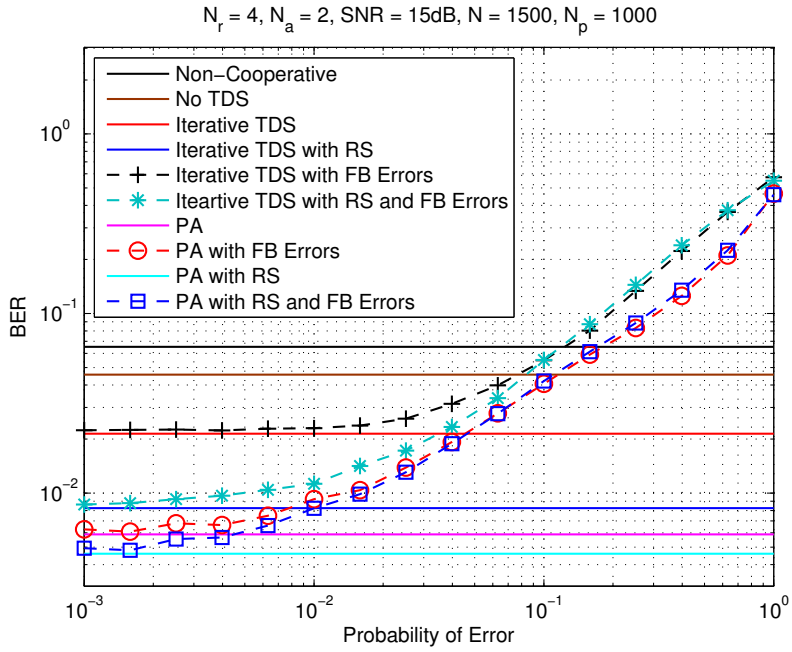

Figure 4.14: BER performance versus the probability of feedback errors for the proposed schemes with optimal linear receivers.

receivers with full backward CSI are used all nodes and the forwarded MSE data from the relays are assumed perfect. All schemes provide improved performance over the non-cooperative system up until the probability of error reaches ≈ 0.1; this is also the point where their performance converges. At this point 57% of the $N_{\mathrm{a}}N_{\mathrm{r}}$ bit packets have at least one or more error. The performance degradation is due to the non-optimal second phase channels being utilised, incorrect total transmit power and incorrect values used in the calculation of the MMSE receiver at the destination node. For the power allocation schemes, 5 bit quantisation in used for the real and imaginary parts and all feedbacks are set to zero to indicate a relay that has been removed through RS. RS improves performance at low error rates but the transition between the performance of power allocation RS and the standard scheme is at a lower error rate than that of the TDS schemes.

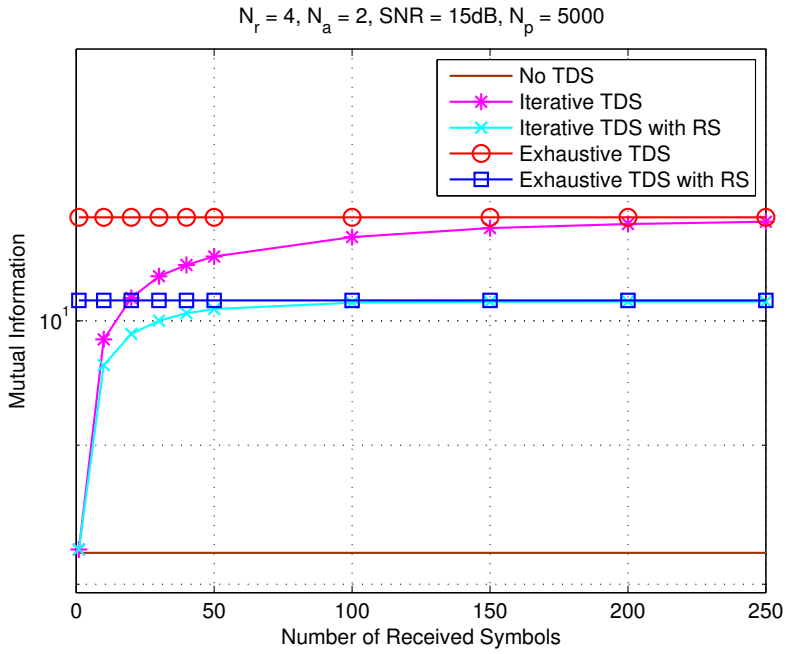

Figure 4.15: Mutual Information performance versus the number of received symbols for the proposed schemes.

Figure 4.15 gives the mutual information of the proposed TDS schemes versus the number of iterations of the DSAs. Both schemes achieve gains over the standard system

but RS results in a small performance loss compared to the TDS scheme. This is due to the MI optimisation given by (4.45) not taking into account the MI of the first phase because of the inherent separation between phases in DF systems. However, the TDS with RS scheme has lower complexity and increased speed of convergence compared to TDS alone due to the refined set $\bar{\Omega}_{\mathrm{T}}$ and its lower cardinality. Additionally, when utilising RS, the probability of the MI/capacity of the first phase being unable to satisfy that of the second phase is reduced.

4.9 Summary

This chapter has presented TDS and RS, and power allocation methods based on DSAs for multi-relay cooperative MIMO systems where RS improves the performance of conventional algorithms. Hybrid continuous-discrete MMSE and MI optimisation problems have been formed and a framework to solve them developed. The resulting joint TDS and power allocation with RS schemes have been shown to operate well with optimal receivers, converge in parallel with low-complexity linear adaptive MMSE receivers and, in the majority of scenarios, converge to the exhaustive solution. Increased diversity and improved interference suppression are obtained by the proposed schemes and full algorithmic implementations have then been given to provide designers with the tools to significantly improve the performance of cooperative MIMO systems.

This and the previous chapter have focussed on resource allocation and interference suppression for the future and current mobile systems. Due to their use of conventional cost functions, reception, and interference suppression techniques that attempt to track the channel coefficients or unfaded symbols, they are suited to low to moderate fading rates and their performance will degrade at high fading rates. The next chapter addresses this degradation and the need for more robust reception and interference suppression in highly time-varying fading channels where conventional techniques are inadequate.

Chapter 5

Bidirectional Algorithms for Interference Suppression in DS-CDMA Systems

Contents

5.1 Introduction

Low-complexity reception and interference suppression are essential in multiuser mobile systems if battery power is to be conserved, data-rates improved and quality of

service enhanced. Conventional adaptive schemes fulfil many of these requirements and have been a significant focus of research literature [2, 29, 51, 52, 60, 72, 113] and Chapters 3 - 4.

However, in time-varying fading channels commonly associated with mobile systems, these adaptive techniques encounter tracking and convergence problems. Optimum closed-form solutions can address these problems but their computational complexity is high and CSI is required. Low-complexity adaptive channel estimation can provide CSI but in highly dynamic channels tracking problems exist due to their finite adaptation rate [38]. An alternative statistical approach is to obtain the correlation structures required for optimal MMSE or LS filtering [114, 115]. Although this relieves the tracking demands placed on the filtering process, in a Rayleigh fading channel, a zero correlator is the result due to the expectation of a Rayleigh fading coefficient, and therefore the cross-correlation vector, equating to zero i.e. $E\left[h_1[n]\right] = 0$ and $E\left[b_1^*[n]\mathbf{r}[n]\right] = 0$. In slowly fading channels this problem may be overcome by using a time averaged approach where the averaging period is equal to or less than the coherence time of the channel. However, in fast fading channels an averaging period equal to the coherence time of the channel is insufficient to overcome the effects of additive noise and characterise the MUI [2].

The inclusion of an optimised convergence parameter(s) into conventional adaptive algorithms, as in Chapter 3 and reference therein, extend their fading range and lead to improved convergence and tracking performance [9, 10, 116–122]. However, the stability of adaptive step-sizes and forgetting factors can be a concern unless they are constrained to lie within a predefined region [123]. In addition, the fundamental problem of obtaining the unfaded symbols whilst suppressing MUI remains. Consequently, the application of such algorithms is restricted to low and moderate fading rates.

The limitations of conventional estimation approaches led to the proposition of methods that attempt to track the faded symbol, such as the channel-compensated MMSE solution [113, 124]. This removed the burden of fading coefficient estimation from the

interference suppression filter; however, a secondary process is required to perform explicit estimation of the fading coefficients in order for symbol estimation to be performed [15].

Approaches that avoid tracking and estimation of the fading coefficients altogether were proposed in [15, 125, 126]. Here it was put forward that although a channel might be highly time variant, two adjacent fading coefficients will be approximately equal and have a significant level of correlation. These properties can then be exploited to obtain a sequence of faded symbols where the primary purpose of the filter is to suppress multiuser interference and track the ratio between successive fading coefficients; thus, not burdening it with estimation of the fading coefficients themselves. However, this scheme has a number of limitations stemming from its use of only one correlation time instant and a single family of adaptive algorithms.

In this chapter, a bidirectional MMSE based interference suppression scheme for highly dynamic fading channels is presented. The non-zero correlation between multiple time instants is exploited to improve the robustness, tracking and convergence performance of existing MMSE schemes. NLMS and CG implementations are presented that overcome a number of problems associated with applying the RLS to bidirectional problems. A range of novel mixing strategies that weight the contribution of the considered time instants and improve the convergence and steady-state performance, and increase robustness against the channel discontinuities are also presented. Analysis of the proposed schemes is given and establishes the mechanisms and factors behind their behaviour and expected performance. The proposed schemes are applied to conventional multiuser DS-CDMA and cooperative DS-CDMA systems to assess their MUI suppression and tracking capabilities. The resulting simulations confirm that the algorithms improve upon existing schemes with minimal increase in complexity.

In this chapter, Section 5.2 presents the proposed optimisation problems and the motivation behind their development. Switching and mixing strategies that enhance performance are proposed and assessed in Section 5.3, followed by the algorithmic

implementations of the proposed presented methods in Section 5.4. Analysis of the proposed algorithms is given in Section 5.5, and simulations and performance evaluation are presented in Section 5.6. Conclusions in Section 5.7 then draw the chapter to a close.

5.2 Proposed Bidirectional Scheme

Adaptive parameter estimation has two primary objectives: estimation and tracking of the desired parameters. When applied to the DS-CDMA systems with short spreading sequences considered in this thesis, these translate into tracking of the desired symbol and suppression of MUI. However, in fast fading channels the combination of these objectives places unrealistic demands on conventional filtering and estimation schemes. Differential techniques reduce these demands by relieving the adaptive filter of the task of tracking fading coefficients. This is achieved by posing an optimisation problem where the ratio between two successive received samples is the quantity to be tracked. Such an approach is enabled by the presumption that, although the fading is fast, there is a significant level of correlation between the adjacent channel samples

$$f_1[i] = E\left[h_1[i]h_1^*[i+1]\right] \geq 0, \tag{5.1}$$

where $h_1[i]$ is the channel coefficient of the desired user. The interference suppression of the resulting filter is improved in fast fading environments compared to conventional adaptive filters but only the ratio of adjacent fading samples is obtained. Consequently, differential MMSE schemes are suited to use with differential modulation where the ratio between adjacent symbols is the data carrying mechanism.

However, limiting the optimisation process to two adjacent samples exposes these processes to the negative effects of uncorrelated samples

$$E\left[h_1[i]h_1^*[i+1]\right] \approx 0, \tag{5.2}$$

but also does not exploit the correlation that may be present between two or more adjacent samples, i.e.

$$\begin{aligned} f_2[i] &= E\left[h_1[i]h_1^*[i-1]\right] > 0 \\ f_3[i] &= E\left[h_1[i+1]h_1^*[i-1]\right] > 0. \end{aligned} \tag{5.3}$$

To address these weaknesses, a bidirectional MSE cost function based on 3 adjacent samples if formed so that the number of channel scenarios under which the differential MMSE performs beneficial adaptations is substantially increased. Termed the bidirectional MMSE, due to the use of the time instants, $i-1$, i, and $i+1$, the motivation behind this proposition is illustrated by the plots of fading/channel coefficients in Figure 5.1, where J_1 represents the 2 sample differential MMSE. There is a low level of correlation present between samples i and $i-1$, thus any adaptation of the filter will bring little benefit. However, the proposed scheme operates over J_1, J_2 and J_3; therefore, it can exploit the correlation between $i+1$ and $i-1$ and past data. Figure 5.1b gives an example of a channel where there is significant levels of correlation between samples. Although the existing differential scheme operates over 2 correlated samples, the proposed scheme is able to exploit the additional correlation present between $i+1$ and i, and $i+1$ and $i-1$; effectively reusing data in a similar method to the affine projection algorithm (AP) [38, 121].

The optimisation problem of the proposed scheme where user 1 is assumed is given by

$$\begin{aligned} \mathbf{w} = \arg\min_{\mathbf{w}} \quad = \quad & E\Big[\left|b[i]\mathbf{w}^H\mathbf{r}[i-1] - b[i-1]\mathbf{w}^H\mathbf{r}[i]\right|^2 && (\mathrm{J}_1) \\ & + \left|b[i]\mathbf{w}^H\mathbf{r}[i-2] - b[i-2]\mathbf{w}^H\mathbf{r}[i]\right|^2 && (\mathrm{J}_2) \\ & + \left|b[i-1]\mathbf{w}^H\mathbf{r}[i-2] - b[i-2]\mathbf{w}^H\mathbf{r}[i-1]\right|^2\Big] && (\mathrm{J}_3) \end{aligned}, \tag{5.4}$$

where $\mathbf{w}$ is the expected value of the filter, $\mathrm{J}_1 - \mathrm{J}_3$ equate to those of Figure 5.1, and the time instants of interest have been altered to avoid the use of future samples. In addition to (5.4), an output power constraint is required to avoid the trivial zero correlator

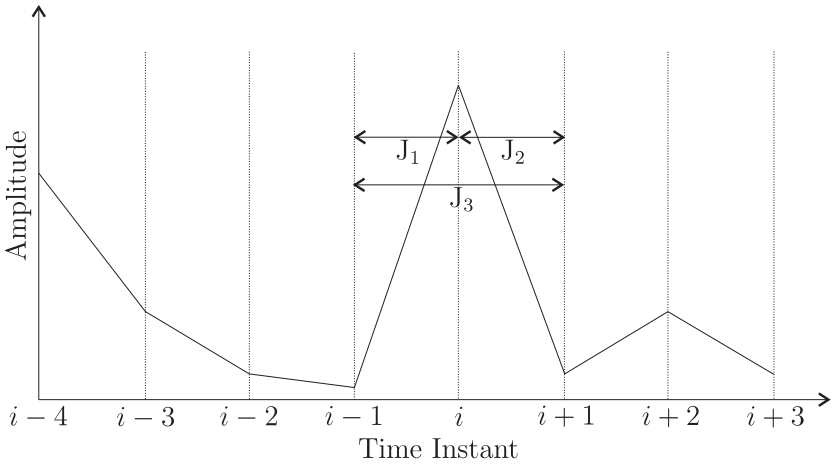

(a) Badly conditioned fading channel

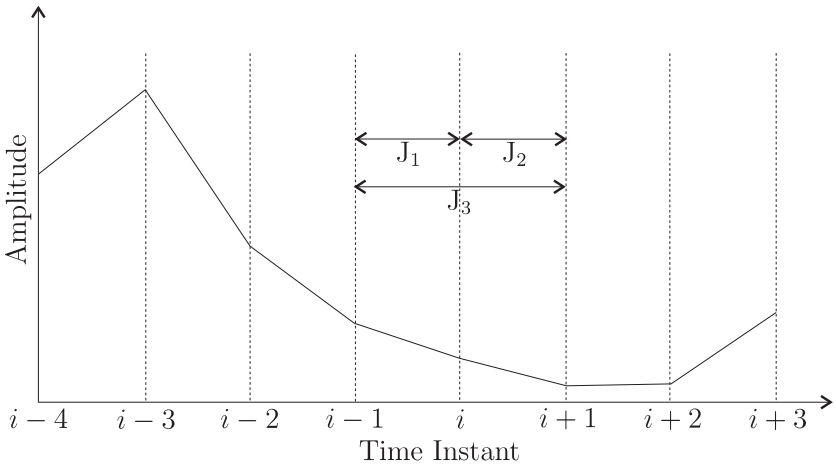

(b) Well-conditioned fading channel

Figure 5.1: Fading channels

solution

$$E\left[\left|\mathbf{w}^H\mathbf{r}[i]\right|^2\right] = 1. \tag{5.5}$$

Basis for (5.4) can be found by considering the output of the filter $\mathbf{w}$ as a scaled version of the faded symbols where the MUI has been suppressed [15]. For J_3 consider the following

$$\begin{aligned}
&\mathbf{w}^H\mathbf{r}[i] \approx \alpha h[i]b[i] \\
&\mathbf{w}^H\mathbf{r}[i-2] \approx \alpha h[i-2]b[i-2] \\
&h[i] \approx h[i-2] \\
&b[i]\mathbf{w}^H\mathbf{r}[i] \approx b[i-2]\mathbf{w}^H\mathbf{r}[i-2] \\
&b[i-2]\mathbf{w}^H\mathbf{r}[i] \approx b[i]\mathbf{w}^H\mathbf{r}[i-2]
\end{aligned} \tag{5.6}$$

where is α is a scaling factor. It is then clear that an optimisation function should focus on the minimisation of

$$b[i-2]\mathbf{w}^H\mathbf{r}[i] - b[i]\mathbf{w}^H\mathbf{r}[i-2] \tag{5.7}$$

in order to track the ratio between faded symbols.

Extension of the bidirectional scheme to any number of time instants is also possible; however, the benefit of doing so is dependent on the fading rate of the channel and the related correlation of the channel coefficients. The generalised form of the bidirectional

problem can be expressed as follows

$$\begin{aligned}\mathbf{w} = \arg\min_{\mathbf{w}} \quad = \quad & E\Big[\Big|b[i]\mathbf{w}^H\mathbf{r}[i-1] - b[i-1]\mathbf{w}^H\mathbf{r}[i]\Big|^2 \\ & \qquad\qquad \vdots \\ & + \Big|b[i]\mathbf{w}^H\mathbf{r}[i-(D-1)] - b[i-(D-1)]\mathbf{w}^H\mathbf{r}[i]\Big|^2 \\ \\ & + \Big|b[i-1]\mathbf{w}^H\mathbf{r}[i-2] - b[i-2]\mathbf{w}^H\mathbf{r}[i-1]\Big|^2 \\ & \qquad\qquad \vdots \\ & + \Big|b[i-1]\mathbf{w}^H\mathbf{r}[i-(D-1)] - b[i-(D-1)]\mathbf{w}^H\mathbf{r}[i-1]\Big|^2 \\ \\ & + \Big|b[i-(D-2)]\mathbf{w}^H\mathbf{r}[i-(D-1)] - b[i-(D-1)]\mathbf{w}^H\mathbf{r}[i-(d-2)]\Big|^2\Big]\end{aligned} \tag{5.8}$$

where D denotes the number of considered time instants. Introducing summations into (5.8) yields a more concise form

$$\mathbf{w} = \arg\min_{\mathbf{w}} = E\left[\sum_{d=0}^{D-2}\sum_{l=d+1}^{D-1}\Big|b[i-d]\mathbf{w}^H\mathbf{r}[i-l] - b[i-l]\mathbf{w}^H\mathbf{r}[i-d]\Big|^2\right], \tag{5.9}$$

where the constraint of (5.5) is required once again.

5.3 Switching Strategies

The advantages of a bidirectional scheme operating over 3 time or more time instants are clear. However, the performance of the scheme may be degraded when received vectors based on uncorrelated fading coefficients are utilised in the update of the interference suppression filter. This is particulary evident from the example channel illustrated in Figure 5.1a, where the contribution to the optimisation function represented by J_3 is unlikely to aid the accurate adaption of $\mathbf{w}$ to the overall trend of the channel due to the incontinuity. To avoid this, a set of switching or mixing parameters is introduced that determines the weighting of the D constituent elements of the bidirectional cost

function. With these modifications the updated 3 time instant bidirectional MSE cost function is given by

$$\begin{aligned}\mathbf{w} = \arg\min_{\mathbf{w}} \quad = \quad & E\Big[\rho_1[i]\left|b[i]\mathbf{w}^H\mathbf{r}[i-1] - b[i-1]\mathbf{w}^H\mathbf{r}[i]\right|^2 && (\mathrm{J}_1)\\ & +\rho_2[i]\left|b[i]\mathbf{w}^H\mathbf{r}[i-2] - b[i-2]\mathbf{w}^H\mathbf{r}[i]\right|^2 && (\mathrm{J}_2)\\ & +\rho_3[i]\left|b[i-1]\mathbf{w}^H\mathbf{r}[i-2] - b[i-2]\mathbf{w}^H\mathbf{r}[i-1]\right|^2\Big] && (\mathrm{J}_3)\end{aligned}, \tag{5.10}$$

where ρ are the weighting factors and $0 \geq \rho_1[i], \rho_2[i], \rho_3[i] \leq 3$. Introducing weighting factors into the generalised bidirectional cost function yields

$$\mathbf{w} = \arg\min_{\mathbf{w}} = E\left[\sum_{d=0}^{D-2}\sum_{l=d+1}^{D-1}\rho_n[i]\left|b[i-d]\mathbf{w}^H\mathbf{r}[i-l] - b[i-l]\mathbf{w}^H\mathbf{r}[i-d]\right|^2\right], \tag{5.11}$$

where $n = d(D-3) + l + 1$. However, for the remainder of this chapter the case where $D = 3$ is considered.

The correct determination of receive vector samples that correspond to the scenarios depicted in Figure 5.1a is essential if correct optimisation of the ρ is to be achieved. The use of CSI to achieve this would be a highly effective but impractical solution due to the difficulty in obtaining the CSI; consequently, other methods must be sought. In this section, the use of two alternative metrics is proposed: the signal power differential after interference suppression between the considered time instants, and the error between the considered time instants.

Firstly, a switching based scheme where $\rho_{1-3} = [0, 1]$ is considered. At each time instant the weighting factors are determined by the following post-filtering power differential metrics

$$\begin{aligned}P_1[i] &= \left|\mathbf{w}[i]^H\mathbf{r}[i]\right|^2 - \left|\mathbf{w}[i]^H\mathbf{r}[i-1]\right|^2\\ P_2[i] &= \left|\mathbf{w}[i]^H\mathbf{r}[i]\right|^2 - \left|\mathbf{w}[i]^H\mathbf{r}[i-2]\right|^2\\ P_3[i] &= \left|\mathbf{w}[i]^H\mathbf{r}[i-1]\right|^2 - \left|\mathbf{w}[i]^H\mathbf{r}[i-2]\right|^2.\end{aligned} \tag{5.12}$$

If the power difference for each of J_{1-3} exceeds a predefined threshold the corresponding

ρ is set to zero, therefore, removing the corresponding element of the cost function from the adaptation process at that time instant. The highly dynamic nature of the channel requires an adaptive threshold which is able to track the changes in the system and determine appropriate time instants based on surrounding samples. Consequently, for each ρ_n a threshold, $T_n[i]$, related to a time-averaged, windowed, root-mean-square of the relevant differential power is used. The value of ρ_n in then determined in the following manner

$$\rho_n[i] = \begin{cases} 0 & \text{if} P_n[i] \geq T_n[i] \\ 1 & \text{otherwise} \end{cases}, \tag{5.13}$$

where

$$T_n[i] = \nu \left[\lambda_P P_{n_{RMS}}[i] + (1 - \lambda_P) P_{n_{RMS}}[i] \right], \tag{5.14}$$

$$P_{n_{RMS}}[i] = \sqrt{\frac{1}{m-1} \sum_{l=i-m}^{i} P_n[l]^2}, \tag{5.15}$$

and ν is a positive user defined constant greater than unity that scales the threshold.

Although the current sample corresponding to J_n may bring no benefit in terms of adaptation, this does not indicate that all previous cost function elements corresponding to J_n should be discarded. An alternative approach is to use a set of convex mixing parameters that are not restricted to 1 or 0. This allows each element of the cost function to be more precisely weighted based on its previous and current values. However, the setting of these mixing parameters is once again problematic if they are to be fixed. Accordingly, an adaptive implementation that can take account of the time-varying channels and previous values which continue to have an impact on the adaptation of the filter is sought. The errors extracted from the cost function (5.10) are chosen as the metric for this implementation. These provide an input to the weighting factor calculation process that is directly related to the cost function of (5.10). The time varying mixing factors are given by

$$\rho_n[i] = \lambda_e \rho_n[i-1] + (1 - \lambda_e) \frac{e_T[i] - |e_n[i]|}{e_T[i]} \tag{5.16}$$

where

$$e_T[i] = |e_1[i]| + |e_2[i]| + |e_3[i]|, \tag{5.17}$$

and the individual errors terms are calculated as

$$\begin{aligned} e_1[i] &= b[i]\mathbf{w}^H[i-1]\mathbf{r}[i-1] - b[i-1]\mathbf{w}^H[i-1]\mathbf{r}[i] \\ e_2[i] &= b[i]\mathbf{w}^H[i-1]\mathbf{r}[i-2] - b[i-2]\mathbf{w}^H[i-1]\mathbf{r}[i] \\ e_3[i] &= b[i-1]\mathbf{w}^H[i-1]\mathbf{r}[i-2] - b[i-2]\mathbf{w}^H[i-1]\mathbf{r}[i-1]. \end{aligned} \tag{5.18}$$

The forgetting factor, $0 \leq \lambda_e \leq 1$, is user defined and, along with normalisation by the total error, $e_T[i]$, and $\sum_{n=1}^{3}\rho_n[0] = 1$, ensures $\sum_{n=1}^{3}\rho_n[i] = 1$ and a convex combination at each time instant.

5.4 Adaptive Algorithms

To commence deriving low-complexity adaptive implementations of the proposed bidirectional schemes, the expected value of the filter $\mathbf{w}$ is replaced with the appropriate instantaneous estimate, yielding

$$\begin{aligned} \mathbf{w}[i] = \arg\min_{\mathbf{w}[i]} = \; & E\Big[\Big|b[i]\mathbf{w}^H[i-1]\mathbf{r}[i-1] - b[i-1]\mathbf{w}^H[i]\mathbf{r}[i]\Big|^2 \\ & + \Big|b[i]\mathbf{w}^H[i-2]\mathbf{r}[i-2] - b[i-2]\mathbf{w}^H[i]\mathbf{r}[i]\Big|^2 \\ & + \Big|b[i-1]\mathbf{w}^H[i-2]\mathbf{r}[i-2] - b[i-2]\mathbf{w}^H[i]\mathbf{r}[i-1]\Big|^2\Big] \end{aligned} \tag{5.19}$$

$$\text{subject to} \qquad E\Big[\Big|\mathbf{w}[i]^H\mathbf{r}[i]\Big|^2\Big] = 1.$$

This cost function then forms the basis of the adaptive algorithms derived in this section. However, to reduce the complexity of the derivations, enforcement of the non-zero constraint is not included and instead enforced in a stochastic manner at each time instant after the adaptation process is complete [15].

5.4.1 Stochastic Gradient Techniques

Here a low-complexity NLMS implementation that utilises an instantaneous gradient in a steepest descent framework is formed.

Firstly, the instantaneous gradient of (5.19) is taken with respect to $\mathbf{w}^H[i]$, yielding

$$\begin{aligned}\nabla_{\mathbf{w}^H[i]}J = \; & -b[i-1]\mathbf{r}[i](b[i]\mathbf{w}^H[i-1]\mathbf{r}[i-1]-b[i-1]\mathbf{w}^H[i]\mathbf{r}[i])^H \\ & -b[i-2]\mathbf{r}[i](b[i]\mathbf{w}^H[i-2]\mathbf{r}[i-2]-b[i-2]\mathbf{w}^H[i]\mathbf{r}[i])^H \\ & -b[i-2]\mathbf{r}[i-1](b[i-1]\mathbf{w}^H[i-2]\mathbf{r}[i-2]-b[i-2]\mathbf{w}^H[i]\mathbf{r}[i-1])^H\end{aligned} \tag{5.20}$$

At this point, in order to improve the convergence performance of the NLMS algorithm, the bracketed error terms of (5.20) are modified by replacing the filters with the most recently calculated one, $\mathbf{w}[i-1]$. The resulting gradient expression is given by

$$\begin{aligned}\nabla_{\mathbf{w}^H[i]}J = \; & -b[i-1]\mathbf{r}[i]\underbrace{\left(b[i]\mathbf{w}^H[i-1]\mathbf{r}[i-1]-b[i-1]\mathbf{w}^H[i-1]\mathbf{r}[i]\right)^H}_{e_1[i]} \\ & -b[i-2]\mathbf{r}[i]\underbrace{\left(b[i]\mathbf{w}^H[i-1]\mathbf{r}[i-2]-b[i-2]\mathbf{w}^H[i-1]\mathbf{r}[i]\right)^H}_{e_2[i]} \\ & -b[i-2]\mathbf{r}[i-1]\underbrace{\left(b[i-1]\mathbf{w}^H[i-1]\mathbf{r}[i-2]-b[i-2]\mathbf{w}^H[i-1]\mathbf{r}[i-1]\right)^H}_{e_3[i]}\end{aligned} \tag{5.21}$$

Placing in the steepest descent filter update expression yields

$$\mathbf{w}[i]=\mathbf{w}[i-1]+\frac{\mu}{M[i]|\mathbf{w}^H[i-1]\mathbf{r}[i-1]|}\left[b[i-1]\mathbf{r}[i]e_1^*[i]+b[i-2]\mathbf{r}[i]e_2^*[i]+b[i-2]\mathbf{r}[i-1]e_3^*[i]\right], \tag{5.22}$$

where μ is the step-size and the normalisation factor, $M[i]$, is given by

$$M[i]=\lambda_M M[i-1]+(1-\lambda_M)\mathbf{r}^H[i]\mathbf{r}[i], \tag{5.23}$$

where λ_M is an exponential forgetting factor [15]. Enforcement of the constraint is performed by the denominator of (5.22) and ensures that the filter, $\mathbf{w}[i]$, does not tend towards a zero correlator as the adaptation progresses.

Incorporation of the variable switching and mixing factors of Section 5.3 has the potential to improve the performance of the above algorithm by optimising the weighting of the error terms of (5.21). Integration of the factors given by (5.13) and (5.16) yields

$$\mathbf{w}[i] = \mathbf{w}[i-1] + \frac{\mu}{M[i]} \left[\rho_1[i] b[i-1] \mathbf{r}[i] e_1[i] + \rho_2[i] b[i-2] \mathbf{r}[i] e_2[i] + \rho_3[i] b[i-2] \mathbf{r}[i-1] e_3[i]\right] \tag{5.24}$$

as the updated filter adaptation equation.

5.4.2 Least Squares Algorithms

To achieve faster convergence and increased robustness to fading a LS based solution is now pursued. Firstly, the bidirectional cost function of (5.4) is cast as a LS problem, yielding

$$\begin{aligned} J = \sum_{l=1}^{i} \lambda^{i-l} \Big[& \left| b[i] \mathbf{w}^H[i-1] \mathbf{r}[i-1] - b[i-1] \mathbf{w}^H[i] \mathbf{r}[i] \right|^2 + \\ & \left| b[i] \mathbf{w}^H[i-2] \mathbf{r}[i-2] - b[i-2] \mathbf{w}^H[i] \mathbf{r}[i] \right|^2 + \\ & \left| b[i-1] \mathbf{w}^H[i-2] \mathbf{r}[i-2] - b[i-2] \mathbf{w}^H[i-1] \mathbf{r}[i-1] \right|^2 \Big] \end{aligned}, \tag{5.25}$$

where λ is an exponential forgetting factor. Proceeding as with the conventional LS derivation, and modifying the equivalent error terms in a similar manner to as in (5.21), the following expressions for the component autocorrelation matrices can be reached

$$\begin{aligned} \bar{\mathbf{R}}_1[i] &= \lambda \bar{\mathbf{R}}_1[i-1] + b[i-1] \mathbf{r}[i] \mathbf{r}^H[i] b^*[i-1] \\ \bar{\mathbf{R}}_2[i] &= \lambda \bar{\mathbf{R}}_2[i-1] + b[i-2] \mathbf{r}[i] \mathbf{r}^H[i] b^*[i-2] \\ \bar{\mathbf{R}}_3[i] &= \lambda \bar{\mathbf{R}}_3[i-1] + b[i-2] \mathbf{r}[i-1] \mathbf{r}^H[i-1] b^*[i-2] \end{aligned} \tag{5.26}$$

and the component cross-correlation vectors

$$\begin{aligned}\bar{\mathbf{t}}_1[i] &= \lambda\bar{\mathbf{t}}_3[i-1] + b[i-1]\mathbf{r}[i]\mathbf{r}^H[i-1]\mathbf{w}[i-1]b^*[i] \\ \bar{\mathbf{t}}_2[i] &= \lambda\bar{\mathbf{t}}_2[i-1] + b[i-2]\mathbf{r}[i]\mathbf{r}^H[i-2]\mathbf{w}[i-1]b^*[i] \\ \bar{\mathbf{t}}_3[i] &= \lambda\bar{\mathbf{t}}_3[i-1] + b[i-2]\mathbf{r}[i-1]\mathbf{r}^H[i-2]\mathbf{w}[i-1]b^*[i-1]\end{aligned} \quad . \tag{5.27}$$

The overall correlation structures are then formed from the summation of the preceding expressions, yielding

$$\bar{\mathbf{R}}[i] = \bar{\mathbf{R}}_1[i] + \bar{\mathbf{R}}_2[i] + \bar{\mathbf{R}}_3[i] \tag{5.28}$$

and

$$\bar{\mathbf{t}}[i] = \bar{\mathbf{t}}_1[i] + \bar{\mathbf{t}}_2[i] + \bar{\mathbf{t}}_3[i]. \tag{5.29}$$

where

$$\mathbf{w}[i] = \bar{\mathbf{R}}^{-1}[i]\bar{\mathbf{t}}[i]. \tag{5.30}$$

As for the NLMS implementation, performance improvements can be expected if the variable switching and mixing factors, (5.13) and (5.16), are incorporated into the correlation expressions. The resulting expressions are

$$\mathbf{R}[i] = \rho_1[i]\mathbf{R}_1[i] + \rho_2[i]\mathbf{R}_2[i] + \rho_3[i]\mathbf{R}_3[i] \tag{5.31}$$

$$\mathbf{t}[i] = \rho_1[i]\mathbf{t}_1[i] + \rho_2[i]\mathbf{t}_2[i] + \rho_3[i]\mathbf{t}_3[i] \tag{5.32}$$

Introducing the above expression into the RLS framework would lead to a low-complexity algorithm with improved convergence and robustness compared to the NLMS of Section 5.4.1. This requires the integration of (5.26) with the matrix inversion lemma (2.47) [38, 127]. However, the derivation requires an expression of the form

$$\mathbf{R}[i] = \mathbf{R}[i-1] + \lambda\mathbf{r}[i]\mathbf{r}^H[i] \tag{5.33}$$

for the autocorrelation matrix; a form which (5.26) is unable to fit into without assumptions that cause a significant performance degradation. Consequently, an alternative low-complexity algorithm to implement the LS solution given by (5.26) - (5.30) is required.

5.4.3 Conjugate Gradient

Due to the incongruent form of the bidirectional LS formulation and the conventional RLS implementation, an alternative low-complexity method is now derived. The CG is chosen due to the lack of a matrix inversion and its excellent convergence properties [57, 58].

Inserting the autocorrelation (5.26) and cross-correlation (5.27) structures of Section 5.4.2 into the standard CG quadratic form yields

$$\mathbf{w}^H[i]\mathbf{R}[i]\mathbf{w}[i] - \mathbf{t}^H[i]\mathbf{w}[i]. \tag{5.34}$$

From [57], the unique minimiser of (5.34) is also the minimiser of

$$\mathbf{R}[i]\mathbf{w}[i] = \mathbf{t}[i]. \tag{5.35}$$

This shows the suitability of the CG algorithm to the bidirectional problem. At each time instant a number of iterations of the following method are required to reach an accurate solution, where the iterations are indexed with the variable j. Other single iteration CG methods are available but these depend upon degeneracy - a term that describes the situation where the successive CG vectors are not orthogonal [128, 129]. Consequently, the conventional method is utilised to ensure satisfactory convergence. At the i^{th} time instant the gradient and direction vectors are initialised as

$$\mathbf{g}_0[i] = \nabla_{\mathbf{w}[i]} J_{LS}(\mathbf{w}[i]) = \mathbf{R}[i]\mathbf{w}_0[i] - \mathbf{t}[i] \tag{5.36}$$

and

$$\mathbf{d}_0[i] = -\mathbf{g}_0[i], \tag{5.37}$$

respectively, where the gradient expression is equivalent to those used in the previous algorithm derivations. The vectors $\mathbf{d}_j[i]$ and $\mathbf{d}_{j+1}[i]$ are $\mathbf{R}[i]$ orthogonal with respect to $\mathbf{R}[i]$ such that $\mathbf{d}_j[i]\mathbf{R}[i]\mathbf{d}_l[i] = 0$ for $j \neq l$. At each iteration, the filter is updated as

$$\mathbf{w}_{j+1}[i] = \mathbf{w}_j[i] + \alpha_j[i]\mathbf{d}_j[i] \tag{5.38}$$

where $\alpha_j[i]$ is the minimiser of $J_{LS}(\mathbf{w}_{j+1}[i])$ such that

$$\alpha_j = \frac{-\mathbf{d}_j^H \mathbf{g}_j[i]}{\mathbf{d}_j^H[i]\mathbf{R}[i]\mathbf{d}_j[i]}. \tag{5.39}$$

The gradient vector is then updated according

$$\mathbf{g}_{j+1}[i] = \mathbf{R}[i]\mathbf{w}_j[i] - \mathbf{t}[i] \tag{5.40}$$

and a new conjugate gradient direction vector found

$$\mathbf{d}_{j+1}[i] = -\mathbf{g}_{j+1}[i] + \beta_j[i]\mathbf{d}_j[i] \tag{5.41}$$

where

$$\beta_j[i] = \frac{\mathbf{g}_{j+1}^H[i]\mathbf{R}[i]\mathbf{d}_j[i]}{\mathbf{d}_j^H[i]\mathbf{R}[i]\mathbf{d}_j[i]} \tag{5.42}$$

ensures the $\mathbf{R}[i]$ orthogonality between $\mathbf{d}_j[i]$ and $\mathbf{d}_l[i]$ where $j \neq l$. The iterations (5.38) - (5.42) are then repeated until $j = j_{max}$.

The variable switching and mixing factors can be incorporated into the algorithm to improve performance. This is achieved by operating the CG algorithm over the modified correlation structures given by (5.31) and (5.32).

5.5 Analysis

In this section, the proposed bidirectional algorithms are analysed to gain an indication of expected performance but also to obtain further insight into the proposed and existing algorithms' operation. The unconventional form of the differential costs function precludes the application of standard MSE analysis. Consequently, the SINR of the proposed algorithms is used in order to analyse their interference suppression and tracking performance. Firstly, the NLMS algorithm and the features of its weight error correlation matrix are studied in order to arrive at an analytical SINR expression. Following this, the analogy between the form of the bidirectional expression and convex combinations of adaptive filters is explored [130–132].

5.5.1 SINR Analysis

To begin consider the SINR expression given by

$$\text{SINR} = \frac{\mathbf{w}^H[i]\mathbf{R}_\text{S}\mathbf{w}[i]}{\mathbf{w}^H[i]\mathbf{R}_\text{I}\mathbf{w}[i]}, \tag{5.43}$$

where $\mathbf{R}_S$ and $\mathbf{R}_I$ are the signal, and interference and noise correlation matrices, respectively. Substituting in the filter error weight vector

$$\boldsymbol{\varepsilon}[i] = \mathbf{w}[i] - \mathbf{w}_o[i], \tag{5.44}$$

where $\mathbf{w}_o$ is the instantaneous standard MMSE receiver, yields

$$\text{SINR} = \frac{\boldsymbol{\varepsilon}^H[i]\mathbf{R}_\text{S}\boldsymbol{\varepsilon}[i] + \boldsymbol{\varepsilon}^H[i]\mathbf{R}_\text{S}\mathbf{w}_o[i] + \overbrace{\mathbf{w}_o^H[i]\mathbf{R}_\text{S}\mathbf{w}_o[i]}^{P_{\text{S,opt}}[i]} + \mathbf{w}_o^H[i]\mathbf{R}_\text{S}\boldsymbol{\varepsilon}[i]}{\boldsymbol{\varepsilon}^H[i]\mathbf{R}_\text{I}\boldsymbol{\varepsilon}[i] + \boldsymbol{\varepsilon}^H[i]\mathbf{R}_\text{I}\mathbf{w}_o[i] + \underbrace{\mathbf{w}_o^H[i]\mathbf{R}_\text{I}\mathbf{w}_o[i]}_{P_{\text{I,opt}}[i]} + \mathbf{w}_o^H[i]\mathbf{R}_\text{I}\boldsymbol{\varepsilon}[i]}. \tag{5.45}$$

Taking the trace and expectation of (5.45) and defining $\mathbf{K}[i] = E[\boldsymbol{\varepsilon}[i]\boldsymbol{\varepsilon}^H[i]]$ and $\mathbf{G}[i] = E[\mathbf{w}_o[i]\boldsymbol{\varepsilon}^H[i]]$, allows the following expression to be formed

$$\text{SINR} = \frac{\mathbf{K}[i]\mathbf{R}_{\text{S}} + \mathbf{G}[i]\mathbf{R}_{\text{S}} + P_{\text{S,opt}}[i] + \mathbf{G}^H[i]\mathbf{R}_{\text{S}}}{\mathbf{K}[i]\mathbf{R}_{\text{I}} + \mathbf{G}[i]\mathbf{R}_{\text{I}} + P_{\text{I,opt}}[i] + \mathbf{G}^H[i]\mathbf{R}_{\text{I}}}. \tag{5.46}$$

From (5.46) it is clear that expressions for $\mathbf{K}[i]$ and $\mathbf{G}[i]$ are required in order to reach an analytical interpretation of the bidirectional NLMS scheme.

Substituting the filter error weight vector into the filter update expression of (5.22) yields a recursive expression for the filter error weight vector

$$\begin{aligned}
\boldsymbol{\varepsilon}[i] \quad &= \boldsymbol{\varepsilon}[i-1] \\
&+ \Big[\mathbf{I} + \mu\mathbf{r}[i]b[i-1]\mathbf{r}^H[i-1]b^*[i] - \mu\mathbf{r}[i]b[i-1]\mathbf{r}^H[n]b^*[i-1] \\
&+\mu\mathbf{r}[i]b[i-2]\mathbf{r}^H[i-2]b^*[i] - \mu\mathbf{r}[i]b[i-2]\mathbf{r}^H[n]b^*[i-2] \\
&+\mu\mathbf{r}[i-1]b[i-2]\mathbf{r}^H[i-2]b^*[i-1] - \mu\mathbf{r}[i-1]b[i-2]\mathbf{r}^H[i-1]b^*[i-2]\Big]\boldsymbol{\varepsilon}[i-1] \;, \\
&+\mu\mathbf{r}[i]b[i-1]e^*_{o,1}[i] \\
&+\mu\mathbf{r}[i]b[i-2]e^*_{o,2}[i] \\
&+\mu\mathbf{r}[i-1]b[i-2]e^*_{o,3}[i]
\end{aligned} \tag{5.47}$$

where the terms $e_{o,1-3}$ denote the errors terms of (5.21) when the optimum filter $\mathbf{w}_o$ is used. Utilising the direct averaging approach given by Kushner [133], and invoked in a number of other texts, the solution to the stochastic difference equation of (5.47) can be approximated by the solution to a second equation [38, 134], such that

$$\begin{aligned}
&E\Big[\mathbf{I} + \mu\mathbf{r}[i]b[i-1]\mathbf{r}^H[i-1]b^*[i] - \mu\mathbf{r}[i]b[i-1]\mathbf{r}^H[n]b^*[i-1] \\
&+\mu\mathbf{r}[i]b[i-2]\mathbf{r}^H[i-2]b^*[i] - \mu\mathbf{r}[i]b[i-2]\mathbf{r}^H[n]b^*[i-2] \\
&+\mu\mathbf{r}[i-1]b[i-2]\mathbf{r}^H[i-2]b^*[i-1] - \mu\mathbf{r}[i-1]b[i-2]\mathbf{r}^H[i-1]b^*[i-2]\Big] \;, \\
&= \\
&\mathbf{I} + \mu\mathbf{F}_1 - \mu\mathbf{R}_1 + \mu\mathbf{F}_2 - \mu\mathbf{R}_2 + \mu\mathbf{F}_3 - \mu\mathbf{R}_3
\end{aligned} \tag{5.48}$$

where $\mathbf{F}$ and $\mathbf{R}$ are correlations matrices. Specifically, $\mathbf{R}_{1-3}$ are autocorrelation matrices

given by

$$\begin{aligned}\mathbf{R}_1 &= E\left[\mu\mathbf{r}[i]b^*[i-1]\mathbf{r}^H[i]b^*[i-1]\right]\\ \mathbf{R}_2 &= E\left[\mu\mathbf{r}[i]b^*[i-2]\mathbf{r}^H[i]b^*[i-2]\right]\\ \mathbf{R}_3 &= E\left[\mu\mathbf{r}[i-1]b^*[i-2]\mathbf{r}^H[i-1]b^*[i-1]\right]\end{aligned} \tag{5.49}$$

and $\mathbf{F}_{1-3}$ cross-time instant correlation matrices, given by

$$\begin{aligned}\mathbf{F}_1 &= E\left[\mu\mathbf{r}[i]b^*[i-1]\mathbf{r}^H[i-1]b^*[i]\right]\\ \mathbf{F}_2 &= E\left[\mu\mathbf{r}[i]b^*[i-2]\mathbf{r}^H[i-2]b^*[i]\right]\\ \mathbf{F}_3 &= E\left[\mu\mathbf{r}[i-1]b^*[i-2]\mathbf{r}^H[i-2]b^*[i-1]\right].\end{aligned} \tag{5.50}$$

Using (5.48) and the independence assumptions of $E\left[e_{o,1-3}[i]\boldsymbol{\varepsilon}[i]\right] = 0$, $E\left[\mathbf{r}^H[i]\mathbf{r}[i-1]\right] = 0$ and $E\left[b_k[i]b_k[i-1]\right] = 0$, an expression for $\mathbf{K}[i]$ is reached

$$\begin{aligned}\mathbf{K}[i] = \;& \left[\mathbf{I}+\mu\mathbf{F}_1-\mu\mathbf{R}_1+\mu\mathbf{F}_2-\mu\mathbf{R}_2+\mu\mathbf{F}_3-\mu\mathbf{R}_3\right]\mathbf{K}[i-1]\cdots\\ & \left[\mathbf{I}+\mu\mathbf{F}_1-\mu\mathbf{R}_1+\mu\mathbf{F}_2-\mu\mathbf{R}_2+\mu\mathbf{F}_3-\mu\mathbf{R}_3\right]\\ & +\mu^2\mathbf{R}_1J_{min,1}[i]\\ & +\mu^2\mathbf{R}_2J_{min,2}[i]\\ & +\mu^2\mathbf{R}_1J_{min,3}[i]\end{aligned} \tag{5.51}$$

where $J_{min,j}[i] = |e_{o,j}|^2$. Following a similar method, an expression for $\mathbf{G}[i]$ can also be reached

$$\mathbf{G}[i] = \mathbf{G}[i-1]\left[\mu\mathbf{F}_1-\mu\mathbf{R}_1+\mu\mathbf{F}_2-\mu\mathbf{R}_2+\mu\mathbf{F}_3-\mu\mathbf{R}_3\right]. \tag{5.52}$$

They preceding expressions can now be studied to gain an insight into the operation of the bidirectional algorithm and the origins of its advantages over the conventional differential scheme. Equivalent expressions for the conventional stochastic gradient scheme are given by

$$\begin{aligned}\mathbf{K}[i] = \;& \left[\mathbf{I}+\mu\mathbf{F}_1-\mu\mathbf{R}_1\right]\mathbf{K}[i-1]\left[\mathbf{I}+\mu\mathbf{F}_1-\mu\mathbf{R}_1\right]\\ & +\mu^2\mathbf{R}_1J_{min,1}[i]\\ \mathbf{G}[i] = \;& \mathbf{G}[i-1]\left[\mu\mathbf{F}_1-\mu\mathbf{R}_1\right].\end{aligned} \tag{5.53}$$

The bidirectional scheme has a number of additional correlation terms compared to the conventional scheme. Evaluating the cross-time instant matrices yields

$$\begin{aligned}\mathbf{F}_1 &= |a_1|^2\mathbf{c}_1\mathbf{c}_1^H \underbrace{E\left[h[i]h^*[i-1]\right]}_{f_1[i]} \\ \mathbf{F}_2 &= |a_1|^2\mathbf{c}_1\mathbf{c}_1^H \underbrace{E\left[h[i]h^*[i-2]\right]}_{f_2[i]} \\ \mathbf{F}_3 &= |a_1|^2\mathbf{c}_1\mathbf{c}_1^H \underbrace{E\left[h[i-1]h^*[i-2]\right]}_{f_3[i]}\end{aligned} \quad . \tag{5.54}$$

From the expressions above, it is clear that the underlying factors that govern the SINR performance of the algorithms are the correlation factors between the considered time instants and data-reuse. Accordingly, it is the additional correlation factors that the bidirectional algorithm possesses that enhances its performance compared to the conventional scheme. This confirms the initial motivation behind the proposition of the bidirectional approach. Lastly, the f_{1-3} expressions of (5.54) can be seen to be the factors that influence the optimum number of time instants to consider.

5.5.2 Combinations of Adaptive Filters

To further our understanding of the bidirectional algorithms, a heuristic and complementary approach is now taken and leads to an analogy with a combination of adaptive filters [131]. The bidirectional LS solution given by (5.30) is made up of 6 constituent correlation structures that result in a filter output of

$$y[i] = \left[(\rho_1\mathbf{R}_1[i] + \rho_3\mathbf{R}_2[i] + \rho_3\mathbf{R}_3[i])^{-1}(\rho_1\mathbf{t}_1[i] + \rho_2\mathbf{t}_2[i] + \rho_3\mathbf{t}_3[i])\right]^H \mathbf{r}[i]. \tag{5.55}$$

Decomposing the expression above leads us to an expression where the signal $y[i]$ is formed from the output of 3 individual adaptive filters

$$\begin{aligned} y[i] &= \left[\left(\mathbf{R}_1[i] + \tfrac{\rho_2}{\rho_1}\mathbf{R}_2[i] + \tfrac{\rho_3}{\rho_1}\mathbf{R}_3[i]\right)^{-1}\mathbf{t}_1[i]\right]^H \mathbf{r}[i] \\ &+ \left[\left(\mathbf{R}_1[i] + \tfrac{\rho_1}{\rho_2}\mathbf{R}_2[i] + \tfrac{\rho_3}{\rho_2}\mathbf{R}_3[i]\right)^{-1}\mathbf{t}_2[i]\right]^H \mathbf{r}[i] \quad . \\ &+ \left[\left(\mathbf{R}_1[i] + \tfrac{\rho_1}{\rho_3}\mathbf{R}_2[i] + \tfrac{\rho_2}{\rho_3}\mathbf{R}_3[i]\right)^{-1}\mathbf{t}_3[i]\right]^H \mathbf{r}[i] \end{aligned} \tag{5.56}$$

This is equivalent to a convex combination of adaptive filters with varying λ [130–132], where each of the 3 filters focuses on the correlation between the 2 of the 3 considered time instants. However, the presence of autocorrelation matrices in the inverses of the expression also indicates that the remaining time instants also influence the structure of each filter. Although the mixing factors are not separable it is possible to interpret them as a form of weighting that is present in conventional combinations of adaptive filters. This therefore partly explains the additional control and performance they provide.

5.6 Simulations

In this section, the proposed adaptive algorithms are applied to conventional multiuser and cooperative DS-CDMA systems with short spreading sequences. The individual Rayleigh fading channel coefficients, $h[i]$, are generated using Clarke's model [79] where 20 scatterers are assumed and the power of the interfering users is between 0dB and 10dB relative to the user of interest. In all simulations the number of packets is denoted by N_p and the fading rate is given by the dimensionless normalized fading parameter, $T_s f_d$, where T_s is the symbol period and f_d is the Doppler frequency shift. The filters' convergence parameters have been optimised resulting in step-sizes forgetting factors of 0.1 and 0.99, respectively, $\lambda_e = 0.95$, $\lambda_M = 0.99$ and the number of CG iterations, $j_{\max} = 5$.

As covered in Section 5.5, the proposed algorithms do not minimise the same MSE as a conventional MMSE receiver; therefore, it is not an adequate performance metric. As a result, BER and SINR based metrics are chosen for the purposes of comparison between existing algorithms and the optimum MMSE solution. Due to the rapidly fading channel, the instantaneous SNR, SNR_i, is highly variable and so the SINR alone is also not a satisfactory metric. To overcome this it is normalised by the instantaneous SNR to give $\frac{SINR}{SNR_\text{i}}$. This value is negative in all simulations and directly reflects the MUI interference suppression and tracking capabilities of the proposed algorithms [15, 125].

5.6.1 Conventional DS-CDMA

Here the adaptive algorithms of Section 5.4 are applied to interference suppression in the uplink of a multiuser DS-CDMA system given by Figure 3.1. Each simulation is averaged over N_p packets and detailed parameters are specified in each plot. The $M \times 1$ received signal after chip-pulsed matched filtering and sampling at the chip rate is given by

$$\mathbf{r}[i] = A_1 b_1[i]\mathbf{H}_1[i]\mathbf{c}_1[i] + \underbrace{\sum_{k=2}^{K} A_k b_k[i]\mathbf{H}_k[i]\mathbf{c}_k[i]}_{\text{MUI}} + \boldsymbol{\eta}[i] + \mathbf{n}[i], \tag{5.57}$$

where $M = N + L - 1$, and $\mathbf{c}_k[i]$ and A_k are the spreading sequence and signal amplitude of the k^{th} user, respectively. The $M \times N$ channel matrix with L paths is given by $\mathbf{H}_k[i]$ for the k^{th} user, $\boldsymbol{\eta}[i]$ ISI vector and $\mathbf{n}[i]$ is noise vector. Conventional schemes use BPSK modulation and the differential and bidirectional schemes utilise differential BPSK where the sequence of data symbols to be transmitted by the k^{th} user are given by $b_k[i] = a_k[i]b_k[i-1]$ where $a_k[i]$ is the unmodulated baseband data.

Analytical Results

Firstly, the analytical expressions derived in Section 5.5.1 and their agreement with simulated results are assessed. Central to the performance of the differential and bidirectional schemes are the correlation factors f_{1-3} and the related assumption of $h_1[i] \approx$

$h_1[i-1]$. Examining the effect of the fading rate on the value of f_{1-3} shows that $f_1 \approx f_2 \approx f_3$ at fading rates of up to $T_s f_d = 0.01$. Consequently, after a large number of received symbols with high total receive power

$$3\left[\mathbf{I} + \mu\mathbf{F}_1 - \mu\mathbf{R}_1\right] \approx \left[\mathbf{I} + \mu\mathbf{F}_1 - \mu\mathbf{R}_1 + \mu\mathbf{F}_2 - \mu\mathbf{R}_2 + \mu\mathbf{F}_3 - \mu\mathbf{R}_3\right], \tag{5.58}$$

due to the decreasing significance of the identity matrix. This indicates that the expected value of the SINR, of the bidirectional scheme, once $f_1 \approx f_2 \approx f_3$ have stabilised, should be similar to the differential scheme. A second implication is that the bidirectional scheme should converge towards the MMSE level due to the equivalence between the differential scheme and the MMSE solution [15]. Figure 5.2 illustrates the analytical performance using the expressions given in Section 5.5.1. The correlation

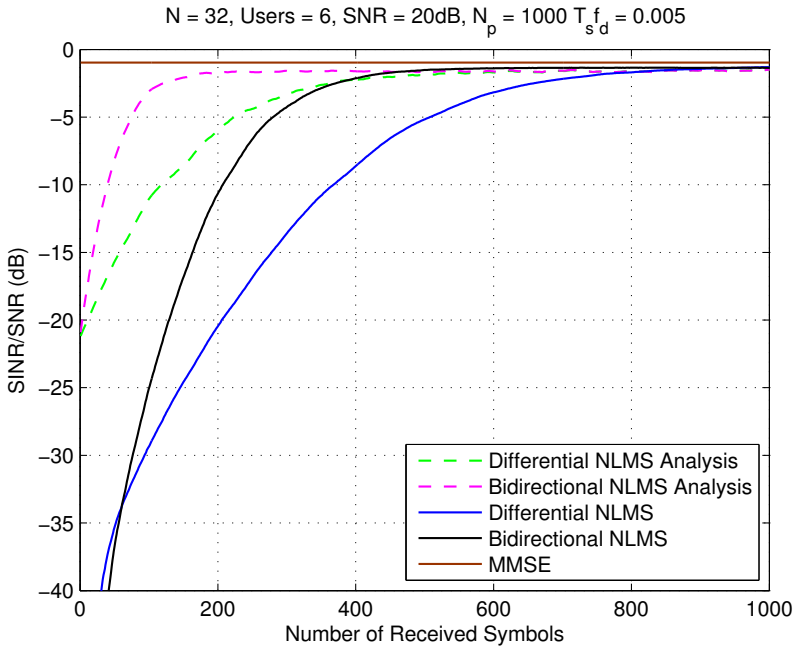

Figure 5.2: SINR performance comparison of simulated and analytical proposed NLMS algorithms over a single path channel.

matrices are calculated via ensemble averages prior to commencement of the algorithm and $\mathbf{G}[0] = \mathbf{K}[0] = \mathbf{I}$. In Figure 5.2 one can see the convergence of the simulated schemes to the analytical and MMSE plots, validating the presented analysis. Due to

the highly dynamic nature of the channel, using the expected values of the correlation matrix alone cannot capture the true transient performance of the algorithms. However, the convergence period of the analytical plots within the first 200 iterations can be considered to be within the coherence time and therefore give an indication of the transient performance relative to other analytical plots. Using this justification and the aforementioned analysis, advantages should be present in the transient phase due to the additional correlation information supplied by $\mathbf{F}_2$ and $\mathbf{F}_3$. This conclusion is supported by Figure 5.2 and the similar forms of the analytical and simulated schemes relative to each other and their subsequent convergence.

SINR Performance

The SINR/SNR performance of the proposed algorithms is given by Figures 5.3 to 5.5. The performance of the CG implementations of the differential and bidirectional algorithms is significantly above that of the RLS during convergence; however, a contributing factor towards this is the extra initialisation flexibility and convergence performance that the CG provides. Figure 5.4 shows in more detail the performance improvement obtained during convergence by the bidirectional CG scheme compared to the CG implementation of the existing differential scheme. This improvement can be attributed to the additional correlation information that the bidirectional scheme utilises. A 1dB gain is present during convergence but as the algorithms approach steady state this margin diminishes; however, this convergence improvement leads to significant BER gains as illustrated in Figure 5.6. As expected from the previous analysis, the differential and bidirectional algorithms converge close to the MMSE optimum and the conventional non-differential schemes are unable to track the unfaded symbols at such a high fading rate and therefore do not converge.

The bidirectional NLMS algorithm provides more significant improvements over the differential scheme, both in the final stages of convergence and steady-state. As with the CG implementations, these differences can be accounted for by the reduced

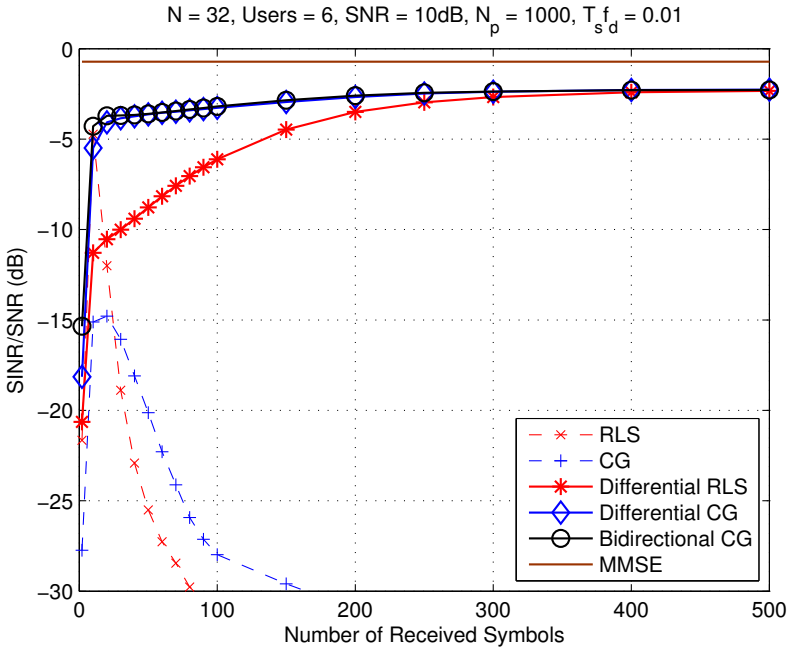

Figure 5.3: SINR/SNR performance comparison of proposed CG algorithms over a single path channel where all schemes have been trained with 150 symbols and then switched to decision directed mode.

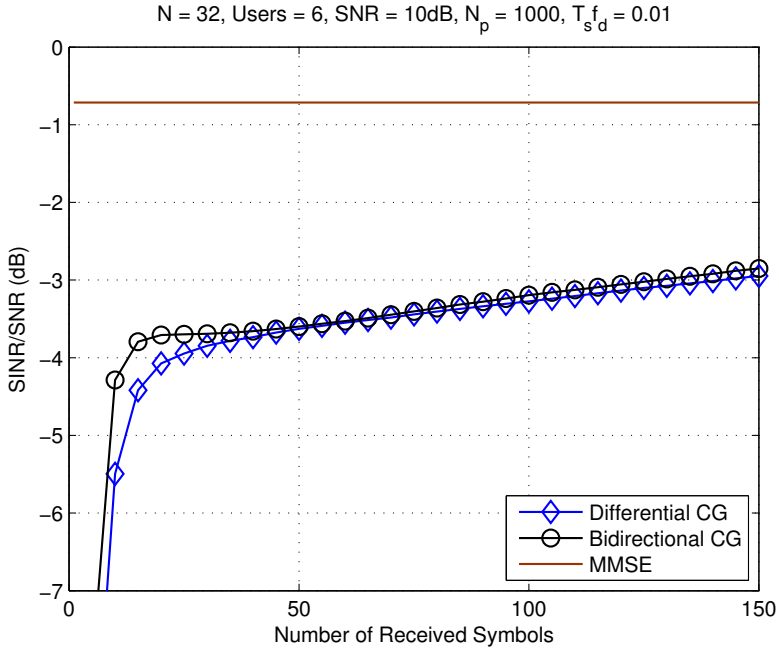

Figure 5.4: Detailed SINR/SNR convergence performance comparison of proposed CG algorithms over a single path channel where all schemes have been trained with 150 symbols and then switched to decision directed mode.

receive signal power; the matrices equivalent to $\mathbf{F}2$ and $\mathbf{F}3$ improving the consistency of the steady-state performance by reducing the impact of weakly-correlated samples; and the NLMS's suitability to data reuse as in the AP algorithm. Once again the conventional adaptive schemes are unable to converge or track the solution due to the more demanding task of tracking both the fading coefficients and suppressing MUI.

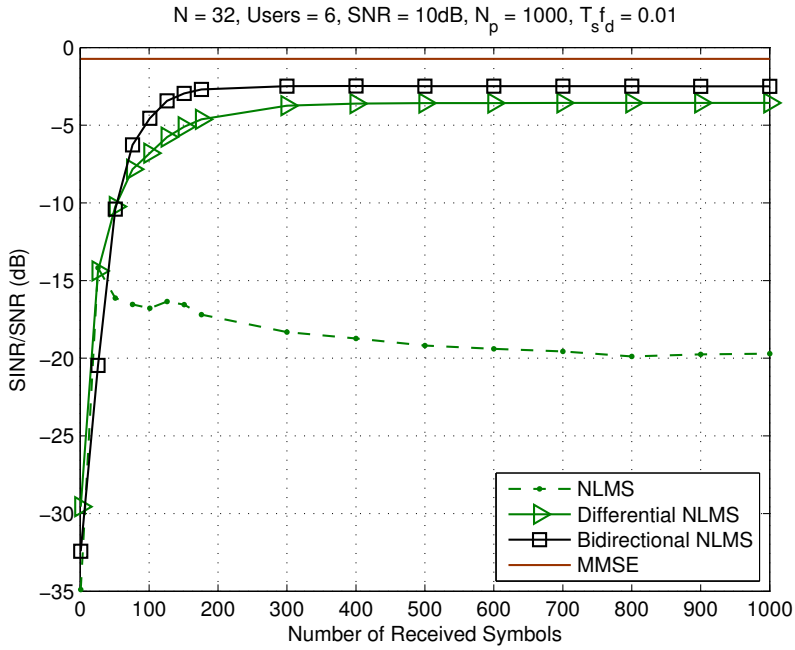

Figure 5.5: SINR/SNR performance comparison of proposed NLMS algorithms over a single path channel where all schemes have been trained with 150 symbols and then switched to decision directed mode.

The BER performance of differential and bidirectional schemes is illustrated in Figure 5.6 where the system parameters are equal to those of Figures 5.3 and 5.5. The RLS and CG algorithms converge to near the MMSE level with the bidirectional scheme providing a significant performance improvement. The NLMS schemes exhibit slower BER convergence compared to their SINR performance but reach a level where decision directed operation can take place in a severely fading channel. Due to the superior performance of the CG and RLS based algorithms it is their performance that is the predominant focus of the remainder of this chapter. As expected, the poor SINR/SNR performance of the conventional schemes has translated into equally poor BER performance in as much that the schemes do not converge and are unable to reliably obtain

the transmitted symbols.

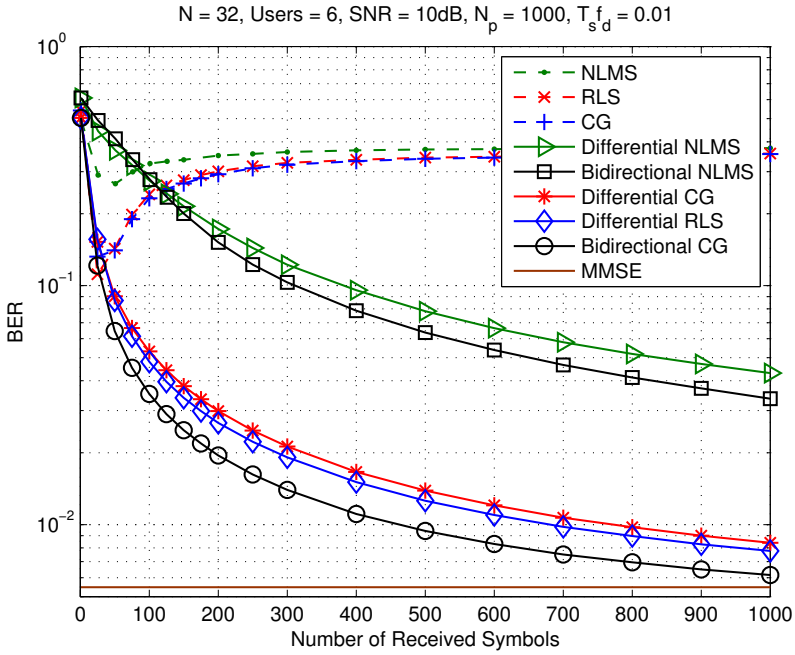

Figure 5.6: BER performance comparison of proposed schemes during training over a single path channel.

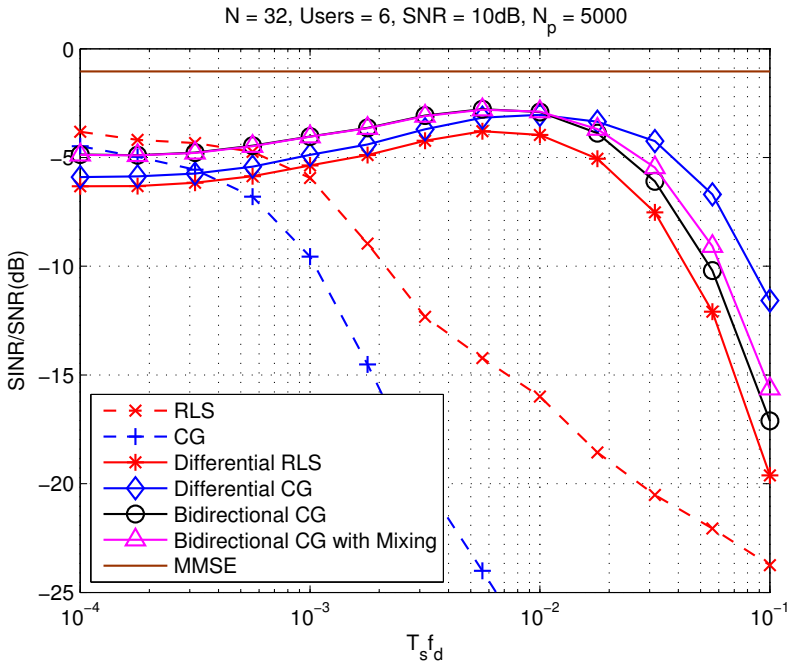

Figure 5.7: SINR/SNR performance versus fading rate of the proposed CG schemes over a single path channel after 200 training symbols.

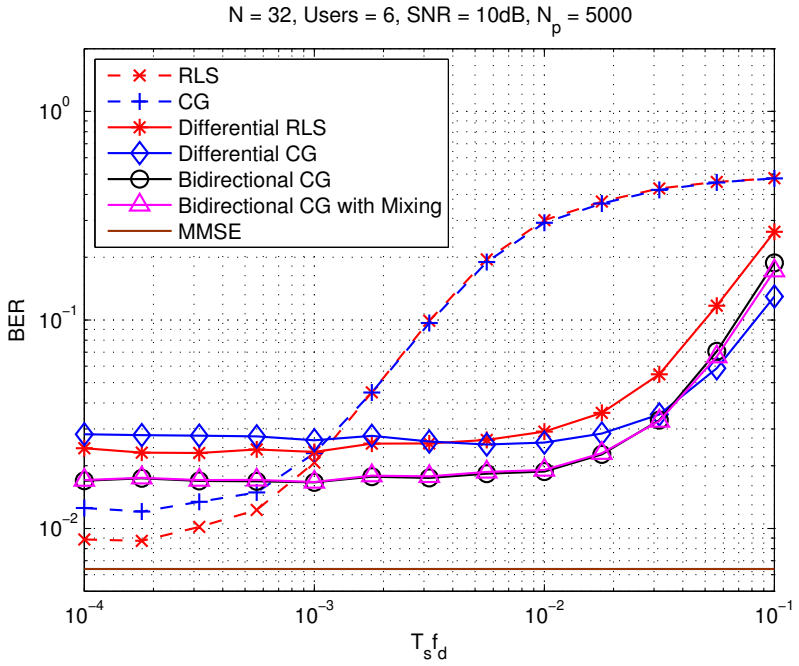

Figure 5.8: BER performance versus fading rate of the proposed CG schemes over a single path channel after 200 training symbols.

Figures 5.7 and 5.8 illustrate the SINR/SNR and BER performance of the proposed CG and RLS algorithms over a range of fading rates. Although the conventional schemes provide good performance at slow fading rates, they are unable to perform adequate interference suppression at fading rates in excess of $T_s f_d = 0.001$. The bidirectional schemes provide improved performance at low fading rates compared to the differential methods but also provide extended performance until fading rates above $T_s f_d = 0.01$ are reached, at which point their performance declines inline with the differential CG. Although the 200 symbol data-record of Figure 5.8 has not allowed the BER plots to fully converge (see Figure 5.6) and the bidirectional and differential schemes to reach their error floor, the advantages of the bidirectional schemes are still evident up to a fading rate of approximately 0.04. Similarly, considering Figure 5.7, the 200 symbol data-record has extended beyond the initial stages of convergence during which the bidirectional CG schemes obtain their SINR/SNR advantage over the differential schemes (see Figure 5.4). Consequently, the full extent of the SINR/SNR gains provided by the bidirectional schemes are not evident in Figure 5.7. Once again, the

increase in performance provided by the bidirectional schemes can be accounted for by the increased correlation information supplied by the matrices $\mathbf{F}_2$ and $\mathbf{F}_3$, and data reuse. The introduction of the mixing factors into the bidirectional algorithm improves performance further, especially at higher fading rates. A first reason for this is the improvement in consistency as previously mentioned. However, a second more significant reason can be established by referring back to the observations on the correlation factors f_{1-3}. Although fading rates of 0.01 may be fast, the assumption $h[i-2] \approx h[i-1] \approx h[i]$ is still valid. Consequently, $f_1 \approx f_2 \approx f_3$ and equal weighting is adequate. However, as the fading rate increases beyond $T_s f_d = 0.01$ this assumption breaks down and the correlation information requires unequal weighting for optimum performance, a task fulfilled by the adaptive mixing factors.

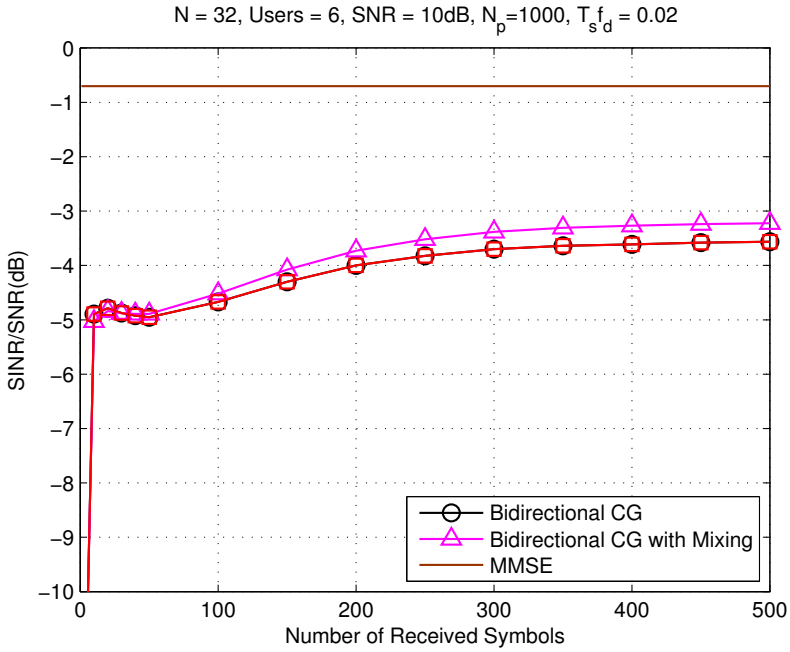

Figure 5.9: SINR/SNR performance over a single path channel of the proposed CG schemes with switching and mixing factors.

A more detailed plot illustrating the performance advantages of the CG switching and mixing parameters presented in Section 5.3 is given by Figure 5.9. The switching approach provides little improvement over the standard bidirectional scheme due to its discrete and non-adaptive operation. As previously covered, a low instantaneous value

of f_{1-3}, as indicated by a large power differential, does not indicate that all information gathered on f_{1-3} is redundant. The mixing parameter implementations address this shortcoming by adaptively setting the parameters via the error weight expression (5.16) that accurately reflects the averaged correlation factors. At a fading rate of $T_s f_d = 0.02$ the assumption of $f_1 \approx f_2 \approx f_3$ begins to diminish in accuracy and therefore unequal weighting is required for performance in excess of the standard bidirectional scheme, as previously mentioned and shown in Figure 5.9.

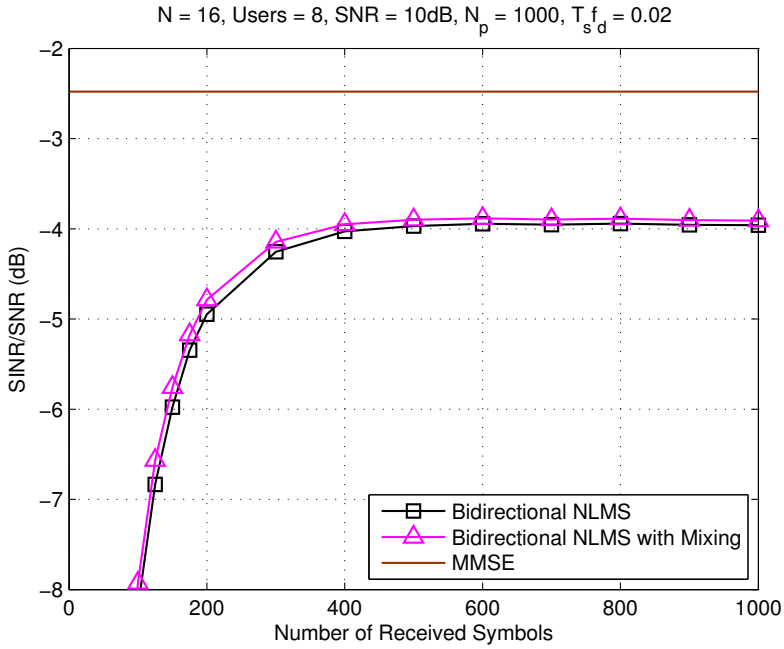

Figure 5.10: SINR/SNR performance over a single path channel of the proposed NLMS schemes with mixing factors.

Figure 5.10 illustrates the performance improvements brought about by introducing the mixing parameters to the bidirectional NLMS schemes. As for the CG scheme, improvements are present both during convergence and steady-state. The origin of these benefits is once again the increased correlation information available to the algorithm and the unequal weighting of the correlation information.

The MUI suppression of the proposed and existing schemes is given by Figure 5.11. The bidirectional scheme has significantly improved multiuser performance compared to the differential algorithms at low system loads but diminishes as the number of users

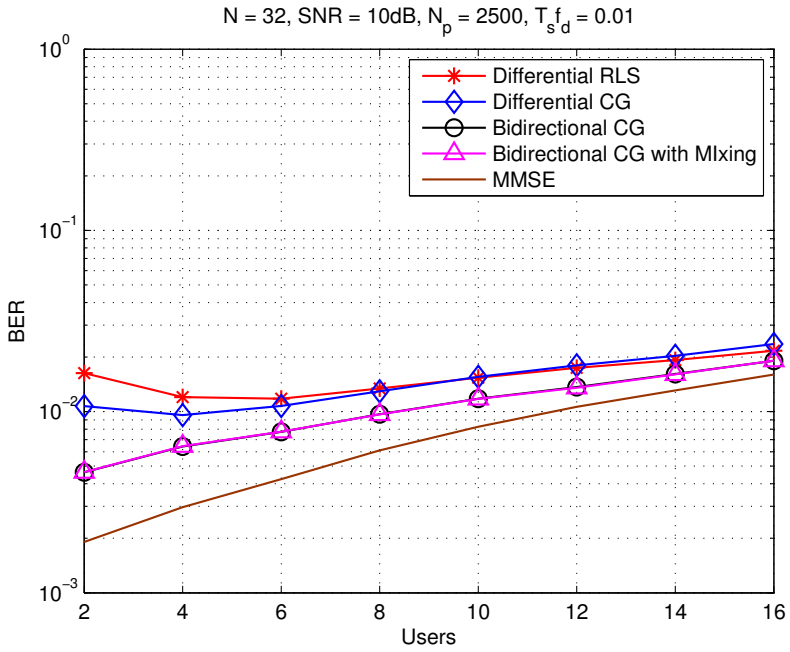

Figure 5.11: BER performance against system loading after 500 symbols of the proposed schemes over a single path channel. Schemes are trained with 150 symbols and then switch to decision directed operation.

increases. This characteristic supports the analytical conclusions of Section 5.5.1 by virtue of the convergence of the differential and bidirectional schemes and the increasing accuracy of (5.58) as system loading, and therefore received power, increases.

5.6.2 Cooperative DS-CDMA

To further demonstrate the performance of the proposed schemes they are now applied to an AF cooperative DS-CDMA system given by Figure 5.12. The expressions for the received signals after chip-pulsed matched filtering and sampling at the n^{th} relay and the destination nodes are given by

$$\mathbf{r}_{\text{sr}_n}[i] = \sum_{k=1}^{K} a_{\text{s}_k}[i] b_k[i] h_{\text{sr}_n}[i] \mathbf{c}_k[i] + \mathbf{n}_{\text{r}_n}[i], \tag{5.59}$$

$$\mathbf{r}_{\text{rd}}[i] = \sum_{n=1}^{N_{\text{r}}} a_{\text{r}_n}[i] h_{\text{r}_n\text{d}}[i] \mathbf{r}_{\text{sr}_n}[i] + \mathbf{n}_{\text{d}}[i] \tag{5.60}$$

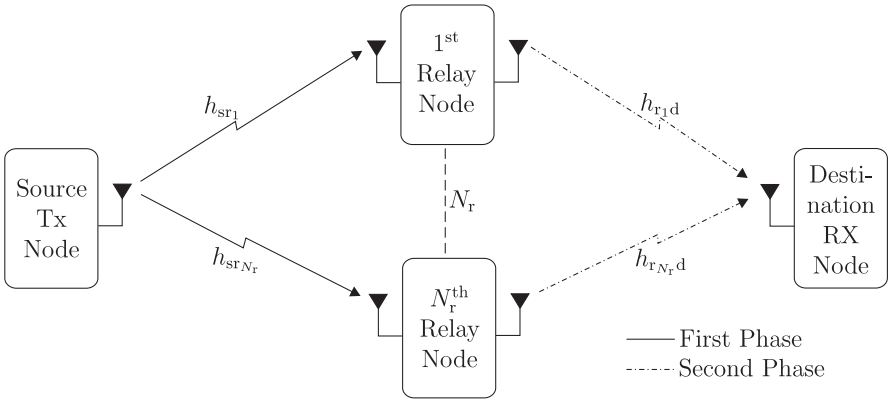

Figure 5.12: Cooperative DS-CDMA System Model

and

$$\mathbf{r}_{\mathrm{rd}}[i] = \sum_{n=1}^{N_\mathrm{r}} \sum_{k=1}^{K} a_{\mathrm{s}_k}[i] a_{\mathrm{r}_n}[i] h_{\mathrm{sr}_n}[i] h_{\mathrm{r}_n\mathrm{d}}[i] \mathbf{c}_k[i] b_k[i] + \sum_{n=1}^{N_\mathrm{r}} a_{\mathrm{r}_n}[i] h_{\mathrm{r}_n\mathrm{d}}[i] \mathbf{n}_{\mathrm{r}_n}[i] + \mathbf{n}_\mathrm{d}[i]. \quad (5.61)$$

where $h_{\mathrm{sr}_n}[i]$ and $h_{\mathrm{r}_n\mathrm{d}}[i]$ are the channel fading channel coefficients between the source and n^{th} relay, and n^{th} relay and the destination, respectively, and $\mathbf{n}_{\mathrm{r}_n}[i]$ and $\mathbf{n}_\mathrm{d}[i]$ are vectors of AWGN at the relays and destination, respectively.

Figure 5.13 shows that the bidirectional scheme obtains performance benefits over the differential schemes during convergence but, as expected, the performance gap closes as steady-state is reached. The inclusion of variable mixing parameters improves performance but to a lesser extent than non-cooperative networks due to the more challenging scenario of compounding highly time-variant channels.

The improvement BER brought about by the bidirectional schemes is evident from Figure 5.14. However, the more challenging environment of a cooperative system with compounded rapid fading has impacted on the BER performance of the schemes, as evidenced by the increased performance gap between the proposed schemes and MMSE reception.

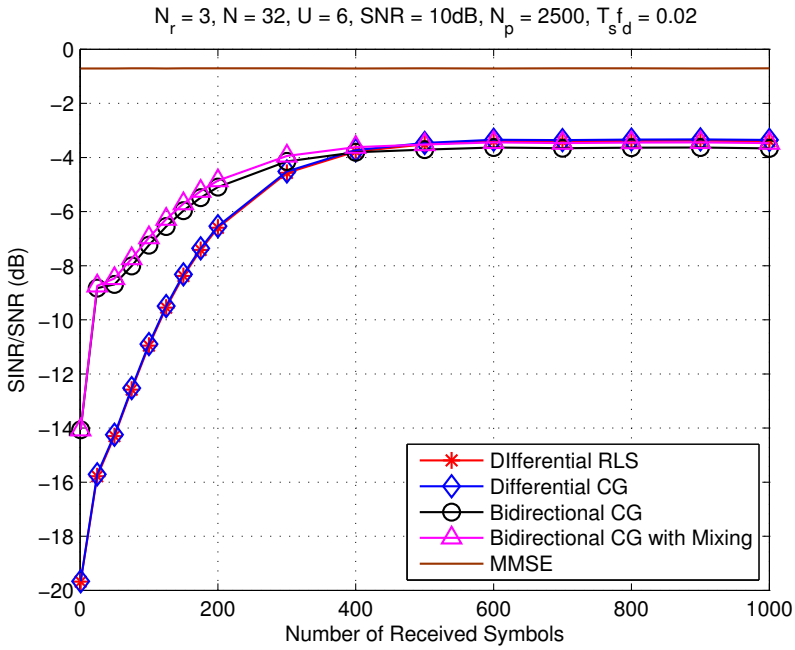

Figure 5.13: SINR/SNR performance of the proposed CG schemes during training in a single path cooperative DS-CDMA system.

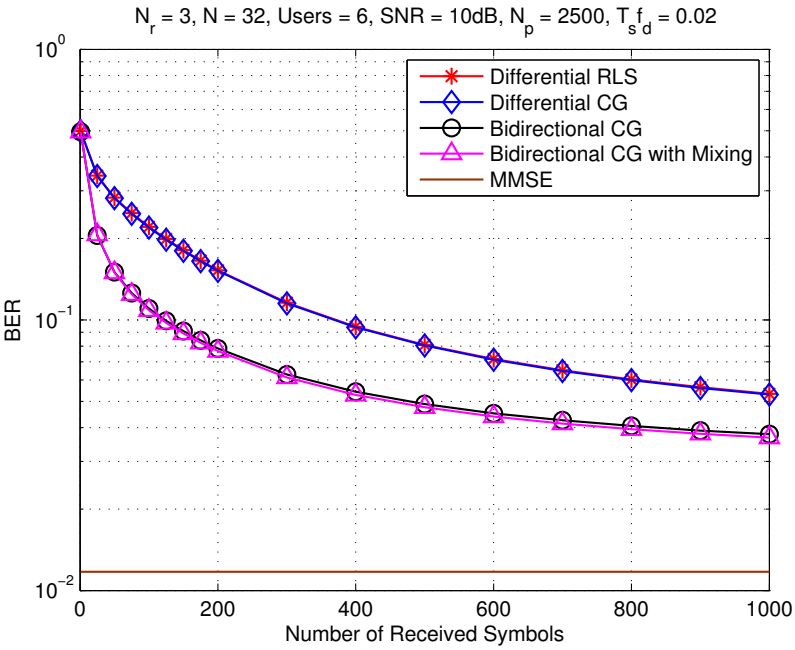

Figure 5.14: BER performance of the proposed CG schemes in a single path cooperative DS-CDMA system.

5.7 Summary

In this chapter, a bidirectional MMSE framework that exploits the correlation characteristics of rapidly varying fading channels to overcome the problems associated with conventional adaptive interference suppression techniques in such channels has been presented. The ratio between successive received vectors is tracked using correlation information gathered at 3 or more time instants in order to avoid tracking of the channel or unfaded symbols. Variable mixing factors were introduced to optimise the weighting of information from each of the considered time instants and was shown to bring further benefits in addition to those obtained by the bidirectional scheme. An analysis of the proposed schemes was performed and the reasons behind the performance improvements shown to be the additional correlation information, data reuse and optimised correlation factor weighting. The conditions under which the differential and bidirectional schemes are equivalent have also been established and the steady-state implications of this detailed. Finally, the proposed algorithms were implemented in standard and cooperative DS-CDMA systems and were shown to outperform both differential and conventional schemes during convergence and steady-state.

Chapter 6

Conclusions and Future Work

Contents

6.1 Summary of Work

In this thesis, efficient interference suppression and resource allocation for mobile networks have been investigated. The current and future mobile systems of DS-CDMA and MIMO have been considered, and the motivation behind their use detailed. Iterative adaptive algorithms were derived and utilised to address the problems of reception in fast-fading channels, computational complexity, interference suppression and resource optimisation, all of which are commonly associated with mobile systems.

In Chapter 3, the problem of interference suppression in multiuser DS-CDMA was considered. The use of extended spreading sequences in DS-CDMA systems increases flexibility and MUI suppression capabilities but complicates the task of reception. To address this, an SM reduced-rank framework based on JIO of adaptive filters was proposed. This enabled the use of direct detection without the requirement of large dimen-

sionality adaptive filters. The application of SM techniques to reduced-rank methods resulted in improved convergence and complexity through the use of optimised convergence parameters and the removal of redundancy associated with SM techniques. NLMS and BEACON algorithm were derived and analysis of their stability and MSE performance presented. Simulations showed equivalent or improved performance of the proposed algorithms compared to existing techniques whilst achieving a significant reduction in computational complexity.

In Chapter 4, the task of resource allocation in cooperative MIMO systems was addressed. The advantages of relaying MIMO systems in terms of diversity, robustness and capacity come at the cost of complex optimisation due to the large number of antennas and nodes. A novel combination of jointly operating DSA was utilised to provide a low-complexity TDS and RS framework that performed antenna and relay optimisation of the second phase whilst avoiding exhaustive searching. The RS process discarded the most poorly performing relays thereby refining and reducing set over which TDS then takes place. This minimises the chance of channel mismatch between the first and second phases, leading to increases in achieved diversity and interference suppression performance over a range of MMSE reception techniques. The use of DSA was extended to joint operation with adaptive continuous power allocation. RS was utilised to constrain the transmit power of poorly performing relays to zero, thereby reducing the dimensionality of structures used in the optimisation process. This led to improved convergence and steady-state performance. Conditions for the convergence of the DSA were stated, and the diversity effects and feedback characteristics of the proposed schemes established. The derived algorithms were applied to a cooperative MIMO system and their interference suppression and diversity performance confirmed. Lastly, non-Wiener performance of LMS interference suppression was exploited in the cooperative system to achieve performance in excess of the 'optimum' linear MMSE interference suppression filter.

In Chapter 5, a bidirectional MMSE scheme that achieves robust interference suppression in severely time-varying fading channels was derived. The proposed algorithms exploit the correlation between 3 or more channel coefficients to track the ratio between successive receive vectors, as opposed to unfaded or faded symbols. Variable mixing factors were introduced to optimise the use of correlation information from the plurality of time instants and extend and improve the performance of the proposed algorithms. NLMS and CG algorithms were given and their improved performance confirmed via simulation in standard and cooperative DS-CDMA systems. An SINR based analytical framework was derived and applied to the proposed algorithm. This provided insight into the operations of the proposed algorithms but also the factors behind their improved convergence and steady-state performance.

6.2 Future Work

The frameworks and algorithms presented in this thesis can be applied to a wide range of systems beyond those covered, including WSN, beamforming, and multi-carrier CDMA. Future extensions of the work presented in this thesis are as follows.

Joint discrete-continuous optimisation problems are found in a large number of communications systems. In the future, OFDM based mobile protocols are anticipated due to their capacity and robustness [18]. The allocation of subcarriers and transmit power in these systems are discrete-continuous optimisation problems, respectively, due to the finite number of subcarrier and data rates. Consequently, the joint DSA and continuous SG algorithms of Chapter 4 have great potential in these systems and is a promising avenue of research.

The bidirectional algorithms of Chapter 5 achieve significantly improved robust-

ness to fast-fading compared to existing DS-CDMA schemes. However, although these schemes also exhibit improved convergence, it is limited by the length of the adaptive filters, which in turn is determined by the length of the channel and spreading sequences. Reduced-rank methods of the sort presented in Chapter 3 and related research literature [70] can address this limitation by performing signal estimation and detection based on bidirectional principles in a reduced-rank subspace. The integration of these methodologies will allow reduced dimensionality adaptive structures to be used in reception and interference suppression; thereby obtaining further improved MUI suppression, convergence and tracking performance.

The application of bidirectional techniques to direct adaptation detection schemes in frequency domain interference suppression and equalisation [135] would be of significant interest. In such a methodology it is envisaged that a process with a similar structure to that presented in Chapter 5 would be performed after an the inverse Fourier transform has been applied to a received signal that has been matched filtering and had any cyclic prefix removed. The bidirectional procedure would then be able to exploit the correlation present in the frequency domain of the received signal, leading to improved convergence and robustness of the direct adaptation process.

The work in this thesis assumes perfect synchronisation between multiuser/multinode transmissions; however, achieving this or suppressing the effects of imperfect synchronisation are not trivial tasks. Investigation into methods of achieving synchronisation in cooperative MIMO networks and the effects of asynchronous transmission on the all proposed schemes would be of great interest and practical importance [31, 33, 136, 137].

List of Symbols

$E[\cdot]$	Expectation
$\mathbf{I}_M$	$M \times M$ Identity matrix
trace$(\cdot)$	Trace of a matrix
∇	Gradient
$\|\| \cdot \|\|$	Euclidean Norm
$\| \cdot \|$	Absolute value
diag[$\mathbf{x}$]	Matrix whose main diagonal is composed of the elements of $\mathbf{x}$
$\sum_{i}^{j}$	Summation with limits $i \rightarrow j$
$\mathfrak{I}(\cdot)$	Imaginary part
$\mathfrak{R}(\cdot)$	Real part
$\otimes$	Kronecker product
$x \in y$	x is an element of Y
$\#(\cdot)$	Cardinality of a set
$\emptyset$	Null set
$x \subset y$	x is a subset of y
sgn$[\cdot]$	Signum function
$\binom{x}{y}$	From x choose y
$x \cap y$	Intersect of x and y

Glossary

AF	Amplify-and-Forward
AoA	Angle of Arrival
AP	Affine Projection
AS	Angle Spread
AVF	Auxiliary-Vector Filtering
AWGN	Additive White Gaussian Noise
BEACON	Bounding Ellipsoid Adaptive Constrained Least Squares
BER	Bit-Error-Rate
BPSK	Binary Phase Shift Keying
CSI	Channel State Information
CG	Conjugate Gradient
DF	Decode-and-Forward
DS	Direct Sequence
DS-CDMA	Direct-Sequence Code-Division Multiple-Access
DSA	Discrete Stochastic Algorithm
EDGE	Enhanced Data Rates for GSM Evolution
FDMA	Frequency Division Multiple Access
FIR	Finite Impulse Response
GSM	Global System for Mobile Communications
GPRS	General Packet Radio Service
IC	Innovation Check

I-METRA	Intelligent Multi-Element Transmit and Receive Antennas
ISI	Intersymbol Interference
JIDF	Joint and Iterative Interpolation, Decimation and Filtering
JIO	Joint Iterative Optimization
LMS	Least Mean-Square
LS	Least Squares
LTE	Long Term Evolution
MAI	Multiple-Access Interference
MAP	Maximum A Posteriori
MI	Mutual Information
MIMO	Multiple-Input Multiple-Output
ML	Maximum Likelihood
MLE	Maximum Likelihood Estimator
MMSE	Minimum Mean-Square Error
MSE	Mean Square-Error
MSWF	Multistage Wiener Filter
MUD	Multiuser Detection
MUI	Multiuser Interference
NLMS	Normalised Least Mean Square
OBE	Optimal Bounding Ellipsoids
OFDM	Orthogonal Frequency Division Multiplexing
PC	Principal Components
PDF	Probability Density Function
PIC	Parallel Interference Cancellation
PR	Pseudo-Random
PSD	Power Spectral Density
QPSK	Quadrature Phase Shift Keying
RLS	Recursive Least Squares

RS	Relay Selection
SG	Stochastic Gradient
SIC	Successive Interference Cancellation
SINR	Signal-to-Interference-plus-Noise Ratio
SISO	Single-Input-Single-Output
SM	Set-Membership
SNR	Signal-to-Noise Ratio
SOP	State Occupation Probability
STBC	Space-Time Block Coding
SVD	Singular Value Decomposition
TDMA	Time Division Multiple Access
TDS	Transmit Diversity Selection
UMTS	Universal Mobile Telecommunications System
UWB	Ultra Wide Band
V-BLAST	Vertical-Bell Laboratories Layered Space-Time
WSN	Wireless Sensor Network
WSS	Wide-Sense Stationary
3GPP	3rd Generation Partnership Project

References

[1] D. Tse and P. Viswanath, *Fundamentals of Wireless Communications*. Cambridge University Press, July 1995.

[2] S. Verdu, *Multiuser Detection*. Cambridge University Press, NY, 1998.

[3] S. W. Peters and R. Heath, "Nonregenerative MIMO relaying with optimal transmit antenna selection," *IEEE Signal Process. Letters*, vol. 15, pp. 421–424, 2008.

[4] L. Zheng and D. N. C. Tse, "Diversity and multiplexing: A fundamental tradeoff in multiple-antenna channels," *IEEE Trans. Inf. Theory*, vol. 49, no. 5, pp. 1073–1096, May 2003.

[5] Z. Yijun, L. Ying, D. Zhiying, L. J. Shan, and H. Hanying, "Optimal design and power allocation for non-regenerative MIMO relay channels," in *IEEE Wireless Commun., Networking and Mobile Computing Conf.*, Dalian, China, 2008.

[6] H. Sun, D. Wang, and X. Y. Sheng Meng, "Optimum power allocation algorithm for MIMO relay channel," in *Int. Conf. on Wireless Commun, Networking and Mobile Computing*, Dalian, October 2008.

[7] M. O. Hasna and M.-S. Alouini, "Optimal power allocation for relayed transmissions over rayleigh fading channels," *IEEE Trans. Wireless Commun.*, vol. 3, no. 6, pp. 1999–2004, November 2004.

[8] Y. Hua, M. Nikpour, and P. Stoica, "Optimal reduced-rank estimation and filtering," *IEEE Trans. Signal Process.*, vol. 49, no. 3, March 2001.

[9] S. Nagaraj, S. Gollamudi, S. Kapoor, and Y. F. Huang, "BEACON: An adaptive set-membership filtering technique with sparse updates," *IEEE Trans. Signal Process*, vol. 47, no. 11, November 1999.

[10] S. Gollamudi, S. Nagaraj, S. Kapoor, and Y. F. Huang, "Set-membership filtering and a set-membership normalized LMS with an adaptive step size," *IEEE Signal Process. Letters*, vol. 5, no. 5, May 1998.

[11] S. Dasgupta and Y. F. Huang, "Asymptotically convergent modified recursive least squares with data dependent updating and forgetting factor for systems with bounded noise," *IEEE Trans. Inform. Theory*, vol. IT-33, pp. 383–392, May 1987.

[12] R. C. de Lamare and R. Sampaio-Neto, "Reduced-rank adaptive filtering based on joint optimization of adaptive filters," *IEEE Signal Process. Letters*, vol. 14, no. 12, December 2007.

[13] ——, "Reduced-rank space–time adaptive interference suppression with joint iterative least squares algorithms for spread-spectrum systems," *IEEE Trans. Vehicular Technology*, vol. 59, no. 3, pp. 1217–1228, March 2010.

[14] S. Andradottir, "A global search method for discrete stochastic optimization," *SIAM Journal on Opt.*, vol. 6, no. 2, pp. 513–530, May 1996.

[15] U. Madhow, K. Bruvold, and L. J. Zhu, "Differential MMSE: A framework for robust adaptive interference suppression for DS-CDMA over fading channels," *IEEE Trans. Commun.*, vol. 53, no. 8, pp. 1377–1390, August 2005.

[16] Ofcom, "Ofcom prepares for 4g mobile auction," http://consumers.ofcom.org.uk/2011/03/ofcom-prepares-for-4g-mobile-auction/, May 2011.

[17] 3rd Generation Partnership Project (3GPP), "3GPP Releases," www.3gpp.org/releases, August 2011.

[18] Y. S. Cho, J. Kim, W. Y. Yang, and C. G. Kang, *MIMO-OFDM Wireless Communications with MATLAB*. John Wiley and Sons (Asia) Pte Ltd., October 2010.

[19] I. Telatar, "Capacity of multi-antenna Gaussian channels," *European Trans. Telecoms.*, vol. 10, no. 6, pp. 585–595, November 1999.

[20] G. Foschine and M. Gans, "On the limits of wireless communications in a fading environment," *Wireless Personal Commun.*, vol. 6, pp. 311–335, March 1998.

[21] A. Paulraj, D. Gore, R. Nabar, and H. Bolcskei, "An overview of MIMO communications - a key to gigabit wireless," *Proc. of the IEEE*, vol. 92, no. 2, pp. 198–218, February 2004.

[22] A. Nosratinia, T. E. Hunter, and A. Hedayat, "Cooperative communications in wireless networks," *IEEE Commun. Magazine*, pp. 74–80, October 2004.

[23] A. Scaglione, D. L. Goeckel, and J. N. Laneman, "Cooperative communications in mobile ad hoc networks," *IEEE Signal Process. Magazine*, pp. 18–29, September 2006.

[24] J. N. Laneman, D. N. C. Tse, and G. Wornell, "Cooperative diversity in wireless networks: Efficient protocols and outage behavior," *IEEE Trans. Inform. Theory*, vol. 50, no. 12, pp. 3062–3080, December 2004.

[25] V. Stankovic, A. Host-Madsen, and Z. Xiong, "Cooperative communications in wireless networks," *IEEE Signal Process. Magazine*, pp. 37–49, September 2006.

[26] R. Krishna, Z. Xiong, and S. Lambotharan, "A cooperative MMSE relay strategy for wireless sensor networks," *IEEE Signal Process. Letters*, vol. 15, pp. 549–552, 2008.

[27] S. Berger and A. Wittneben, "Distributed multiuser MMSE relaying in wireless ad-hoc networks," in *IEEE Asilomar Conf. on Signals, Systems and Computers*, Monterrey, CA, November 2005.

[28] H. S. Ryu, C. G. Kang, and D. S. Kwon, "Transmission protocol for cooperative MIMO with full rate: Design and analysis," in *IEEE Vehicular Technology Conf.*, Dublin, Ireland, May 2007.

[29] W. Huang, Y. Wong, and C. Kuo, "Decode-and-forward cooperative relay with multi-user detection in uplink CDMA networks," in *IEEE Global Telecoms. Conf.*, Pheonix, November 2007.

[30] A. Sendonaris, E. Erkip, and B. Aazhang, "User cooperation diversity - parts I and II," *IEEE Trans. Commun.*, vol. 51, no. 11, pp. 1927–1948, Novmeber 2003.

[31] S. Wei, D. Goeckel, and M. Valenti, "Asynchronous cooperative diversity," *IEEE Trans. Wireless Commun.*, vol. 5, no. 6, pp. 1547–1557, June 2006.

[32] T. M. Cover and A. A. E. Gamal, "Capacity theorems for the relay channel," *IEEE Trans. Info. Theory*, vol. 25, no. 5, pp. 572–584, September 1979.

[33] K. Vardhe, D. Reynolds, and M. Valenti, "The performance of multiuser cooperative diversity in an asynchronous CDMA uplink," *IEEE Trans. Wireless Commun.*, vol. 7, no. 5, pp. 1930–1940, May 2008.

[34] S. Kay, *Fundamentals of Statistical Signal Processing: Estimation Theory*. Prentice Hall, 1993.

[35] H. V. Trees, *Detection, Estimation and Modulation Theory*. John Wiley and Sons, September 2001.

[36] M. Hayes, *Statistical Signal Processing and Modeling*. John Wiley and Sons, April 1996.

[37] H. Hsu, *Theory and Problems of Probability, Random Variables and Random Processes*. McGraw-Hill, October 1996.

[38] S. Haykin, *Adaptive Filter Theory*, 4th ed. NJ: Prentice Hall, 2002.

[39] Z. Tian, H. Ge, and L. L. Scharf, "Low-complexity multiuser detection and reduced-rank Wiener filters for ultra-wideband multiple access," in *IEEE ICASSP*, March 2005.

[40] L. Scharf, "The SVD and reduced rank signal processing," *Signal Processing*, vol. 25, no. 2, pp. 113–133, November 1991.

[41] J. Goldstein and M. Honig, "Adaptive reduced-rank interference suppression based on the multistage Wiener filter," *IEEE Trans. Commun.*, vol. 50, no. 6, pp. 986–994, June 2002.

[42] J. Goldstein, I. Reed, and L. Scharf, "A multistage representation of the Wiener filter based on orthogonal projections," *IEEE Trans. Inform. Theory*, vol. 44, no. 11, pp. 2943–2959, November 1998.

[43] J. S. Goldstein and I. S. Reed, "Reduced rank adaptive filtering," *IEEE Trans. Signal Process.*, vol. vol. 45, p. 492–496, February 1997.

[44] A. M. Haimovich and Y. Bar-Ness, "An eigenanalysis interference canceler," *IEEE Trans. on Signal Process.*, vol. 39, no. 1, pp. 78–84, January 1991.

[45] H. Hotelling, "Analysis of a complex of statistical variables into principal components," *Journal of Educational Psychology*, vol. 24, no. 6/7, pp. 417–441, 498–520, September/October 1933.

[46] D. A. Pados, L. Fernado J, and S. N. Batalama, "Auxiliary-vector filters and adaptive steering for DS/CDMA single-user detection," *IEEE Trans. Vehicular Technology*, vol. 48, no. 6, pp. 1831–1839, November 1999.

[47] H. Qian and S. Batalama, "Data record-based criteria for the selection of an auxiliary vector estimator of the MMSE/MVDR filter," *IEEE Trans. Commun.*, vol. 51, no. 10, pp. 1700–1708, October 2003.

[48] G. N. Karystinos, H. Qian, M. J. Medley, and S. N. Batalama, "Short data record adaptive filtering: The auxiliary-vector algorithm," *Elsevier Science Digital Signal Processing*, vol. 12, pp. 193–222, August 2002.

[49] R. C. de Lamare and R. Sampaio-Neto, "Adaptive reduced-rank MMSE filtering with interpolated FIR filters and adaptive interpolators," *IEEE Signal Process. Letters*, vol. 12, no. 3, pp. 177–180, March 2005.

[50] ——, "Adaptive interference suppression for DS-CDMA systems based on interpolated FIR filters with adaptive interpolators in multipath channels," *IEEE Trans. Vehicular Technology*, vol. 56, no. 5, pp. 2457–2474, September 2007.

[51] S. Moshavi, "Multi-user detection for DS-CDMA communications," *IEEE Commun. Magazine*, pp. 124–136, October 1996.

[52] U. Madhow and M. Honig, "MMSE interference suppression for direct-sequence spread spectrum CDMA," *IEEE Trans. Commun.*, vol. 42, no. 12, pp. 3178–3188, December 1994.

[53] E. Viterbo and J. Boutros, "A universal lattice code decoder for fading channels," *IEEE Trans. Info. Theory*, vol. 45, no. 5, pp. 1639–1642, July 1999.

[54] M. Damen, H. E. Gamal, and G. Caire, "On maximum-likelihood detection and the search for the closest lattice point," *IEEE Trans. Info. Theory*, vol. 49, no. 10, pp. 2389–2402, October 2003.

[55] B. Widrow and M. E. Hoff, "Adaptive switching circuits," Stanford Electron Labs., Stanford, CA, Tech. Rep., June 1960.

[56] ——, "Adaptive switching circuits," in *IRE Western Electric Show and Convention Record, Part 4*, August 1960, pp. 96–104.

[57] D. G. Luenburger and Y. Ye, *Linear and Nonlinear Programming*, 3rd ed. Springer, 2008.

[58] C. Meyer, *Matrix Analysis and Applied Linear Algebra*. SIAM, February 2001.

[59] P. Li, R. C. de Lamare, and R. Fa, "Multiple feedback successive interference cancellation with shadow area constraints for MIMO systems," in *Int. Symposium on Wireless Communs. Systems*, York, September 2010.

[60] R. C. de Lamare and R. Sampaio-Neto, "Minimum mean squared error iterative successive parallel arbitrated decision feedback detectors for DS-CDMA systems," *IEEE Trans. Commun.*, vol. 5, no. 56, pp. 778–789, May 2008.

[61] J. Li, X.-D. Zhnag, and Q. Gao, "Successive interference cancellation for DS-CDMA downlink/uplink," in *IEEE Wireless Commun. and Networking Conf.*, Lax Vegas, USA, March 2008.

[62] Z. Han and K. R. Liu, *Resource Allocation for Wireless Networks: Basics, Techniques and Applications*. Cambridge University Press, April 2008.

[63] R. C. de Lamare, "Joint power allocation and interference suppression techniques for cooperative CDMA systems," in *IEEE Vehicular Technology Conf.*, Barcelona, Spain, April 2009.

[64] L. L. Scharf and D. W. Tufts, "Rank reduction for modeling stationary signals," *IEEE Trans. Acoustics, Speech and Signal Process.*, vol. 35, no. 3, pp. 350–355, March 1987.

[65] L. L. Scharf and B. van Veen, "Low rank detectors for Gaussian random vectors," *IEEE Trans. Acoustics, Speech and Signal Process.*, vol. 35, no. 11, pp. 1579–1582, November 1987.

[66] X. Wang and H. V. Poor, "Blind multiuser detection: A subspace approach," *IEEE Trans. on Infom. Theory*, vol. 44, no. 2, pp. 677–690, March 1998.

[67] Y. Song and S. Roy, "Blind adaptive reduced-rank detection for DS-CDMA signals in multipath channels," *IEEE Journal on Selected Areas in Communications*, vol. 17, no. 11, pp. 1960–1970, November 1999.

[68] M. L. Honig, "A comparison of subspace adaptive filtering techniques for DS-CDMA interference suppression," in *IEEE MILCOM*, Monterrey, CA, November 1997.

[69] D. A. Pados and G. N. Karystinos, "An iterative algorithm for the computation of the MVDR filter," *IEEE Trans. Signal Process.*, vol. 49, no. 2, pp. 290–300, February 2001.

[70] R. C. de Lamare and R. Sampaio-Neto, "Adaptive reduced-rank processing based on joint and iterative interpolation, decimation and filtering," *IEEE Trans. Signal Process.*, vol. 57, no. 7, pp. 2503–2514, July 2009.

[71] P. Clarke and R. C. de Lamare, "Adaptive set-membership reduced-rank interference suppression for DS-UWB systems," in *IEEE ISWCS*, September 2009.

[72] R. C. de Lamare and R. Sampaio-Neto, "Minimum mean-squared error iterative successive interference parallel arbitrated decision feedback detectors for DS-CDMA systems," *IEEE Trans. Commun.*, vol. 56, no. 5, pp. 778–789, May 2008.

[73] R. Singh and L. B. Milstein, "Adaptive interference suppression for DS-CDMA," *IEEE Trans. Commun.*, vol. 50, no. 12, pp. 1902–1905, December 2002.

[74] R. C. de Lamare and P. S. R. Diniz, "Set-membership adaptive algorithms based on time-varying error bounds for CDMA interference suppression," *IEEE Trans. Vehicular Technology*, vol. 58, no. 2, pp. 644–565, February 2009.

[75] L. Huo and Y.-F. Huang, "Set-membership adaptive filtering with parameter-dependent error bound tuning," in *Int. Conf. on Acoustics, Speech and Signal Process.*, Philadelphia, USA, March 2005.

[76] I. Akyildiz, W. Su, Y. Sankarasubramaniam, and E. Cayirci, "A survey on sensor networks," *IEEE Commun. Magazine*, vol. 40, no. 8, pp. 102–114, August 2002.

[77] M. L. Honig and H. V. Poor, *Wireless Communications: Signal Processing Prospectives*. Eds. Englewood Cliffs, NJ: Prentice-Hall, 1998, ch. 2 - Adaptive Interference Suppression, pp. 64–128.

[78] *Third Generation Partnership Project (3GPP)*, specifications 25.101, 25.211-25.215, versions 5.x.x.

[79] W. Jakes, *Microwave Mobile Communications*. Wiley-IEE Press, May 1994.

[80] P. Liu and Z. Xu, "Linear multiuser detection for uplink long-code CDMA systems," in *IEEE ICASSP*, California, April 2003.

[81] Z. Xu, P. Liu, and M. D. Zoltowski, "Diversity -assisted channel estimation and multiuser detection for downlink CDMA with long spreading codes," *IEEE Trans. Signal Process.*, vol. 52, no. 1, pp. 190–201, January 2004.

[82] B. Widrow and M. A. Lehr, "30 years of adaptive neural networks: Perceptron, madaline, and backpropagation," *Proceedings of the IEEE*, vol. 78, no. 9, September 1990.

[83] R. Gaudel, F. Bonnet, J. b. Domelevo-Entfellner, and A. Roumy, "Noise variance estimation in DS-CDMA and its effects on the individually optimum receiver," in *IEEE Workshop on Signal Process. Advances in Wireless Commun.*, Cannes, France, July 2006.

[84] J. Wu, C. Xiao, and K. Letaief, "Estimation of additive noise variance for multiuser CDMA systems," in *Int. Conf. on Commun., Circuits and Systems*, Hong Kong, China, May 2005.

[85] P. S. R. Diniz and S. Werner, "Set-membership binormalized data-reusing LMS algorithms," *IEEE Trans. Signal Process.*, vol. 51, no. 1, pp. 124–134, January 2003.

[86] S. Werner, M. L. R. Campos, and P. S. R. Diniz, "Partial-update NLMS algorithms with data selective updating," *IEEE Trans. Signal Process.*, vol. 52, no. 4, pp. 938–949, April 2004.

[87] R. C. de Lamare, L. Wang, and R. Fa, "Adaptive reduced-rank LCMV beamforming algorithms based on joint iterative optimization of filters: Design and analysis," *Elsevier Signal Process.*, vol. 90, no. 2, pp. 640–652, February 2010.

[88] Y. Fan and J. Thompson, "MIMO configurations for relay channels: Theory and practice," *IEEE Trans. Wireless Commun.*, vol. 6, no. 5, pp. 1774–1786, May 2007.

[89] S. W. Peters, A. Y. Panah, K. T. Truong, and R. W. Heath, "Relay architectures for 3GPP LTE-advanced," *EURASIP Journal on Wireless Commun. and Networking*, vol. 2009, p. 14, March 2009.

[90] Z. Fang, Y. Hua, and J. C. Koshy, "Joint source and relay optimization for a non-regenerative MIMO relay," in *Fourth IEEE Workshop on Sensor Array and Multichannel Processing*, Waltham, MA, USA, July 2006.

[91] I. Berenguer, X. Wang, and V. Krishnamurhty, "Adaptive MIMO antenna selection via discrete stochastic optimization," *IEEE Trans. Signal Process.*, vol. 53, no. 11, pp. 4315–4329, November 2005.

[92] L. Qiu, Y. Zhang, C. Dai, M. Song, and D. Wang, "Cross-layer design for relay selection and power allocation strategies in cooperative networks," in *Commun. Networks and Services Research. Conf.*, New Brunswick, May 2009.

[93] X. Li, S. Jin, X. Gao, and K.-K. Wong, "Near-optimal power allocation for MIMO channels with mean or covariance feedback," *IEEE Trans. Commun.*, vol. 58, no. 1, pp. 289–299, January 2010.

[94] M. A. Torabi and J. Frigon, "Semi-orthogonal relay selection and beamforming for amplify-and-forward MIMO relay channels," in *IEEE Wireless Commun. and Networking Conf.*, Las Vegas, USA, March 2008.

[95] G. J. Foschini, "Layered space-time architecture for wireless communication in a fading environment when using multiple antennas," *Bell Laboratories Technical Journal*, vol. 1, no. 2, pp. 41–59, Autumn 1996.

[96] H. D. Hongyuan Zhang and B. L. Hughes, "Analysis on the diversity-multiplexing tradeoff for ordered MIMO SIC receivers," *IEEE Trans. Commun.*, vol. 57, no. 1, pp. 125–133, January 2009.

[97] R. Fa and R. C. de Lamare, "Multi-branch successive interference cancellation for MIMO spatial multiplexing systems: design, analysis and adaptive implementation," *IET Commun.*, vol. 5, no. 4, pp. 484–494, May 2010.

[98] P. Li, R. C. de Lamare, and R. Fa, "Multiple feedback successive interference cancellation detection for multiuser MIMO systems," *IEEE Trans. Wireless Commun.*, vol. 10, no. 8, pp. 2434–2439, August 2011.

[99] Y. Cai, D. le Ruyet, and D. Roviras, "Joint interference suppression and power allocation techniques for multiuser multiantenna relay broadcast systems," in *Int. Symposium on Wireless Commun. Systems*, York, September 2010.

[100] R. C. de Lamare, "Joint iterative power allocation and interference suppression algorithms for cooperative spread spectrum networks," in *Int. Conf. on Acoustics, Speech and Signal Process.*, Dallas, USA, March 2010.

[101] M. Ding, S. Liu, H. Luo, and W. Chen, "MMSE based greedy antenna selection scheme for AF MIMO relay systems," *IEEE Signal Process. Letters*, vol. 17, pp. 433–436, May 2010.

[102] I. Bahceci, T. M. Duman, and Y. Altunbasak, "Antenna selection for multiple-antenna transmission systems:performance analysis and code construction," *IEEE Trans. Inform. Theory*, vol. 49, no. 10, pp. 2669–2681, October 2003.

[103] S. Chen, W. Wang, X. Zhang, and D. Zhao, "Performance of amplify-and-forward MIMO relay channels with transmit antenna selection and maximal-ratio combining," in *IEEE Wireless Commun. and Networking Conf.*, Budapest, Hungary, April 2009.

[104] B. C. Lim, W. A. Krzymien, and C. Schlegel, "Efficient sum rate maximization and resource allocation in block-diagonalized space-division multiplexing," *IEEE Trans. Vehicular Technology*, vol. 58, no. 1, pp. 478–484, January 2009.

[105] F.-S. Tseng and W.-R. Wu, "MMSE-SIC transceiver design in amplify-and-forward MIMO relay systems," in *IEEE Vehicular Technology Conf.*, Taipei, Taiwan, June 2010.

[106] C. S. Park and K. B. Lee, "Transmit power allocation for successive interference cancellation in multicode MIMO systems," *IEEE Trans. Commun.*, vol. 56, no. 12, pp. 2200–2213, December 2008.

[107] S. Talwar, Y. Jing, and S. Shahbazpanahi, "Joint relay selection and power allocation for two-way relay networks," *IEEE Signal Process. Letters*, vol. 18, no. 2, pp. 91–91, February 2011.

[108] A. Hedayat and A. Nosratinia, "Outage and diversity of linear receivers in flat fading MIMO channels," *IEEE Trans. Signal Process.*, vol. 55, no. 12, pp. 5868–5873, December 2007.

[109] I. Telatar, "Capacity of multi-antenna Gaussian channels," *European Trans. Telecommun.*, vol. 10, no. 6, pp. 585–595, November 1999.

[110] L. Schumacher, K. I. Pedersen, and P. Mogensen, "From antenna spacings to theoretical capacities - guidelines for simulating MIMO systems," in *IEEE International Symposium on Personal, Indoor and Mobile Radio Commun.*, Lisbon, September 2002.

[111] T. Irkuma, A. Beex, and J. Zeidler, "Non-Wiener weight behavior and LMS transversal equalizers," *IEEE Trans. Signal Process.*, vol. 56, no. 9, pp. 4521–4525, September 2008.

[112] M. Reuter and J. Zeidler, "Nonlinear effects in LMS adaptive equalizers," *IEEE Trans. Signal Process.*, vol. 47, no. 6, pp. 1570–1579, June 1999.

[113] M. Honig, M. Shensa, S. Miller, and L. Milstein, "Performance of adaptive linear interference suppression for DS-CDMA in the presence of flat rayleigh fading," in *IEEE Vehicular Technology Conf.*, Pheonix, May 1997.

[114] D. Sadler and A. Manikas, "MMSE multiuser detection for array multicarrier DS-CDMA in fading channels," *IEEE Trans. Signal Process.*, vol. 53, no. 7, pp. 2348–2358, July 2005.

[115] R. Schoder, W. Gerstacker, and A. Lampe, "Noncoherent MMSE interference suppression for DS-CDMA," *IEEE Trans. Commun.*, vol. 50, no. 4, pp. 577–587, April 2002.

[116] S. Haykin, A. Sayed, J. Zeidler, P. Yee, and P. Wei, "Adaptive tracking of linear time variant systems by extended RLS algorithms," *IEEE Trans. Signal Process.*, vol. 45, no. 5, pp. 1118–1128, May 1997.

[117] J. Wang, “Fast tracking RLS algorithm using novel variable forgetting factor with unity zone,” *IEEE Electronics Letters*, vol. 27, no. 23, pp. 2550–2551, November 1991.

[118] R. Kwong and E. Johnston, “A variable step size LMS algorithm,” *IEEE Trans. Signal Process.*, vol. 40, no. 7, pp. 1633–1642, May 1992.

[119] B. Toplis and S. Pasupathy, “Tracking improvements in fast RLS algorithm using a variable forgetting factor,” *IEEE Trans. Acoust., Speech, Signal Process.*, vol. 36, no. 2, pp. 206–227, February 1988.

[120] S.-H. Leung and C. So, “Gradient-based variable forgetting factor RLS algorithm in time-varying environments,” *IEEE Trans. Signal Process.*, vol. 53, no. 8, pp. 3141–3150, August 2005.

[121] S. Hyun-Chool, A. Sayed, and S. Woo-Jin, “Variable step-size NLMS and affine projection algorithms,” *IEEE Signal Process. Letters*, vol. 11, no. 2, pp. 132–135, February 2004.

[122] Y. Zhang, N. Li, J. Chambers, and Y. Hao, “New gradient-based variable step size LMS algorithms,” *EURASIP Journal on Adv. in Signal Process.*, January 2008.

[123] S. Gelfand, Y. Wei, and J. Krogmeier, “The stability of variable step-size LMS algorithms,” *IEEE Trans. Signal Process.*, vol. 47, no. 12, pp. 3277–3288, December 1999.

[124] H. V. Poor and X. Wang, “Adaptive multiuser detection in fading channels,” in *Annual Allerton Conf. Commun., Control and Computing*, Monticello, October 1996.

[125] L. J. Zhu and U. Madhow, “Adaptive interference suppression for direct sequence CDMA over severely time-varying channels,” in *IEEE Global Telecoms. Conf.*, Pheonix, Novmeber 1997.

[126] M. Honig, S. Miller, M. Shensa, and L. Milstein, "Performance of adaptive linear interference suppression in the presence of dynamic fading," *IEEE Trans. Commun.*, vol. 49, no. 4, pp. 635–645, April 2001.

[127] P. S. R. Diniz, *Adaptive Filtering: Algorithms and Practical Implementation*, 3rd ed. Springer, August 2008.

[128] P. S. Chang and A. N. Wilson, "Analysis of conjugate gradient algorithms for adaptive filtering," *IEEE Trans. Signal Process.*, vol. 48, no. 2, pp. 409–418, February 2000.

[129] ——, "Adaptive filtering using modified conjugate gradient," in *MWSCS*, Rio de Janeiro, August 1995.

[130] N. J. Bershad, J. C. M. Bermudez, and J.-Y. Yourneret, "An affine combination of two LMS adaptive filters - transient mean square analysis," *IEEE Trans. Signal Process.*, vol. 56, no. 8, May 2008.

[131] M. Martinez-Ramon, J. Arenas-Garcia, A. Navia-Vazquez, and A. R. Figueiras, "An adaptive combination of adaptive filters for plant identification," in *14th International Conf. on Digital Signal Processing*, Santorini, Greece, 2002.

[132] J. Arenas-Garcia, A. Figueiras-Vidal, and A. Sayed, "Mean-square performance of a convex combination of two adaptive filters," *IEEE Trans. Signal Process.*, vol. 45, no. 3, pp. 1078–1090, March 2006.

[133] H. Kushner, *Approximation and Weak Convergence Methods for Random Processes with Applications to Stochastic System Theory*. MIT Press, April 1984.

[134] A. Sayed, *Adaptive Filters*. John Wiley & Sons, May 2008.

[135] S. Li and R. C. de Lamare, "Adaptive linear interference suppression based on block conjugate gradient method in the frequency domain for DS-UWB systems," in *IEEE ISWCS*, Siena, October 2009.

[136] T.-D. Nguyen, O. Berder, and O. Sentieys, “Impact of transmission synchronisation error and cooperative reception techniques on the performance of cooperative MIMO systems,” in *IEEE Conf. on Commmun.*, May 2008.

[137] S. Hsin-Yi and S. Kalyanaraman, “Asynchronous cooperative MIMO communication,” in *Modeling and Optimization in Mobile, Ad Hoc and Wireless Networks and Workshops*, April 2008.